Prion propagation and molecular chaperones

Habilitation Thesis

Author(s):
Zahn, Ralph

Publication date:
2002

Permanent link:
https://doi.org/10.3929/ethz-a-004399625

Prion propagation and molecular chaperones

RALPH ZAHN

Institut für Molekularbiologie und Biophysik, Eidgenössische Technische Hochschule, Hönggerberg, CH-8093 Zürich, Switzerland

Abbreviations: BSE, bovine spongiform encephalopathy; CD, circular dichroism; CHO, chinese hamster ovary cell line; chPrP, chicken PrP; CJD, Creutzfeldt-Jakob disease; CNS; central nervous system; DLPC, detergent-lipid-protein complexes; Dpl, doppel protein; ER, endoplasmic reticulum; FFI, fatal familial insomnia; GPI, glycosyl phosphatidylinositol; GSS, Gerstmann-Sträussler-Scheinker syndrome; hPrP, human PrP; mPrP, mouse PrP; NMR, nuclear magnetic resonance; NOE, nuclear Overhauser enhancement; nvCJD, new variant CJD; PIPLC, cellular membranes by phosphatidylinositol phospholipase C; PK, proteinase K; *Prnp*, PrP gene; PrP, prion protein; PrP 27–30, protease-resistant core fragment of PrP^{Sc}; PrP^{C}, cellular isoform of PrP; PrP-res, PK-resistant PrP isoform, PrP^{Sc}, scrapie isoform of PrP; SAF, scrapie-associated fibrils; ScN_2a, scrapie-infected mouse neuroblastoma cell line; shPrP, Syrian hamster PrP; TSE, transmissible spongiform encephalopathy.

1. INTRODUCTION

Although the central paradigm of protein folding (Anfinsen, 1973), that the unique three-dimensional structure of a protein is encoded in its amino acid sequence, is well established, its generality has been questioned due to two recent developments in molecular biology, the "prion" and "molecular chaperone". Biochemical characterization of infectious scrapie material causing central nervous system (CNS) degeneration indicates that the necessary component for disease propagation is proteinaceous (Prusiner, 1982), as first outlined by Griffith (1967) in general terms, and involves a conversion from a cellular prion protein, denoted PrP^{C}, into a toxic scrapie form, PrP^{Sc}, which is facilitated by PrP^{Sc} acting as a template for PrP^{C} to form new PrP^{Sc} molecules (Prusiner, 1987). The "protein-only" hypothesis implies that the same polypeptide sequence, in the absence of any posttranslational modifications, can adopt two considerably different stable protein conformations (Fig. 1). Thus, in the case of prions it is possible, although not proven, that they violate the central paradigm of protein folding. There is some indirect evidence that another factor, provisionally named "protein X", might be involved in the conformational conversion process (Prusiner *et al*., 1998), which includes a dramatic change from α-helical into β-sheet secondary structure (Fig. 1). This factor has not been identified yet, but it has been proposed that protein X may act as a molecular chaperone. The idea that molecular chaperones play a critical role in the generation of PrP^{Sc} is appealing also from a theoretical point of view, because PrP^{Sc} formation involves changes in protein folding and possibly intermolecular aggregation (Fig. 1), processes in which chaperones are known to participate (Musgrove & Ellis, 1986). The discovery and functional analysis of more than a dozen molecular chaperones made it clear that these proteins do not complement folding information that is not already contained in the genetic code (Ellis *et al*., 1989), rather they facilitate the folding and assembly of proteins by preventing misfolding and refolding misfolded proteins (Hartl, 1996). Whether a molecular chaperone or another type of macromolecule is identified as the conversion factor, therefore, the molecular chaperone concept is likely to contribute to the understanding of the molecular nature of the PrP^{C} to PrP^{Sc} conversion.

In this review I consider the prion concept from the view of a structural biologist whose main interest focuses on spontaneous and chaperone-mediated conformational changes in proteins. As a starting point for those who are not prion experts section 2 summarizes some of the key experiments leading to the prion concept and the main arguments supporting the protein-only hypothesis. A more comprehensive discussion of this issue can be found in the Nobel Lecture of Prusiner (1998). Although historically scrapie isoforms of PrP were the first to be described, they have been only marginally been characterized. The lack of structural information on PrP^{Sc} originates from its tendency to form detergent-insoluble aggregates of different types which makes a characterization difficult (section 3). For the cellular isoform, solution structures have been defined using nuclear magnetic resonance (NMR) spectroscopy for monomeric forms of recombinant PrP of the two most widely used laboratory animals in prion research, the mouse and the hamster. Recently, our lab determined the NMR structure of the human prion protein to provide a direct basis for future structure based arguments on the propagation of human prions (section 4). So far, the biological role of the cellular prion protein remains an enigma, but the situation might change in the near future due to the recent discovery of a gene encoding a

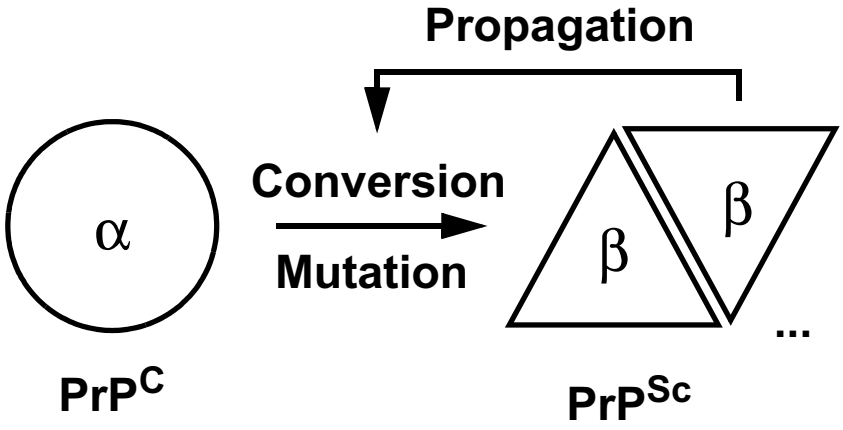

Fig. 1. Proposed mechanism for the propagation of prions causing TSE (Prusiner, 1987). The host encoded PrP^{C} is a monomeric protein which contains mainly α-helical secondary structure. The detergent-insoluble PrP^{Sc} isoform contains large amounts of β-sheet secondary structure, and tends to form fibrillar protein aggregates. Prion propagation includes a PrP^{C} to PrP^{Sc} conformational conversion, which is promoted by the PrP^{Sc} isoform. The conversion reaction is also facilitated by genomic or somatic mutations in the PrP gene leading to inherited or spontaneous forms of TSE, respectively. Transmission of exogenous PrP^{Sc} into humans or animals causes infectious TSE forms.

PrP-like protein designed "doppel" (Dpl) with about 25% identity with all known prion proteins. The conversion of PrP^{C} into PrP^{Sc} has been the focus on intense research and although it is still not clear how the conversion occurs, the characteristics and minimal requirements have been defined as described in section 5. One of the striking features of prion diseases is the existence of species barriers and prion strains. It appears now well established that the species barrier is due to differences in the amino acid sequence between PrP^{Sc} and PrP^{C}, and that different prion strains within a given species are invariant in amino acid sequence but exist in different conformations. There is accumulating evidence that the prion strain found in "new variant" Creutzfeldt-Jakob disease (nvCJD) patients originates from transmission of the bovine spongiform encephalopathy (BSE) agent to humans. These phenomena are also reviewed in section 5. To better understand the conversion process numerous mutants of the PrP gene (*Prnp*) leading to familial transmissible spongiform encephalopathy (TSE) have been recombinantly expressed and their consequence defined (section 6). From these results it has been concluded that other molecular mechanisms are important in facilitating the structural conversion of PrP isoforms during familial TSE besides thermodynamical destabilization of the PrP^{C} isoform. Synthetic peptide fragments of PrP defined as crucial from genetic analysis have been investigated by biophysical methods. Although there is so far no evidence that synthetic PrP fragments can spontaneously transform into infectious PrP^{Sc}, many of them do tend to form β-sheet structure and aggregate into amyloid fibrils. These results are reviewed in section 7. Various lines of evidence indicate that the cofactor protein X participates in prion propagation as described in section 8. The partially mapped protein X epitope on PrP^{C} coincidences with the location of species variations observed when comparing the three-dimensional structures of human, mouse, and hamster PrP^{C} C-terminal domain and with the epitopes for immune reactions with PrP isoform-specific antibody. The possibility that protein X is a molecular

chaperone is reviewed in section 9, where the discussion focuses on the chaperonin Hsp60 as this is the only chaperone for which there is evidence suggesting a specific interaction with the prion protein involving a conformational change. Fortuitously, the chaperonins probably represent the best understood family of molecular chaperones in terms of structure-function relationships. This section closes with the arguments that support the hypothesis that prion propagation is mediated by chaperonin (Table 1). In section 10 I propose a connection between the prion and molecular chaperone concepts on the basis of proposed molecular mechanisms for PrP conversion.

2. Protein-only hypothesis

The protein-only hypothesis evolved from a collection of radiobiological data on the agent causing scrapie disease in sheep (Alper *et al*., 1966; 1967; Latarjet *et al*., 1970). The agent was found to be extremely resistant to inactivation by ultra-violet and ionizing radiation, as was later shown for the agent causing Creutzfeldt-Jakob disease (CJD) in humans (Gibbs *et al.*, 1978), excluding the possibility that a scrapie-specific nucleic acid containing virus or viroid is the infectious component of prions. The availability of the prion protein gene *Prnp* facilitated testing the model that the scrapie agent contains a PrP-related nucleic acid by using hybridization techniques (Oesch *et al.*, 1985). Purified preparations of hamster prions were found to contain less than 0.004 single-stranded DNA or RNA molecules per infectious unit, and return refocusing gel electrophoresis limited the size of homogeneous nucleic acid molecules to less than 80 nucleotides in length per infectious unit (Kellings *et al*., 1992; 1994).

Conclusive evidence that the agent was associated with protein was shown by demonstrating that the activity of partially purified scrapie agent was sensitive to proteinase digestion and was inactivated by chemical reagents that are known to denature protein, including sodium dodecyl sulfate, urea, guanidinium thiocyanate, and phenol (Prusiner *et al*., 1980; 1981*b*; McKinley *et al*., 1981). As will be outlined in the following section, highly purified protein was identified to purify with the scrapie agent, and was not found in a similar fraction from uninfected brain.

Ablation of the PrP gene in knockout mice ($Prnp^{0/0}$) was found to prevent both prion disease and prion propagation after intracerebral inoculation of prions, whereas reintroduction of PrP transgenes restored susceptibility to prion (Büeler *et al*., 1993; Sailer *et al*., 1994). Conversely, overexpression of PrP^{C} increased the rate of PrP^{Sc} formation and shortened the incubation time of prions (Prusiner *et al.*, 1990). Mutations in the open reading frame of *Prnp* are genetically linked to inherited prion disease and are associated with formation of PrP^{Sc} (Carlson *et al*., 1986). The P102L mutation was the first PrP mutation to be genetically linked to CNS in Gerstmann-Sträussler-Scheinker (GSS) syndrome (Doh-ura *et al*., 1989; Goldgaber *et al*., 1989; Hsiao *et al*., 1989), and has since been found in many GSS families throughout the world (Kretzschmar *et al*., 1991). Transgenic mice expressing the P102L mutation at high levels develop spontaneous disease of the CNS similar to that seen in the brains of human who die as a consequence of the mutation (Hsiao *et al*., 1990).

Many lines of evidence converge on the thesis that prions are composed of PrP^{Sc} molecules and devoid of nucleic acid (Prusiner, 1998). Although each individual piece of evidence described above could be explained in several ways, the conjunction of the data strongly supports the proposal that the prion is composed partly or entirely of PrP^{Sc} and that

protein-encoding nucleic acid is not an essential component (Weissmann, 1999). The final proof, however, would be the demonstration that biosynthetic, pure PrP^C can be converted to infectious scrapie agent under defined conditions.

3. THE SCRAPIE PRION PROTEIN PrP^{Sc}

3.1 *Purification of PrP 27–30*

The development of a purification protocol for the scrapie agent and its biochemical and biophysical characterization not only support the protein-only hypothesis, but also forms the platform from which many other branches in prion research have emerged. A biochemical purification method requires the ability to follow biological activity during single purification steps. An efficient bioassay for the detection of scrapie activity has been originally described by Prusiner and colleagues. The assay is based on the length of the incubation period after intracerebral inoculation of prions into hamster, where the incubation period is defined as the time interval from inoculation to the onset of clinically detectable neurological illness or as the interval from inoculation to death (Prusiner *et al.*, 1980). Both of these intervals are inversely proportional to the size of the dose injected, and are a linear function of the logarithm of the inoculum size over a wide range of dosages (Prusiner *et al*., 1981*a*). The development of the incubation time assay substantially reduced the number of animals needed for quantitating the agent in a given sample by a factor of fifteen when compared to the end point titration method (Chandler, 1963) and reduced the time required to measure prions in samples with high titers. Employment of hamsters or genetically manipulated Tg20 mice (Fisher *et al*., 1996) further reduced the assay time to 70 days instead of 360 days for non-manipulated mice.

Initial attempts to purify the scrapie agent were unsuccessful because of the difficulty to separate the agent from cellular membranes. Prusiner *et al.* (1977) were able to study the sedimentation characteristics of the scrapie agent in fixed angle rotors using the technique of analytical differential centrifugation. These studies indicated that the scrapie agent is a discrete infectious particle which can be sedimented at a particular w^2t value. A significant purification of the scrapie agent could be achieved by using a combination of low-speed centrifugation, polyethylene glycol precipitation, limited proteinase K (PK) digestion, ammonium sulfate precipitation, and discontinuous sucrose gradient sedimentation (Bolton *et al*., 1982; Prusiner *et al*., 1982). Infectivity analysis of the discontinuous sucrose gradients by the incubation time bioassay showed that approximately half of the agent sedimented in a fraction near the bottom of the gradient, but infectivity was also found in fractions at the top of the gradient. Analyses of ^{125}I-labeled sucrose gradient fractions by gel electrophoresis revealed a diffuse protein band with a molecular size of 27 to 30 kDa in those fractions enriched for the infectious agent. Because of this size heterogeneity the purified protein was designed PrP 27–30 (Bolton *et al*.,1984; Prusiner *et al*., 1984). This was the first time that the prion protein became “visible” – from a biochemist’s point of view. The distribution of infectivity in various sucrose gradient fractions indicated the tendency of PrP 27–30 to form detergent-insoluble aggregates. Employment of zonal rotor centrifugation (Prusiner *et al*., 1983) allowed large scale purification of extensively purified prions containing only one major protein, whose concentration correlated with the titer of the scrapie agent over a 10^4-fold range (McKinley *et al*., 1983).

3.2 *Proteinase K resistance*

When the *Prnp* was identified by Oesch and Weissmann in 1985 they demonstrated by immunostaining of brain extracts that PrP 27–30 is in fact a proteolytic product of a larger prion protein, initially termed PrP 33–35^{Sc}. The index "Sc" was used to distinguish the scrapie form of the prion protein from the cellular form, PrP 33–35^{C}, which was detected in both infected and uninfected brain. Hence, the protease-resistance of the scrapie isoform is traditionally linked to the presence of prion infectivity (McKinley *et al*., 1983; Bolton *et al*., 1984), making it a good marker for disease, although in some experimental setups PrP 27–30 can not be detected in samples that contain prion infectivity. Transgenic mice overexpressing the mouse prion protein gene carrying the P102L mutation of GSS spontaneously develop disease which is not derived from protease-resistant PrP^{Sc} molecules (Hsiao *et al*., 1990; Telling *et al.*, 1996*a*). Moreover, after inoculation of infectious brain extracts from these mice into healthy mice no PK resistance protein can be detected. Conversely, protease-resistant PrP is not necessarily infectious. The organic solvent dimethyl sulfoxide inhibits the accumulation of PrP^{Sc} in scrapie-infected neuroblastoma (ScN_2a) cells presumably by stabilizing a soluble protein conformation (Tatzelt *et al*., 1996). When membranes prepared from brains of hamsters terminally ill with scrapie are incubated in the presence of dimethyl sulfoxide and detergents, part of the PK-resistant PrP 27–30 molecules can no longer be precipitated by high speed centrifugation nor do they aggregate into very large structures (Shaked *et al*., 1999). When inoculated into hamster brains, only traces of scrapie infectivity are associated with these soluble PrP 27–30 molecules. Infectivity is also not regained upon amorphic aggregation and removal of dimethyl sulfoxide from the protease-resistant protein. In agreement with these studies, different solvent conditions abolish PK resistance in PrP 27–30 equally well but have different effects on scrapie infectivity. These results suggest that the conversion of PrP^{C} into protease-resistant PrP molecules is not a crucial step in prion replication.

3.3 *Scrapie associated fibrils*

The scrapie isoform of the prion protein appears to contain an intrinsic tendency to form fibrillary-organized protein aggregates. Merz and co-workers discovered that subfractions of brains from scrapie-infected animals contain abnormal fibrillary structures, designated "scrapie-associated fibrils" (SAF), when examining negative stain electron microscope preparations (Merz *et al*., 1981). They observed SAF in all combinations of scrapie agent species and host examined, regardless of their histopathology, in particular the presence or absence of amyloid plaques. The fibrils consist of either two or four filaments, and they were morphologically dissimilar to the normal brain fibrils – microtubules, neurofilaments, glial filaments, and actin filaments. Similar SAF were observed in sucrose gradient enriched fractions of brains and spleens infected with CJD or scrapie in humans or animals (Merz *et al*., 1983, Diringer *et al*., 1983). Ultrastructurally purified SAF appear as short, straight, unbranched fibrils. They disperse freely as single fibrils, or in clusters, sometimes associated with proteinaceous or membrane-like structures. Two types of SAF have been identified in a variety of preparations from scrapie-infected animals. Type I SAF are composed of two 4 to 6 nm

diameter filaments, each of which is apparently supercoiled with a periodicity of 40 to 80 nm, yielding a 11 to 14 nm diameter fiber. The length of the fibrils range from 100 to 500 nm in length. The more rare type II SAF, observed in only some of the scrapie strains, are composed of four helically wound filaments, but with a periodicity of 100 to 200 nm. The morphology of the SAF is the same in naturally occurring, or in experimentally transmitted disease, and is different from those of "amyloid fibrils" in size and periodicity (Merz *et al*., 1984).

Prusiner and co-workers determined that the higher molecular weight fraction of their PrP 27–30 preparations forms rod-shaped particles 10 to 20 nm in diameter and 100 to 200 nm in length in the electron microscope (Prusiner *et al*., 1983). They estimated that about one thousand PrP molecules with a molecular weight of 27 to 30 kDa are packed in a single prion "rod", which resemble in morphology purified amyloid as confirmed by the green birefringence observed in samples stained with Congo red dye under a polarisation microscope. It was concluded that prion rods represent a polymeric form of the scrapie prion, and that the amyloid plaques observed in TSEs might consist of prion rods. However, in new purification protocols for PrP^{Sc} including proteinase inhibitors no prion rods were found in the purified fractions (McKinley *et al*., 1991*a*). The absence of prion rods was puzzling, since it was previously reported that the detergent extraction of microsomal membrane alone resulted in the formation of prion rods (Meyer *et al*., 1986). To determine whether both detergent extraction and limited proteolysis are required for the formation of prion rods, microsomal membranes were detergent-extracted as well as protease-digested. Neither detergent-extraction with sarkosyl nor limited PK digestion alone produced prion rods. Only after combining both purification steps were prion rods observed, indicating that the prion rods represent an artificial protein aggregate generated by the purification procedure.

The development of an efficient protocol for preparing PrP 27–30 made it possible to produce rabbit antiserum and localize the scrapie protein in hamster brains (Bendheim *et al.*, 1984). The structures observed, especially in the hippocampus of hamster brain stained with PrP antiserum, were discrete, measured up to 40 μm in diameter and had a fluffy, cotton-like appearance. When adjacent sections were stained with Congo red dye, these same structures exhibited green birefringence with polarized light, suggesting that the structures staining with PrP antiserum are composed of paracrystalline arrays of prion proteins that exhibit the staining characteristics of amyloid plaques. The same antiserum to hamster scrapie PrP 27–30 also reacted with proteins purified from the brains of mice with experimental CJD – that is mice infected with the CJD agent – indicating that these two diseases share antigenic determinants (Bendheim *et al*., 1985). In the brains of such mice extracellular prion "filaments" of up to 1500 nm in length and with a diameter of 16 nm that occasionally narrow to 8 nm have been identified by using immunocytochemical techniques and affinity-purified antibodies (DeArmond *et al.*, 1985). The prion filaments were reported to form the major element of the plaques in the brain of scrapie-infected hamsters, and to be morphologically identical with purified prion rods and amyloid fibrils (Barry *et al*., 1985). The antiserum directed against prion filaments also decorates SAF in scrapie-infected brain and reacts with a broad protein band at 33 to 35 kDa in Western blot analysis of scrapie preparations (Merz *et al*., 1987).

In conclusion, both SAF and prion rods copurify with infectivity and are biochemically and antigenically related, although they differ in morphology. It seems that the protein fibrils observed under different conditions represent different aggregation states of the same protein,

and that their morphology is dependent on the preparation and purification procedure. Whether natural prion protein aggregates in amyloid plaques contain fibrillar or amorphic structure and whether amyloid plaques or fibrils are a necessary and sufficient prerequisite of pathogenicity remain to be established.

3.4 *Smallest infectious unit*

The reversible dissociation of prion rods into detergent-lipid-protein complexes (DLPC) and liposomes with full retention of scrapie infectivity (Gabizon *et al*., 1987) raises the question about the size of the smallest infectious unit for prions. Incorporation of prion rods into liposomes can be achieved by removal of cholate from mixtures of the detergent and phospholipid, which have been found to solubilize purified PrP 27–30 in the form of DLPC. Infectious liposomes contain, on average, between two and four PrP 27–30 molecules. Inactivation of scrapie activity by ionizing radiation exhibits single-hit kinetics and gives a target size of 55 ± 9 kDa (Bellinger-Kawahara *et al*., 1988), where the inactivation profile is independent of the form of the prion: samples containing purified amyloid rods yield the same inactivation profile as brain homogenates, microsomal fractions, detergent-extracted microsomes, and liposomes. These data are consistent with earlier radiation studies on brain homogenates estimating the molecular size of the scrapie and CJD agent to be less than 100 kDa (Alper *et al*., 1966; Latarjet *et al.*, 1970; Gibbs *et al*., 1978). They also agree with the identification of low molecular size prion forms during size exclusion chromatography (Bolton *et al.*, 1982), and the finding that "miniprions", although they are soluble in detergent, contain the propensity for transmission of infectivity (Muramoto *et al.*, 1996; see also section 5.3). Together, these studies argue that the smallest infectious particle causing TSE contains only a few PrP molecules.

3.5 *Conformational properties*

Clearly defining the conformational properties of different forms of PrP is crucial to defining the transition and disease mechanisms. In the case of prions this proves challenging because the most powerful methods for determining protein conformation rely on soluble homogenous samples precluding the investigation of aggregates. Fourier transform infrared (FTIR) spectroscopy permits the determination of the relative amounts of different types of secondary structure for proteins in aqueous media. The advantage of this technique is that it does not require that a molecule is in solution. Second-derivative analysis of the infrared spectra reveals that PrP 27–30, purified from highly infectious hamster brain fibril preparations (Bolton *et al*., 1987) and suspended in phosphate-buffered saline by sonication, contains 47% β-sheet, 31% turn, and 17% α-helix secondary structure – curiously, the amount of secondary structure in non-proteinase-treated PrP^{Sc} could initially not be determined, because of the tendency of PrP^{Sc} to aggregate into particles too large to be introduced into short pathlength measuring cells (Caughey *et al*., 1991*a*). The high content of β-sheet secondary structure in PrP 27–30 is consistent with its amyloid-like properties (Prusiner *et al*., 1983), and similar to but not identical with data obtained from attenuated total reflection FTIR (Gasset *et al*., 1993). The major

rP

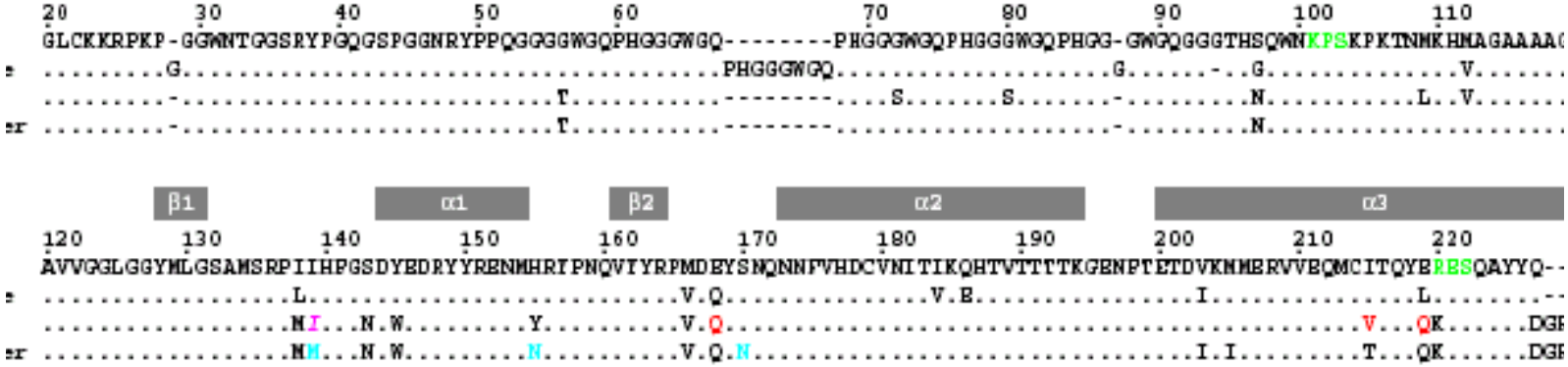

roEL / Hsp60

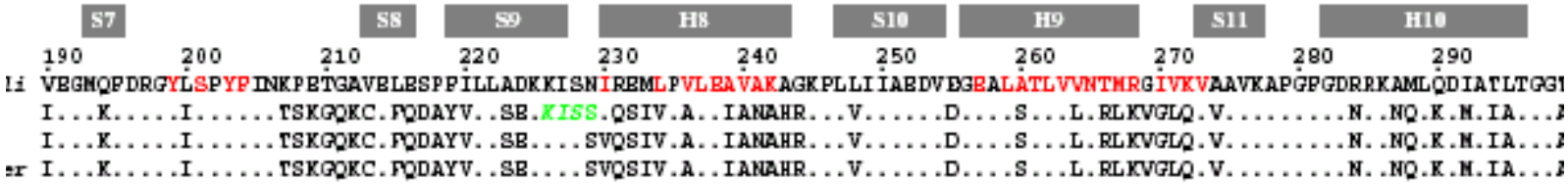

that the analyte is manipulated as a thin hydrated film (Goormaghtigh *et al.*, 1990). Prion rods analysed by attenuated total reflection FTIR consist of 54% β-sheet, 10% turn, and 25% α-helix. In spectra the low frequency β-sheet component that maximizes at 1621.5 cm^{-1} accounts for one-third of the overall secondary structure and presumably reflects the presence of intermolecular β-sheet. Perturbations in the secondary structure of PrP 27–30 correlate well with changes in scrapie infectivity (Gasset *et al.*, 1993). Conditions that reduce β-sheet structure are accompanied by disassembly of the prion rods and a diminution of infectivity. Similar results are obtained when PrP 27–30 is analysed by circular dichroism (CD) spectroscopy in the solid state in dried films (Safar *et al.*, 1993*b*). Acidic pH induces a reversible change in secondary structure under conditions that do not destroy infectivity, whereas basic conditions produce an irreversible structural change and a loss of infectivity. The most profound alterations are associated with sodium dodecyl sulfate, which increases α-helix- and turn-content at the expense of β-sheet structure and infectivity. Conversely, disruption of the prion rods by dispersion into infectious DLPC occurs without a change in either secondary structure or prion infectivity. These results suggest that the additional β-sheet secondary structure contained in the scrapie isoform of PrP is a necessary prerequisite for its pathogenicity.

PrP^{Sc} has a slightly lower content of β-sheet (43%) and a higher content of α-helix (30%), when compared with the proteinase-resistant core form measured under similar conditions using FTIR (Gasset *et al.*, 1993; Pan *et al.*, 1993). A similar behavior is observed when measurements are carried out on proteins reconstituted into liposomes (Safar *et al.*, 1993*a*): the secondary structure of PrP^{Sc} in liposomes deduced from analysis of CD spectra contains 34% β-sheet, 20% α-helix, and 46% β-turn and random coil; N-terminal truncation generating PrP 27–30 gives 43% β-sheet, no α-helix, and 57% β-turn and random coil. Hence, independent of the environment, the removal of the N-terminus seems to induce a structural rearrangement in the prion protein that is accompanied by a conversion of α-helical into β-sheet secondary structure.

The polymerization of PrP 27–30 into ordered arrays offers opportunities to determine additional structural features of the scrapie isoform by X-ray diffraction. The preparation of PrP 27–30 samples is confounded by the tendency of the rods to lose morphology in water solutions (Nguyen *et al.*, 1995*b*), but samples of prion rods dried from water give circular reflections that are indexed by an orthogonal unit cell with the dimensions $a = 9.25$ Å, $b = 6.45$ Å, $c = 7.99$ Å. The relatively strong reflection at 4.63 Å is broad, indicating that only a few β-strands are hydrogen bonded to each other in this state. A very weak reflection at 8.00 Å indicates the

Fig. 2. (A) Amino acid sequence comparisons of the PrP segment 20–230 of the bovine, mouse and Syrian hamster prion proteins, with the human sequence as a reference (Schätzl *et al.*, 1995). The following color code was used to identify the known species-specific PrP^{C} epitopes: red, residues of the protein X epitope of mouse PrP involved in the human/mouse species barrier (Kaneko *et al.*, 1997*c*); cyan, residues of the PrP^{Sc} epitope of hamster PrP involved in the hamster/mouse species-barrier (Kocisko *et al.*, 1995); magenta, residues of the PrP^{Sc} epitope of mouse PrP involved in the mouse/hamster species barrier (Priola & Chesebro, 1995). (B) Alignment of the fragments 190–300 of the human, mouse, and hamster Hsp60 amino acid sequences, with the *E. coli* GroEL sequence as a reference. The residues indicated in red form the peptide binding site of GroEL (Fenton *et al.*, 1994; Buckle *et al.*, 1997; Kobayashi *et al.*, 1999; Tanaka & Fersht, 1999). At the top in (A) and (B) the locations of the regular secondary structures of human PrP and GroEL are indicated, respectively. Potential phosphorylation sites in human PrP and human Hsp60 are indicated in green (Edelman *et al.*, 1987).

intersheet spacing. Diffraction patterns obtained from prion rods in sucrose solution, which preserves the morphology of rods, show a sharp but weak spacing at 4.72 Å, and a broad intersheet band at 8.82 Å, indicating a larger domain and a uniform geometric distribution in the hydrogen bonding direction. The relatively small intersheet spacing of PrP 27–30 in prion rods argues that small side chains are involved in the β-sheet structure formation. The region of PrP between residues 113 and 124 is the only region entirely devoid of bulky aliphatic and aromatic residues (see Fig. 2A).

Discovering conditions for functional solubilization of PrP^{Sc} with retention of associated scrapie infectivity would greatly facilitate studies defining the molecular structure of the infectious particle. Unfortunately, the solubilization of PrP 27–30 in DLPC interferes with crystallization so that the use of phospholipids to solubilize scrapie proteins has not been helpful in structural studies of the prion protein. Intermediate levels of guanidine hydrochloride moderately solubilize prion aggregates (Safar *et al*., 1993*b*), but again do not permit crystallographic studies. The use of 0.2% sodium dodecyl sulfate and sonication leads to disaggregation of PrP 27–30 into non-infectious, spherical particles with a relatively homogeneous size distribution of about 10 nm (Riesner *et al*., 1996). In these studies sodium dodecyl sulfate denaturation causes prion infectivity to diminish and PrP 27–30 to become sensitive to protease digestion. More recently, biochemical studies have been initiated employing organic solvents in combination with a variety of nondenaturing detergents for solubilization of PrP 27–30 prion rods (Wille & Prusiner, 1999). Through a process of liquid-liquid extraction *via* reverse micelles and an organic phase, PrP 27–30 could be solubilized into predominantly monomers and dimers. The best conditions for production of reverse micelles turned out to be in the presence of the solvents trifluoropropanol or hexafluorophenylpropanol and the detergent dioctysulfosuccinate. Only the combination of solvents and detergents leads to a complete disappearance of rod-shaped aggregates in the electron microscope. Organic solvents alone only slightly reduce the aggregate size, and detergents alone barely change the rod shape and ultra structure. Although solubilization is not accompanied by any recognizable change in secondary structure, it unfortunately results in a loss of prion infectivity. However, examination of some negatively stained preparations of solubilized PrP 27–30 by electron microscopy revealed conditions under which PrP crystallized into two- and three-dimensional crystals (Wille & Prusiner, 1999). Formation of these crystals required uranyl salts containing acetate, formate, or nitrate. Lattice spacings of various crystal forms could be determined from electron micrographs and by electron diffraction. The PrP crystals were described as suitable for structural analysis by electron crystallography or by X-ray crystallography.

3.6 *Dissociation and stability*

Characterizing folding intermediates of PrP^{Sc} iscritical for understanding prion propagation as they are direct thermodynamic and conformational precursors of the infectious scrapie isoform. With increasing guanidine hydrochloride concentration, the turbidity, fluorescence emission maxima, and circular dichroism of PrP^{Sc} undergoes complex changes (Safar *et al*., 1993*a*). The non-overlapping midpoints of transitions from associated to dissociated states and from folded to unfolded states suggests the existence of stable intermediates with different conformational

stability of protein domains. Aggregated PrP^{Sc} dissociates initially into monomers or oligomers, designed intermediates I_1 (Safar *et al*., 1994), with substantial secondary structure, partially denatured tertiary structure, and with solvent exposed Trp residues. The transition midpoint for conversion from PrP^{Sc} to I_1 is at 1.5 M guanidine hydrochloride concentration when measured by CD spectroscopy (Safar *et al*., 1993*a*). With increasing denaturant concentration, oligomeric PrP^{Sc} unfolds to a stable intermediate I_2 with a transition midpoint at about 3.2 M guanidine hydrochloride. An additional increase in denaturant concentration causes complete unfolding of I_2 into random coil conformation. The transitions between apparent folding intermediates of PrP 27–30 are sharper than in PrP^{Sc}, and the transition midpoint for the conversion of intermediate I_2 to fully unfolded protein is shifted to a guanidine hydrochloride concentration between 4.5 and 5.5 M, suggesting a higher thermodynamic stability of the truncated scrapie isoform. The dissociation of PrP 27–30 is fully reversible up to 2.5 M guanidine hydrochloride, and the irreversible loss of infectivity at higher denaturant concentration correlates with irreversible unfolding and rapid formation of amorphous misfolded aggregates upon dilution (Safar *et al*., 1993*b*). The equilibrium intermediate I_1 of PrP 27–30 has multiple high-affinity hydrophobic binding sites for 8-anilino-1-naphthalenesulfonate (ANS), some close to the Trp residues (Safar *et al*., 1994). The far-UV circular dichroism of an acid-induced intermediate is similar to the guanidine hydrochloride-induced intermediate and suggests the presence of a molten globule-like conformation (Kuwajima, 1989) with a significant portion of α-helical and β-turn secondary structure.

An important characteristic of agents causing TSEs is their exceptional thermal resistance. Under some circumstances a portion of scrapie or CJD infectivity is heat resistant for more than one hour at 132 °C (Brown *et al.*, 1990). This heat resistance of infectivity implies reversibility of protein conformation upon thermal unfolding or a very unusual conformational heat resistance. Experiments with purified PrP 27–30 indicate no change of infectivity upon heating to 100 °C and only a minor drop upon heating to 132 °C in dehydrated thin films (Safar *et al.*, 1993*b*). During heating the secondary structure of this protein is heat-resistant in the solid state with no significant changes after exposure to 132 °C. The slightly diminished infectivity at 132 °C correlates with the formation of higher molecular weight aggregates, and is most likely explained by side chain cross-linking (Jaenicke & Rudolph, 1986). The secondary structure of PrP 27–30 apparently has the necessary thermal stability to be a carrier of infectivity, in agreement with the protein-only hypothesis.

4. The cellular prion protein PrP^{C}

4.1 *Prnp expression*

The unexpected finding by Weissmann and colleagues that mRNA transcribed from *Prnp* is present in normal and scrapie-infected brain at similar levels (Oesch *et al.*, 1985; Basler *et al*., 1986) suggested that PrP^{Sc} constitutes a posttranslationally modified isoform of a host encoded cellular precursor protein, PrP^{C}. The single-copy chromosomal *Prnp* contains a single exon and is highly conserved among mammals (Schätzl *et al*., 1995). The prion protein is synthesized with an N-terminal signal sequence that targets the protein to the endoplasmic reticulum (ER) where the peptide is removed, leaving Lys23 as the N-terminal residue (Hope *et al*., 1986; Turk

et al., 1988). At the C-terminus the *Prnp* encodes a 23 residue signal sequence for attachment of a glycosyl phosphatidylinositol (GPI) anchor on the external surface of the plasma membrane (Stahl *et al*., 1987; 1990*a*). As shown in figure 3A, the mature human protein of 208 amino acids contains two cysteine residues at position 179 and 214 forming an intramolecular disulfide bond (Turk *et al*., 1988), and two consensus acceptor sites at positions Asn181–Thr183 and Asn197–Thr199 for the addition of N-linked sugars (Fig. 2A), both of which are glycosylated at Asn in the majority of protein molecules (Endo *et al*., 1989; Haraguchi *et al*., 1989; Rogers *et al.*, 1990). Striking features of the amino acid sequence are the four adjacent octapeptide repeats PHGGGWGQ of residues 60 to 91 (Fig. 3A), with an analogues nonapeptide on the adjacent N-terminal side (positions 51 to 59), and a transmembrane region comprising residues 110 to 135 containing a completely conserved AGAAAAGA palindrome sequence (Figs. 2A and 3A). The prion protein is primarily expressed in cells of the central nervous system (Kretzschmar *et al.*, 1986) and abundantly in several peripheral tissues (Mobley *et al*., 1988; Manson *et al*., 1992). Expression regionally increases during ontogenesis, with regional differences persisting into adulthood.

Recently, a gene encoding a PrP-like protein has been discovered (Moore *et al*., 1999). The novel locus *Prnd* is 16 kb downstream of the mouse *Prnp* and encodes a 179 residue protein designed “doppel” with about 25% identity with all known prion proteins. Mouse and human Dpl proteins share 76% identity, where most of the sequence differences are conservative amino acid replacements. A comparative model based on the sequence similarity with PrP suggests that Dpl shares many structural features with PrP^{C} including an N-terminal signal sequence, a cluster of basic residues adjacent to the signal sequence, and a structured C-terminal domain containing two Asn-linked glycosylation sites and a GPI anchor attached to the C-terminus. The octapeptide repeats and the transmembrane region are missing in the doppel protein. Like the prion protein, Dpl is expressed during embryogenesis but, in contrast to PrP, it is expressed minimally in the central nervous system.

Initial studies of knockout mice deficient for functional *Prnp* were not able to clarify the biological role of the prion protein (Büeler *et al*., 1993; Collinge *et al*., 1994; Lledo *et al*., 1996). Subsequent studies with other $Prnp^{0/0}$ lines, however, suggested that PrP may play a role in the maintenance of cerebellar Purkinje neurons (Sakaguchi *et al*., 1996; Moore, 1997) and in sleep regulation (Tobler *et al*., 1996). This controversy could be explained after the discovery of the *Prn* gene structure. The two $Prnp^{0/0}$ lines which developed late-onset ataxia and Purkinje cell degeneration were found to express chimeric mRNAs derived from splicing of *Prnp* to *Prnd*, suggesting that overexpression of Dpl provokes neurodegeneration. The $Prnp^{0/0}$ lines with intact splice acceptor expressing low levels of *Prnd* mRNA do not develop dysfunction presumably because Dpl can complement functional PrP. Healthy $Prnp^{0/0}$ lines expressing mouse PrP(121–231) develop cerebellar astrophy during neonatal development (Shmerling *et al*., 1998), whereas addition of either residues 95–107 or 108–121 to the gene product renders the transgene non-lethal (Muramoto *et al*., 1997). From these findings it is tempting to speculate that the C-terminal part of PrP avidly binds to a receptor protein (e.g. Martins *et al*., 1997; Rieger *et al*., 1997), which must be activated by amino acids located within the N-terminal PrP polypeptide chain.

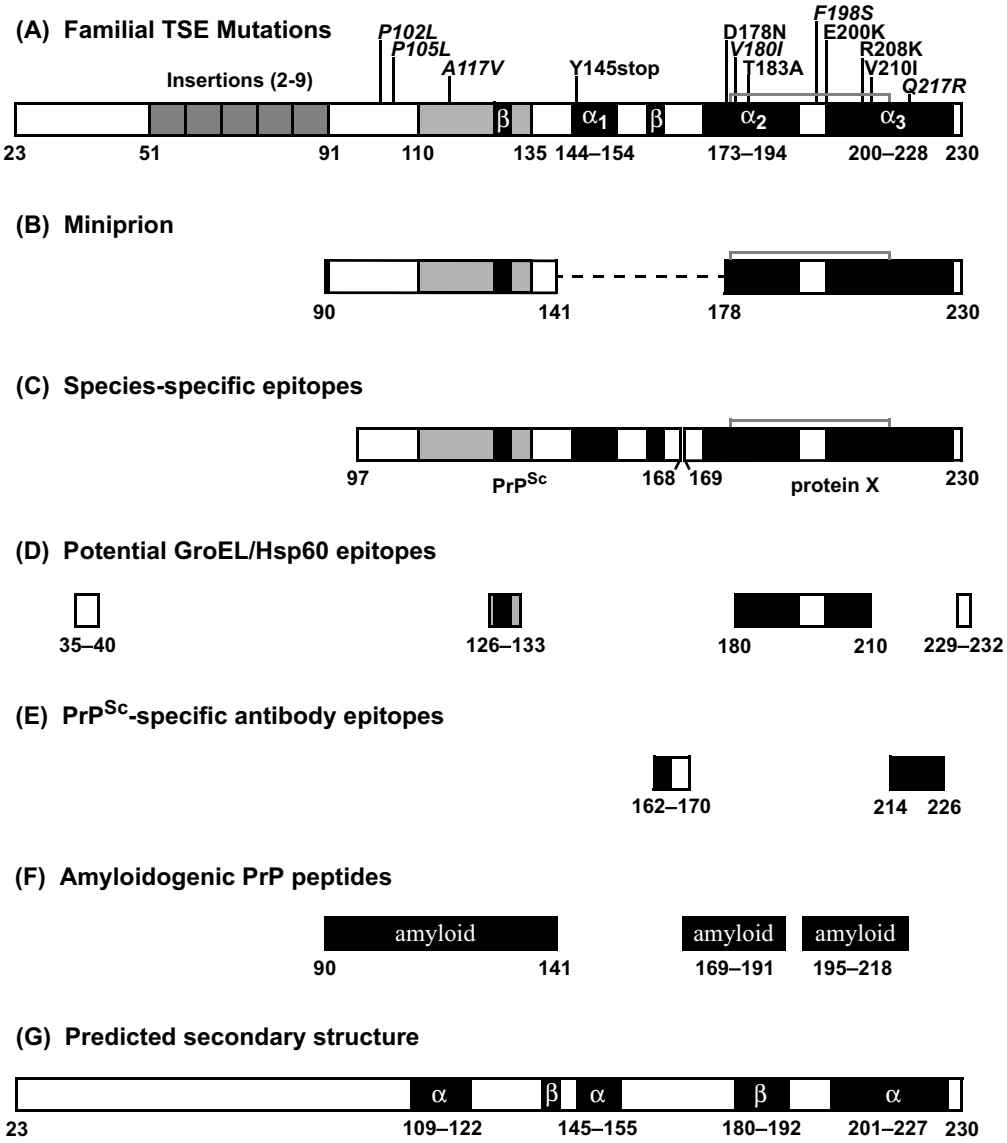

Fig. 3. (A) Primary structure of the mature human prion protein. At the top are indicated the known amino acid replacements related to inherited human prion diseases: CJD and FFI mutations in plain letters, GSS mutations in italic letters. Regular secondary structure elements are represented in black. The dark grey and light grey boxes show respectively the octapeptide repeats and the transmembrane region. The disulfide bond between Cys179 and Cys214 is indicated with a grey line. (B) Minimal PrP sequence required for prion propagation in mice and mouse neuroblastoma cell line (Fisher *et al*., 1996; Muramoto *et al*., 1996; Supattapone *et al*., 1999). Residue numbering is according to the human sequence. (C) Epitopes on PrP^{C} for binding to PrP^{Sc} (residues 97 to 168) and protein X (residues 169 to 230) as evaluated from transgenic mice experiments (Telling *et al*., 1994; 1995). Residue numbering is according to the human sequence. (D) Epitopes on PrP^{C} for binding of GroEL as determined from immunoblotting (residues 180–210; Edenhofer *et al*., 1996) or predicted from the consensus sequence of peptides binding to GroEL and Hsp60 (other segments shown; Chatellier *et al*., 1999). (E) PrP^{Sc} isoform-specific epitopes on PrP^{C} recognized by monoclonal antibody 15B3 (Korth *et al*., 1997). (F) Polypeptide regions of PrP where synthetic peptides form amyloid fibrils as indicated from electron microscopy and observation of green-gold birefringence by polarized microscopy after Congo red staining (Gasset *et al.*, 1992; Come *et al*., 1993; Forloni *et al*., 1993; Goldfarb *et al*., 1993; Selvaggini *et al*., 1993; Tagliavini *et al*., 1993; De Gioia *et al*., 1994; Kaneko *et al.*, 1995; 1997*b*; Nguyen *et al*., 1995*a*,*b*; Zhang *et al*., 1995; Heller *et al.,* 1996; Inouye & Kirschner, 1997; 1998; Pillot *et al.*, 1997; Chabry *et al*., 1998; Sharman *et al*., 1998; Liu *et al*., 1999*b*; Salmona *et al*., 1999). (G) Secondary structure prediction was performed using the hierarchal neuronal network method (Guermeur, 1997; available at http://pbil.ibcp.fr/NPSA/npsa_hnn.html).

4.2 *Biosynthetic pathway*

Biosynthesis of mammalian PrP has been studied in mouse neuroblastoma cell clones (Caughey *et al*., 1989). Biosynthetic processing begins within the lumen of the rough ER, where the GPI anchor and high mannose glycans are added to the polypeptide chain concurrent with or soon after translation and translocation, and the signal peptide is removed by a signal peptidase. Presumably during passage through the Golgi apparatus, the high-mannose glycans are processed to yield complex hybrid glycans on PrP, which is then shuttled to the plasma membrane and GPI-anchored. The transport through the rough ER and Golgi to the cell surface takes about 60 minutes, and has a half-life on the plasma membrane of approximately three to six hours (Borchelt *et al*., 1990).

Harris and colleagues have used chicken (ch) PrP as a model system to demonstrate that PrP is constitutively endocytosed from the plasma membrane and recycles back to the cell surface (Shyng *et al*., 1993; 1994; 1995). Electron microscopy and biochemical evidence suggest that chPrP is internalized *via* coated pits when expressed in cultured neuroblastoma cells: immunogold-labeled particles can be seen in coated vesicles and deeply invaginated coated pits that are in the progress of pinching off from the plasma membrane. Internalization of chPrP is blocked by incubation of cells in hypertonic medium, a treatment which causes inhibition of clathrin-mediated endocytosis. The half-time for cycling of chPrP between plasma membrane and the endosome is about 60 minutes, and at steady-state the protein is equally divided between surface and internal compartments (Shyng *et al*., 1993). More than 95% of the molecules returning to the cell surface after one cycle are intact, but the remainder are intracellularly cleaved between residues Thr114 and Met137, corresponding to residues Thr107 and Met129 in the human protein (Fig. 2A). Interestingly, the cleavage site is located in the transmembrane region of PrP, where amino acid sequences are largely identical in the chicken and mammalian prion protein. Because chPrP lacks a cytoplasmic domain and thus cannot interact directly with components of the clathrin coat, Shyng *et al*. (1994) proposed a model according to which the polypeptide chain of chPrP binds to the extracellular domain of a transmembrane protein that contains a coated pit localization signal in its cytoplasmic domain. Investigation of structural features of the chPrP molecule revealed that sequences in the N-terminal half are essential for this process (Shyng *et al*., 1995). Progressive deletions between residues 25 and 91 of chPrP caused graded reductions of internalization and concentration in coated pits. Furthermore, two deletions within the hexapeptide region NPGYPH corresponding to the octapeptide repeat region in mammalian PrP, and one within the conserved segment comprising residues 117 to 135 are about equally effective in reducing endocytosis. The fact that mouse PrP, as well as two mouse/chicken chimeras, are internalized as efficiently as chPrP, argues that conserved structural features are involved in interaction with the endocytic machinery.

On the other hand there is evidence that endogenous PrP^{C} is associated with detergent-insoluble membrane domains generally rich in cholesterol, glycosphingolipids, and GPI-anchored protein, termed caveolae, originally identified with electron microscopy as flask-shaped membrane invaginations 50 to 100 nm in diameter on the surface of endothelial and epithelial cells (Anderson, 1998). The striped coats that characterize caveolae are easily distinguished from the polygonal lattices of clathrin-coated pits under the electron microscope.

Subsequent studies of endothelial cells suggested that the caveolae form plasmalemmal vesicles that move across the cell during transcytosis. Recently, caveolae have been identified as the vehicle for receptor-mediated internalization of small molecules and proteins by a process called potocytosis (Anderson *et al*., 1992). Potocytosis and receptor-mediated endocytosis are parallel, but not redundant, endocytic pathways, with caveolae and clathrin-coated pits being specialized to internalize different types of molecules (Anderson, 1998). GPI anchored PrP^C has been localized to invaginated caveolae in both fibroblasts and neuronal cells (Ying *et al*., 1992) and has been demonstrated to fractionate with caveolae and its marker protein caveolin during purification (Harmey *et al*., 1995; Vey *et al*., 1996; Naslavsky *et al*., 1997; Wu *et al*., 1997), although caveolae have not been found in cultured neuroblastoma cells (Shyng *et al*., 1994).

4.3 *NMR structures*

Considering that the protein-only hypothesis suggests a change of protein conformation as a possible cause of the onset of TSEs, the three-dimensional prion protein structures have attracted keen interest. So far, nuclear magnetic resonance solution studies have been described for monomeric forms of recombinant PrP of the two most widely used laboratory animals in prion research, the mouse (m) and the Syrian hamster (sh), using the constructs mPrP(121–231) (Riek *et al*., 1996; 1998), shPrP(90–231) (James *et al*., 1997; Liu *et al*., 1999*a*), mPrP(23–231) (Riek *et al*. 1997) and shPrP(29–231) (Donne *et al*., 1997). Both of these prion proteins contain a globular domain that extends approximately from residues 125–228, and an N-terminal flexibly disordered "tail". The globular domain contains a short two-stranded anti-parallel β-sheet and three α-helices. Because of the similarity in secondary structure of recombinant PrP when compared with native PrP^C purified from brain tissue, which contains 42% α-helical and only 3% β-sheet when measured by FTIR or CD (Meyer *et al*., 1986), the recombinant PrP most probably resembles the PrP^C isoform. The extensive sequence homology (Schätzl *et al*, 1995) indicates that the mammalian prion proteins should all have a common polypeptide fold.

Recently, our lab determined the NMR structures of the intact recombinant human prion protein, hPrP(23–230), and the two C-terminal fragments hPrP(90–230) and hPrP(121–230) to provide a direct basis for future structure–function arguments on human prion protein (Zahn *et al*., 2000). The NMR structure of hPrP(23–230) contains a globular domain that extends approximately from residues 125–228, a flexibly extended N-terminal tail of residues 23–124, and a short flexible C-terminal segment consisting of residues 229–230 (Fig. 4), which is similar to the previously described structural models of mPrP(23–231) and shPrP(29–231). The flexibly disordered tail occurs in all prion protein constructs characterized so far and is qualitatively manifested in the small dispersion of the ^1H chemical shifts and negative values of the $^{15}N\{^1H\}$-heteronuclear Overhauser enhancements for residues 23–124, as described in detail for mPrP(23–231) (Riek *et al*., 1997). This contrasts with the corresponding parameters for the residues 125–228, which have values typical for a globular folded domain. A superposition for best fit of the backbone atoms N, C^α and C' of residues 125–228 of hPrP(23–230), hPrP(90–230) and hPrP(121–230) shows that the three-dimensional structure of the domain in the intact protein is very similar to that in the two C-terminal fragments (Fig. 5). The regular secondary structure elements coincide exactly in the three structures, with the residues 128–131 forming the first β-strand, 144–154 the first α-helix, 161–164 the second β-strand, 173–194 the second α-helix and 200–228 the third α-helix (Fig. 4). There is a

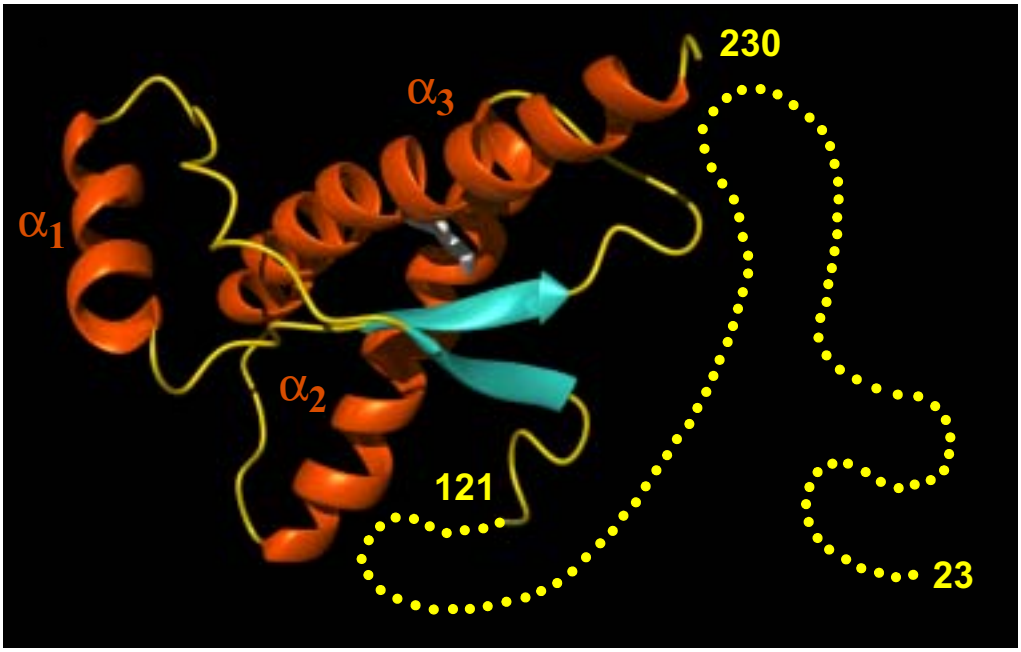

Fig. 4. Ribbon diagram of the three-dimensional structure of the intact human prion protein, hPrP(23–230). Helices are orange, β-strands cyan, segments with non-regular secondary structure within the C-terminal domain yellow, and the flexibly disordered tail of residues 23–121 is represented by yellow dots. Reproduced with permission from Zahn *et al*. (2000).

hydrogen bond from the amide proton of Met134 to the carbonyl oxygen of Asn159, which is reminiscent of an irregular, β-bulge-type elongation of the β-sheet toward helix 1. The three proteins have nearly identical side chain conformations for the hydrophobic amino acids and the single disulfide bond Cys179–Cys214, and in all three proteins most of the regular secondary structures are well defined, with small backbone displacements. Increased disorder is seen in the loop of residues 167–171 between β-strand 2 and helix 2, at the end of helix 2 and the following loop, and for the last two turns of helix 3 (Fig. 5), where the reduced precision of the structure determination of the polypeptide segment 167–171 seems to arise from slow exchange between two or more polypeptide backbone conformations in the millisecond time-scale. The local conformational state of the polypeptide segments 187–193 in helix 2 and 219–226 in helix 3 is measurably influenced by the length of the N-terminus. Since identical patterns of $^{13}C^{\alpha}$ shifts were obtained at three different protein concentrations between 0.l and 1 mM, we concluded that the observed variations are due to transient intramolecular interactions of the globular domain with the flexible tail (Fig. 4). The interaction sites coincide with the aforementioned disordered ends of the helices 2 and 3, which appear to be slightly stabilized in the presence of the intact tail, leading to an increase in helix population amounting to a few percent.

4.4 *Copper binding*

The octapeptide repeat region is among the most conserved parts of PrP in mammals, implying some functional and structural roles for the octapeptides. As early as 1992 it was suggested that

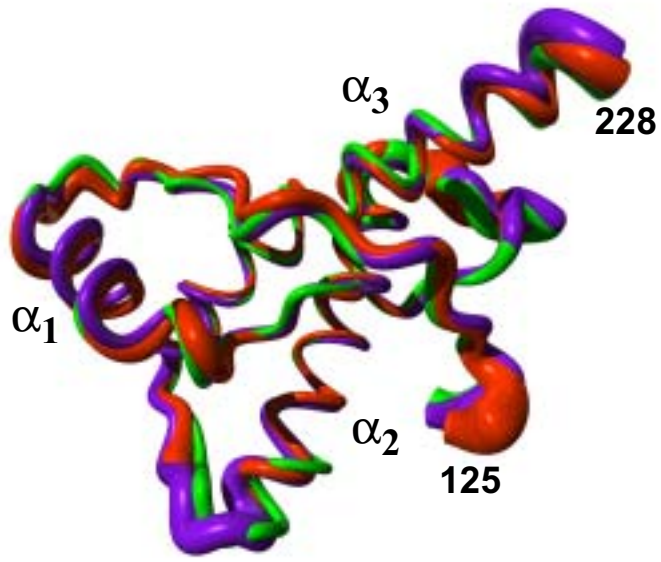

Fig. 5. Comparison of the mean NMR structures of the polypeptide segments comprising residues 125 to 228 for hPrP(23–230) (green), hPrP(90–230) (orange) and hPrP(121–230) (violet). A spline function is drawn through the C^{α} positions. The variable radius of the cylindrical rods is proportional to the mean global backbone displacement per residue (Billeter *et al*., 1989), as evaluated after superposition for best fit of the atoms N, C^{α} and C′ of the residues 125–228 in the 20 energy-minimized conformers used to represent each of the three solution structures. Reproduced with permission from Zahn *et al*. (2000).

the octapeptide repeat region, rich in His and Trp residues (Fig. 2A), may have a role in binding of metal ions (Sulkowski, 1992). In fact, a copper-chelated affinity column was essential for the purification of intact PrP^{C} (Pan *et al.*, 1992). Mass spectrometry initially showed that the octapeptide repeat provides a specific binding site for divalent metal ions, preferentially binding Cu(II) (Hornshaw *et al.*, 1995), and peptides from the analogous hexapeptide region of chicken PrP showed similar specificity for copper. The binding mode of Cu(II) to a number of PrP fragments in the octapeptide region has been studied using a combination of spectroscopic techniques (Viles *et al*., 1999). Visible absorption, visible CD, and electron spin resonance spectra suggest that the coordination sphere of the copper is identical for two, three, or four octapeptide peptide repeats, consisting of a square-planar geometry with three nitrogen ligands and one oxygen ligand. Proton NMR spectroscopy indicates that the histidine residues in each octapeptide are coordinated to the Cu(II) ion. These data are consistent with a model for the structure of the Cu(II) complex showing the four histidine residues in successive octapeptide repeats bridged between two copper ions, with both the $N^{\varepsilon 2}$ and $N^{\delta 1}$ imidazole nitrogen of each histidine residue coordinated and the remaining coordination sites occupied by a backbone amide nitrogen and water molecule (Viles *et al*., 1999). This structural model is not consistent with Raman spectroscopy studies suggesting that metal binding induces formation of α-helical structure (Miura *et al*., 1996), but is reminiscent of the structure of other copper binding enzymes (Parge *et al.*, 1992). The pH-dependent binding of copper to histidine explains the disagreement in the literature as to the number of Cu(II) ions that bind PrP^{C} with high affinity (Brown *et al*., 1997*a*; Stöckel *et al*., 1998): four copper ions bind tightly to the octapeptide region at pH 7.4 with a dissociation constant in the micro molar range; protonation of one or

more imidazoles at pH values between 7.4 and 6.0 decreases the number of effective binding sites; below pH 6, copper does not tightly bind to the cellular prion protein.

Total Cu(II) concentration is estimated in human serum at 16 to 20 μM, between 0.5 to 2.5 μM in the cerebrospinal fluid, and 15 μM in the synaptic cleft (Hartter *et al*., 1988; Linder, 1991). Although the precise free copper concentration in the brain is not known, it seems likely that PrP^C could be copper-complexed *in vivo*. Knockout mice deficient in PrP^C have been reported to exhibit more than ten-fold reductions in the copper content of membrane-enriched brain extracts relative to wild-type mice and similar reductions in synaptosomal and endosome-enriched subcellular fractions (Brown *et al*., 1997*a*). They also showed altered cellular phenotypes, including a reduction in the activity of copper/zinc superoxide dismutase (SOD) and altered electrophysical responses in the presence of excess copper. The opposite is true for SOD from transgenic mice that overexpress PrP^C (Brown & Besinger, 1998). This is in agreement with results obtained with neurons cultured from $Prnp^{0/0}$ mice which display increased sensitivity to oxidative stress, because of reduced SOD activity (Brown *et al*., 1997*c*). Moreover, PC12 cells selected for resistance to copper toxicity have increased expression of PrP^C (Brown *et al.*, 1997*b*). These data argue that PrP^C expression is important for cellular resistance to oxidative stress and may regulate SOD activity by influencing copper incorporation into the SOD molecule. In fact, recent experiments have shown that mouse PrP^C, either as recombinant protein or immunoprecipitated from brain tissue, has an intrinsic SOD activity, which is abolished by deletion of the octapeptide repeat region (Brown *et al*., 1999). These results suggest that PrP^C has an enzymatic function that depends on copper incorporation, consistent with its cellular location and indicating that it has a direct role in cellular resistance to oxidative stress.

Using mouse neuroblastoma lines Pauly & Harris (1998) have demonstrated that copper ions rapidly and reversibly stimulate the constitutive endocytosis of PrP^C from the cell surface and its passage into an early endocytic compartment. Amino-terminally deleted forms of PrP^C that are missing some or all of the octapeptide repeats are less efficiently endocytosed than the intact protein in response to extracellular copper. This effect together with the established affinity of the octapeptide repeat for copper suggests the hypothesis that PrP^C could serve as a recycling receptor for uptake of copper ions from the extracellular milieu (Pauly & Harris, 1998). PrP^C might bind copper ions on the cell surface and then deliver them to an endocytic compartment within which the bound ions dissociate because of an acidic environment (Viles *et al*., 1999). Stimulation of endocytosis might be triggered by a conformational change in PrP^C upon copper binding, leading to an increase in affinity for the putative endocytic receptor that localizes PrP^C in clathrin-coated pits (Harris *et al.*, 1996; see also section 4.2). Finally, the dissociated ions may be transferred to other copper-carrier proteins that move the ions into the cytosol where they interact with cytoplasmic SOD and other enzymes.

5. Post-translational PrP conversion

5.1 *Conformational isoforms*

When comparing the biophysical and biochemical properties of PrP^C and PrP^{Sc} as described in the two previous sections, some major differences between the two isoforms can be

summarized: (*i*) PrP^{Sc} has a high content of β-sheet secondary structure, whereas PrP^{C} has a high α-helix content and only very little β-sheet secondary structure; (*ii*) PrP^{Sc} is insoluble in detergents, while PrP^{C} is readily solubilized under nondenaturing conditions; (*iii*) PrP^{Sc} is partially hydrolyzed by proteases to form a fragment designed PrP 27–30, while PrP^{C} is completely degraded under the same conditions; and (*iv*) PrP^{Sc} accumulates *in vivo*, while PrP^{C} turns over rapidly. All these isoform-specific properties can be fully explained by a change in protein conformation, suggesting that the key event in prion disease is a conformational change from the host protein PrP with mainly α-helical secondary structure into a new protein conformation, where some of the α-helices convert to β-sheets. Whether the change in PrP conformation is triggered by covalent posttranslational modifications has been studied in detail over the last fifteen years or so and will be discussed in the following.

An intramolecular disulfide bond connecting Cys179 and Cys214 is formed in both PrP isoforms (Turk *et al*., 1988), suggesting that reduction of the two cysteine residues within mature PrP is not necessary for PrP^{C} to PrP^{Sc} conversion. The effect of disulfide bond reduction on the efficiency of conversion has been examined in cell-free system (Herrmann & Caughey, 1998). In the *in vitro* conversion assay (Kocisko *et al.*, 1994) the PrP^{Sc} is partially denatured in 3 M guanidine hydrochloride, before adding in fifty-fold excess over metabolically labeled ^{35}S-PrP^{C} at a 1 M final guanidine hydrochloride final concentration. Under these conditions PrP^{C} is converted into PrP-res, a PrP isoform resistant to limited PK proteolysis. The products of cell-free conversion reactions have not yet been proven to be infectious (Hill *et al*., 1999), because there are major technical difficulties associated with such an analysis (Horiuchi & Caughey, 1999*b*). In any case, the species and strain specificities of the cell-free conversion reactions as described in sections 5.4 and 5.5 argue that this experimental system is relevant to prion research. The addition of the disulfide reducing agent dithiothreitol inhibits the conversion reaction resulting in half the amount of converted material at a concentration of 2 to 2.5 mM. Separate pretreatment of either PrP^{C} or PrP^{Sc} with dithiothreitol and an alkylating agent to prevent reoxidation also inhibits the conversion, indicating that preservation of the disulfide bond in both isoforms is important. Further support for this view is derived from the mutation C178A which prevents the formation of PrP^{Sc} in ScN_2a cells (Muramoto *et al*., 1996). On the other hand, the treatment of protein fractions enriched for scrapie infectivity with either 2% mercaptoethanol or 100 mM dithiothreitol does not diminish prion titers (Prusiner *et al*., 1980). Thus a consistent explanation for these data is that a successful conversion requires that the disulfide bond in PrP^{C} is retained during conformational change into PrP^{Sc}, resulting in a disulfide bond which is very resistance to reduction.

There are unidentified modifications at Arg25 and Arg37 in PrP^{Sc} based on absent or novel signals at the corresponding Edman cycles (Hope *et al*., 1988; Turk *et al*., 1988). It seems doubtful that these putative arginine modifications are important for conversion since PrP lacking the segment 32–80 is susceptible for prion propagation and allows efficient prion replication (Fisher *et al*., 1996). Moreover, an absent signal in the Edman cycle of Arg25 has also been observed for the PrP^{C} isoform (Turk *et al*., 1988). Another possible chemical modification of amino acid side chains is the deamidation, isomerization, and racemization of asparaginyl and aspartyl residues in proteins. The major products of these reactions are the normal L-aspartate and the abnormal L-isoaspartate, with D-aspartate and D-isoaspartate being formed to a lesser extent (Geiger & Clarke, 1987). Interestingly, abnormal aspartyl residues

appear to be the predominant isoform found in β-amyloid peptides, isolated from the brains of Alzheimer's disease victims (Roher *et al*., 1993*a*,*b*). However, for PrP^{Sc} it has been shown that the levels of altered aspartyl residues detected are low (Weber *et al*., 1998). It thus seems unlikely that the conversion to PrP^{Sc} is due to the stoichiometric accumulation of isoaspartyl residues in the PrP^{C}polypeptide chain.

Several experiments suggest that the N-linked carbohydrate, although constituting up to 20% of the mass of the PrP molecule, does not play a pivotal role in the PrP^{Sc} formation (Butler *et al*., 1988; Taraboulos *et al.*, 1990*a*). For example, removal of the two Asn-linked glycosylation sites by *in situ* mutagenesis similarly results in the syntheses of a PK-resistant and detergent-insoluble unglycosylated PrP species in ScN_2a cells (Taraboulos *et al.*, 1990*a*). It was found that PrP^{Sc} is produced more rapidly when the scrapie-infected cells are treated with tunicamycin, an inhibitor of *N*-acetylglucosamine transferases. Several investigators have observed that PrP^{Sc} synthesized in scrapie-infected cells displays a preponderance of lower molecular weight glycoforms (see Caughey & Raymond, 1991; Tatzelt *et al*., 1996), suggesting that less glycosylated molecules may be preferred substrates in the generation of the PrP^{Sc} isoform. This interpretation is consistent with studies on the efficient *in vitro* conversion of unglycosylated PrP^{C} in the cell-free system (Kocisko *et al*., 1994). Finally, an inherited form of spongiform encephalopathy has recently been described in a Brazilian family with an Thr to Ala substitution at residue 183 (Nitrini *et al*., 1997), which abolishes one of the consensus sites for glycosylation.

A GPI anchor is attached to the C-terminus of both PrP isoforms, but these differ in their ability to be released from cellular membranes by phospholipase (Caughey *et al.*, 1990; Stahl *et al*., 1987; 1990*b*). The polypeptide backbone of PrP^{C} appears not to span the plasma membrane bilayer, since the protein can be released from the membrane solely by phosphatidylinositol phospholipase C (PIPLC). Using membranes isolated from scrapie-infected hamster brains, however, the PrP^{Sc} isoform is resistant to release, whereas purified denatured PrP^{Sc} is sensitive to digestion with phospholipase (Stahl *et al*., 1990*b*). The most likely explanation for this difference is that oligomerization of membrane-bound PrP^{Sc} prevents access of PIPLC to the carboxy terminus (Narwa & Harris, 1999). Approximately 15% of purified PrP^{Sc} molecules are truncated at the C-terminus resulting in loss of the tripeptide Gly228–Arg229–Arg230 (Stahl *et al*., 1990*a*), and there is also spontaneous release of PrP^{C} from cultured cells with a half-time of five hours accounting for 10% of the total immunoprecipitated PrP^{C} (Borchelt *et al*., 1990; 1993). Thus, although both isoforms display similar chemical posttranslational modifications introduced at the C-terminus, the complex structures of the glycolipids within the GPI anchor provide ample possibility for variation between the two isoforms. Nevertheless, neither these nor other covalent modifications have been shown to originate the conformational change in PrP (Stahl et *al*., 1993).

5.2 *Location of propagation*

The subcellular location of the molecular events underlying the post-translational conversion of the prion protein have been investigated preferentially in cultured cells. In ScN_2a cells bearing an efficient expression vector for epitope-tagged prion protein (Scott *et al*., 1992), about one third of expressed PrP polypeptide chains acquire protease resistance and are found to primarily

accumulate in the perinuclear Golgi region (Caughey *et al*., 1990; Taraboulos *et al.*, 1990*b*). No differences in biosynthesis of PrP^{C} are observed between uninfected *versus* scrapie-infected cells, indicating that scrapie infection does not modify PrP biosynthesis (Caughey *et al*., 1989). Synthesis and degradation of PrP^{Sc} are much slower when compared with PrP^{C}, with half-times for turnover of 15 hours and more than 24 hours, respectively (Borchelt *et al*., 1990). Because the PrP^{Sc} precursor is located at least transiently on the cell surface (Caughey & Raymond, 1991), the intracellular accumulation of PrP^{Sc} must result from the internalization of PrP^{Sc} or its precursor from the plasma membrane rather than the retention of PrP^{Sc} in the Golgi apparatus during biosynthesis. Assigning the plasma membrane as the subcellular location of PrP^{Sc} propagation is consistent with the finding that C-terminal truncation that deletes the signal sequence for GPI anchor also substantially reduces PrP^{Sc} formation (Rogers *et al*., 1993). Moreover, release of PrP^{C} molecules from the surface of cultured cells by PIPLC digestion prevents PrP^{Sc} formation (Caughey *et al*., 1991*b*; Borchelt *et al*., 1992).

From the localization of PrP^{C} to caveolae described in the section 4.2 and finding that PrP^{Sc} formation is inhibited by lovastatin, which diminishes cellular cholesterol levels, it was suggested that glycosphingolipid- and cholesterol-rich caveolae-like domains (CLDs) might be the site where prions are propagated (Taraboulos *et al*., 1995; Vey *et al.*, 1996). Like caveolae, CLDs contain detergent-insoluble domains enriched for GPI-anchored proteins, but unlike caveolae do not depend on the marker protein caveolin. The increase in formation of PrP^{Sc} after depletion of sphingolipid in neuroblastoma cells infected with prion further supports that propagation of the scrapie isoform requires targeting of GPI anchored protein to CLDs of the plasma membrane (Naslavsky *et al.*, 1999), before it accumulates within them as well as in lysosomes (Gorodinsky & Harris, 1995). Whether conversion takes place in raft-like membranous domains or in coated invaginations of plasma membranes and by which mechanism CLDs regulate formation of PrP^{Sc} remains to be established. One possibility is that rafts provide a physical platform that laterally concentrate PrP^{C} substrate and PrP^{Sc} template within cellular membranes (Naslavsky *et al.*, 1997), thereby enhancing the opportunity of these molecules to interact.

Based on the finding that PrP^{C} is continuously internalized into endosomes, it is also possible that formation of PrP^{Sc} may occur in endosome-like organelles, where the pH varies between 4.7 and 5.8 (Lee *et al*., 1996). This view is supported by biochemical and immunogold electron microscopy studies of scrapie-infected mouse brain, indicating that PrP^{Sc} is enriched in subcellular structures containing endosome-specific proteins (Arnold *et al*., 1995) and is localized to an internal vesicular compartment largely constituted of secondary lysosomes (McKinley *et al*., 1991*b*). The fact that PrP^{Sc} is truncated at the N-terminus by leupeptin- and ammonium chloride-sensitive proteases provides further evidence that PrP^{Sc} follows the endocytic pathway to the lysosomes (Caughey *et al*., 1991*b*). Since PrP^{Sc} is not completely degraded in the lysosomes, its conversion to the proteinase-resistant state confirms that conversion must occur prior to its exposure to proteases within endolysosomes and secondary lysosomes. However, contracting these data, redirection of PrP^{C} in ScN_2a cells to clathrin-coated pits by C-terminal fusion of transmembrane segments prevents PrP^{Sc} formation (Kaneko *et al*., 1997*a*).

5.3 *Minimal PrP sequence*

Truncation of residues 23 to 88 comprising the N-terminus of mature prion protein does not prevent PrP^{Sc} synthesis in ScN_2a cells (Roger *et al*., 1993), indicating that more than one third of the amino acids in PrP^{C} including the octapeptide repeat region is not required for prion propagation (Fig. 3A). Further mapping of polypeptide regions revealed that additional deletion of the segments 95–107, 108–121, 122–140, 177–200, and 201–217, but not 141–176 does prevent prion propagation in scrapie-infected cells (Muramoto *et al*., 1996). Thus, in addition to the 66 residues at the N-terminus, 36 residues including the first α-helix and the first strand of the β-sheet can be deleted without altering PrP^{Sc} propagation (Fig. 3B). Interestingly, the remaining segments of residues 90–141 and 178–230 contain all the single point mutations in the human PrP gene leading to familial TSE as a consequence of amino acid substitution (Fig. 3A). The resulting construct of 106 amino acids, termed PrP106 or "miniprion" (Prusiner, 1998), is expressed as GPI-anchored protein on the cell surface, and its solubility is intermediate between intact PrP^{C} and PrP^{Sc} (Muramoto *et al*., 1996). Although PrP^{C} is soluble in a combination of 0.5% Triton X-100 and 0.5% deoxycholate, $PrP^{Sc}106$ is not, but becomes soluble when sarkosyl is added under conditions where intact PrP^{Sc} remains insoluble. Hence, protease-resistance in miniprions is not necessarily coupled to detergent-insolubility.

Transgenic mice studies confirmed that segments 23–88 and 141–176 do not play a critical role in the formation of PrP^{Sc}, transmissibility of prions, or pathogenesis of prion disease (Fisher *et al*., 1996; Supattapone *et al*., 1999). Prions containing intact $mPrP^{Sc}$ produce CNS dysfunction between 200 and 400 days after intracerebral inoculation in knockout mice expressing miniprions, Tg(PrP106)$Prnp^{0/0}$, while brain homogenates prepared from these mice inoculated into Tg(PrP106)$Prnp^{0/0}$ mice produce neurologic disease between 50 and 80 days later. The initial prolongation of incubation time is equivalent to the "prion species barrier" as mentioned in the introduction and further elaborated in section 5.4 and has thus been termed "prion transmission barrier" (Supattapone *et al*., 1999). When intact $mPrP^{Sc}$ is inoculated into Tg(PrP106)$Prnp^{+/0}$ mice the incubation period is significantly shortened, indicating that the products of prion replication directed by the single copy of intact mPrP are driving the production of PrP106 prion, thereby acting in *trans* to accelerate the passage across the prion transmission barrier. Presumably, the $mPrP^{Sc}$ facilitates the conversion of PrP106 by providing a source of the PrP^{Sc} template. The $PrP^{Sc}106$ purified from transgenic mice tends to form particles that resemble prion rods composed of PrP 27–30 (Supattapone *et al*., 1999). Deconvolution of FTIR spectra of transgenic $PrP^{Sc}106$ yields estimates of 27 to 31% α-helix and 36 to 37% β-sheet. Similarly, PrP106 recombinantly expressed in *E. coli* is also rich in β-sheet secondary structure, displays a partial resistance to PK digestion, is soluble at a concentration of 10 mg/ml, but forms relatively uniform spherical particles of about 9 nm in diameter.

Not all the aforementioned experiments with scrapie-infected cell cultures (Muramoto *et al*., 1996) can be repeated using the transgenic mice model system (Muramoto *et al*., 1997): the PrP transgene encoding the 122–140 deletion fails to express in transgenic mice; mice with PrP transgenes in which the segments 177–200 or 201–217 are deleted develop heritable PrP disorder that resembles neuronal storage disease, but which differs considerably from that of the prion diseases. Ultrastructurally, enlarged nerve cell bodies are filled with a proliferation of the

ER suggesting that mutant PrP may accumulate in this cellular compartment. This raises the possibility that the absence of either helix 2 or helix 3 prevents the trafficking of nascent PrP^{C} molecules from the ER into the Golgi apparatus. It is unlikely that only altered glycosylation can make PrP pathogenic, because transgenic mice expressing Syrian hamster PrPs with point mutations to block Asn-linked glycosylation do not produce any of the reported pathological findings (DeArmond *et al*., 1997).

5.4 *Prion species barrier*

One interesting phenomenon associated with TSE agents is the barrier to interspecies transmission which is manifested statistically as an increase in the incubation period between the time of infection and clinical disease. This "prion species barrier", first described more than 30 years ago (Pattison, 1965; Pattison & Jones, 1968), varies depending on the species being infected and the species from which the TSE agent stems. For instance, mouse scrapie prion can be transmitted to Syrian hamsters with an incubation time of 380 days but transmission into mice is about threefold faster (Kimberlin & Walker, 1978; Kimberlin *et al*., 1987). Conversely, hamster scrapie prion agent has a 60 day incubation period in hamsters but has not been successfully transmitted to mice (Kimberlin *et al*., 1989). After the first passage, prions reflect the sequence of the host PrP gene and not that of the PrP^{Sc} molecules in the inoculum derived from the donor (Bockman *et al*., 1987). On subsequent passage in a homologous host, the incubation time shortens to that recorded for all subsequent passages.

The development of transgenic mice for prion studies confirmed that the species barrier is due to differences in the amino acid sequence of PrP^{Sc} in the inoculum and PrP^{C} expressed in the recipient animal. Transgenic mice co-expressing shPrP inoculated with hamster scrapie prion exhibit scrapie infectivity, incubation times, and PrP amyloid plaques characteristic of hamsters (Scott *et al*., 1989). Conversely, if the same mice are inoculated with mouse scrapie prions they synthesize mouse prions and exhibit neuropathological changes similar to those in non-transgenic mice (Prusiner *et al*., 1990). Thus, when the sequence of PrP^{Sc} in the inoculum matches that of PrP^{C} expressed in the recipient mouse, a pronounced reduction in the length of the incubation time is observed. These findings argue that prion synthesis is initiated by a species-specific interaction between PrP^{Sc} in the inoculum and endogenous PrP^{C}.

Direct evidence for this concept is supported by the finding that prion species barrier can be mimicked during the *in vitro* conversion of purified PrP^{C} with partially denatured PrP^{Sc} (Kocisko *et al.*, 1994). When the reaction is performed with $shPrP^{Sc}$ and $mPrP^{C}$, little conversion to protease-resistant products is observed (Kocisko *et al.*, 1995). This result correlates with the lack of transmission of hamster scrapie to mice. In contrast, when $shPrP^{C}$ is incubated with either $mPrP^{Sc}$ or $shPrP^{Sc}$, similar amounts of protease-resistant products are generated. This result correlates with the fact that mouse scrapie can be transmitted to hamsters, albeit with a longer incubation time than when transmitted into mice. Glycosylation of the PrP^{C} isoform is not required for species specifity in the conversion reaction, implying that the PrP^{Sc} epitope of PrP^{C} does not contain glycosyl groups. Conversion experiments performed with chimeric mouse/hamster PrP indicate that the PrP^{Sc} epitope of hamster PrP^{C} includes the residues Met139, Asn155, and Asn170 (Fig. 2A). Conversely, only replacement of residue Ile138 in mouse PrP against the corresponding residue in hamster PrP at position 139 (Fig. 2A),

affects conversion efficiency in scrapie-infected neuroblastoma cells (Priola & Chesebro, 1995), indicating that PrP^{Sc} epitopes of mouse and hamster PrP^{C} have different topology or include different regions of the polypeptide chain.

5.5 *Prion strains*

Studies of scrapie in goats originally demonstrated reproducible variations in disease phenotype with the passage of "prion strains" in genetically inbred host (Pattison & Millson, 1961). Prion strains are now defined to produce a specific phenotype of prion disease as manifested by the length of incubation time, the topology of PrP^{Sc} accumulation and the distribution of pathological lesions in the brain (Fraser & Dickinson, 1968; Scott *et al*., 1997*a*). Isolation of prion strains from mink by passage to hamsters (Bessen & Marsh, 1994; Bessen *et al*., 1995) and passage of inherited human prion diseases to transgenic mice (Telling *et al*., 1996*b*) indicate that the properties of prion strains are "enciphered" in the conformation of the PrP^{Sc} isoform. For example, extracts from the brains of fatal familial insomnia (FFI) patients carrying the mutation D178N and a methionine residue at the polymorphism site 129 have been shown to transmit disease into mice expressing a chimeric human/mouse transgene, Tg(MHu2M)$Prnp^{0/0}$, about 200 days after inoculation and induce formation of a 19 kDa PrP^{Sc} protease-resistant fragment, whereas familial CJD (E200K) and spontaneous CJD produce a 21 kDa fragment. Similar protease-resistant fragments of PrP^{Sc} are found in brain extracts of FFI and familial CJD (E200K) patients, respectively (Monari *et al*., 1994), where the difference in molecular size has been shown to originate from different proteolytic cleavage sites at the amino-terminus. On second passage, Tg(MHu2M)$Prnp^{0/0}$ mice inoculated with FFI prions show an incubation time of about 130 days, while those inoculated with CJD (E200K) prions exhibit and incubation time of about 170 days, with the protease-resistant core of the two prion strains remaining unchanged (Prusiner, 1997). These data demonstrate that PrP^{Sc} molecules invariant in amino acid sequence can exist in different conformations or "strains", and argue that PrP^{Sc} acts as a template for the conversion of PrP^{C} into nascent PrP^{Sc} molecules during prion replication.

Employing a sensitive conformation-dependent immunoassay confirmed that the variation in incubation time of eight prion strains is related to the relative protease sensitivity of PrP^{Sc} and thus to conformation of prion strain (Safar *et al*., 1998). The immunoassay used is based on the observation that the immunoreactivity of PrP^{Sc}, but not PrP^{C}, with monoclonal antibody 3F4 is greatly enhanced by denaturation (Kascsak *et al*., 1987). This is because the transformation of PrP^{C} into PrP^{Sc} is accompanied by burial of epitopes involving residues 90 to 120, whereas C-terminal epitopes remain exposed (Peretz *et al*., 1997). In graphs of the ratio of antibody binding to denatured *versus* native PrP plotted as a function of the concentration of PrP^{Sc} or PrP 27–30 found in the brains of hamsters, each strain occupies a unique position, indicative of a particular PrP conformation. When the difference in concentrations of PrP^{Sc} and PrP 27–30 is plotted as a function of the incubation time, a linear relationship is found suggesting that strain-specific incubation time arises from distinct rates of PrP^{Sc} cellular degradation rather than from different rates of PrP^{Sc} formation (Prusiner *et al*., 1998).

An important marker of prion strain variation is the pattern of PrP^{Sc} glycosylation, namely the relative occurrence of diglycosylated, monoglycosylated, and unglycosylated PrP^{Sc} forms

which can be easily distinguished by gel electrophoresis (Kascsak *et al*., 1986). Variation in glycosylation pattern of PrP^{Sc} after protease digestion has been noted in strains from patients with sporadic CJD (Parchi *et al*., 1996), familial CJD (Monari *et al*., 1994), and nvCJD (Collinge *et al*., 1996). Because both nvCJD and BSE prions exhibit the same molecular size and preponderance of the doubly glycosylated isoform of PrP 27–30 molecules it has been argued that the BSE agent may have been transmitted to humans (Raymond *et al*., 1997), which is in agreement with the recent finding that Tg(BoPrP)$Prnp^{0/0}$ mice inoculated with nvCJD and BSE brain extracts exhibit indistinguishable neuropathology and incubation times (Scott *et al*., 1999). The suggestion that differences in glycosylation may actually play a causal role in the propagation of strains by targeting each prion variant to distinctive subpopulation of neurons in the brain (Hecker *et al*., 1992) is difficult to reconcile with the fact that modification of Asn-linked carbohydrates attached to PrP^{C} is completed before the PrP^{C} is distributed to the cell surface (Borchelt *et al*., 1990; Caughey & Raymond, 1991), where the conversion into PrP^{Sc} presumably takes place.

6. Effect of familial TSE mutations

Whereas the transmission of prion disorders requires direct interaction between exogenous PrP^{Sc} and endogenous PrP^{C}, the conversion process in hereditary spongiform encephalopathies appears to occur spontaneously leading to the conclusion that the characteristic mutations favor spontaneous conversion of the prion protein to the PrP^{Sc} isoform (Cohen *et al*., 1994). This view is confirmed by the spontaneous neurodegeneration of transgenic mice expressing mutations in *Prnp* (Hsiao *et al*., 1990), and the transmission of neurodegeneration by brain extracts prepared from these mice (Hsiao *et al*., 1994; Telling *et al.*, 1996*a*). Familial TSEs include one-tenth of the cases of CJD and all cases of GSS and FFI (see Prusiner & Hsiao, 1994; Parchi & Gambetti, 1995; Young *et al.*, 1999), and are all linked to dominantly inherited, germline mutations in the human *Prnp* on chromosome 20. Twelve specific point mutations and several insertions in the open reading frame of the human *Prnp* have been linked with familial TSE forms (see Fig. 3A). Eight of the single point mutations occur in the region containing helices 2 and 3 of the well structured C-terminal domain of PrP^{C}, and are associated with either CJD, GSS, or FFI. The three single point mutations in the flexibly disordered N-terminus and the amber mutation at codon 145 are linked to GSS. Insertion mutations in the octapeptide repeat region are associated with a variable phenotype that can include features of CJD or GSS, and consist of two to nine additional octapeptide segments. Initiation of sporadic disease may follow from somatic mutation and thus would follow a path similar to that for the germline mutations in inherited disease.

6.1 *Thermodynamic Stability of* PrP^{C}

Based on structural modeling of the PrP^{C} to PrP^{Sc} conversion it has been hypothesized that amino acid substitutions associated with inherited TSE disease decrease the thermodynamic stability of the PrP^{C} isoform and thus facilitate its conversion into the PrP^{Sc} isoform (Cohen *et al*., 1994; Huang *et al*., 1994; 1995). However, the three-dimensional structure of PrP^{C} shows convincingly that familial TSEs generally cannot be rationalized by the assumption of reduced

stability of the PrP^C isoform of the mutant proteins. First, three point mutations that segregate with inherited TSEs are located in the flexibly disordered polypeptide segment (Fig. 3A), where it is unlikely that individual amino acid substitutions would measurably affect the global protein stability. Second, for the eight protein species with disease-related amino acid changes in the globular C-terminal domain the three-dimensional structure predicts widely varying effects on protein stability (Fig. 6). The Glockshuber lab has separately introduced all eight TSE mutations located in the structured domain of PrP^C into recombinantly expressed mPrP(121–231) fragment (Liemann and Glockshuber, 1999). The biophysical characterization of these variants with CD spectroscopy showed that none of the mutations affect the global protein structure, indicating that these mutations do not *per se* cause a PrP^{Sc}-like conformation. Moreover, the mPrP(121–231) variants showed different degrees of destabilization of the native conformation: while amino acid replacements D178N, T183A, F198S, and Q217R considerably decrease protein stability, the stability of the other four variants and the nonpathogenic Met/Val polymorphism at position 129 remains unchanged. There is no correlation between stability of the PrP^C isoform with any particular TSE phenotype. Similar observations were made during the investigation of human PrP(90–231) variants carrying the mutations D178N and P102L associated with CJD/FFI and GSS, respectively (Swietnicki *et al*., 1998). From these results it can be concluded that other molecular mechanisms are important in facilitating the structural conversion of PrP isoforms during human TSE than changes in the thermodynamic stability of the PrP^C isoform. Such mechanisms may include a stabilizing effect of the mutation on PrP^{Sc} or its folding transition state, or an altered interaction with protein X. This view is supported by the findings that mice overexpressing a murine PrP transgene with the non-destabilizing GSS mutation P102L spontaneously develop infectious scrapie-like disease (Hsiao *et al*., 1990; 1994), whereas the slightly destabilizing E200K mutation does not cause illness (Telling *et al.*, 1996*a*). Along similarly lines the expression of murine PrP with the mutation D178N in Chinese hamster ovary (CHO) cells results in protease-resistant and detergent-insoluble protein (Lehmann & Harris, 1996*a*), whereas the same mutation expressed in transfected human neuroblastoma cell line results in protease-sensitive prion protein (Petersen *et al*., 1996).

6.2 *De novo synthesis of PrP^{Sc}*

There are differences in the steps underlying PrP^{Sc} formation when comparing infected cells and cells expressing mutant forms of the prion protein. Mouse PrP molecules carrying disease-related mutations display a number of biochemical markers characteristic of PrP^{Sc} when stably expressed in CHO cells (Lehmann & Harris, 1995; 1996*a*,*b*), but all of these biochemical markers develop with different kinetics during pulse-chase experiments (Daude *et al*., 1997). According to Harris and colleagues mutant PrPs are initially synthesised in the PrP^C isoform and then acquire the characteristics of PrP^{Sc} in a stepwise fashion during passage through various cellular compartments. The initial step takes place during translation of the PrP polypeptide chain in the ER and alters the membrane association of the PrP molecule so that it is inefficiently released by PIPLC. Phospholipase resistance is most probably the consequence of a structural change of PrP which makes the GPI anchor inaccessible to other proteins (Narwa & Harris, 1999). Since PrP^{Sc} from scrapie-infected brain and cultured cells is also inefficiently

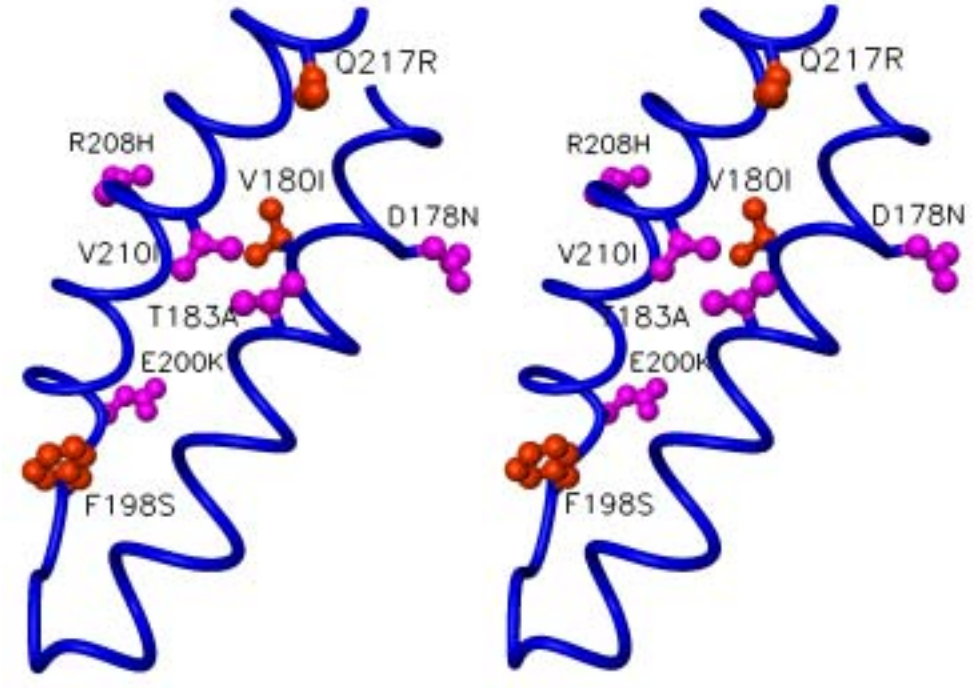

Fig. 6. Stereoview of the polypeptide segment 173–218 in the human prion protein (Zahn *et al*., 2000), where the backbone (blue) is represented as a spline function drawn through the C^{α} positions. The side chains mutated in Creutzfeldt-Jacob-Disease and Gerstmann-Sträussler-Scheinker syndrome within this segment are drawn in magenta and orange, respectively. The figure was prepared with the program MOLMOL (Koradi *et al*., 1996).

released from membranes by PIPLC as described in section 5.1, resistance to the action of phospholipase may be a general property of the scrapie isoform. The second step in the transformation of mutant PrP is acquisition of detergent insolubility, and occurs at the plasma membrane or on the endocytic pathway. The third step is acquisition of protease resistance and takes place several hours after acquisition of detergent insolubility. These results demonstrate that conversion to the PrP^{Sc} isoform may begin at an early point in the biosynthetic pathway and that acquisition of detergent insolubility and protease resistance are temporally distinct steps connected by an intermediate PrP species. The accumulation of a conversion intermediate has also been observed during studies on brains of heterozygous CJD patients carrying the E200K mutation (Gabizon *et al*., 1996).

Analysis of transfected CHO cells that express abnormally glycosylated forms of mouse PrP, generated by substitution of alanine for threonine at codon 182, which is homologous to the T183A mutation in CJD patients (see Figs. 3A and 6), blocks the delivery of the protein to the cell surface, but nevertheless displays all the aforementioned properties of PrP^{Sc} observed in this assay system (Lehmann & Harris, 1997). The intracellular compartment where the T182A mutant accumulates is likely to be proximal to the mid-Golgi stack. Most importantly, the fact that mutant PrP is converted to a PrP^{Sc}-like isoform without being expressed on the cell surface indicates that transit to the plasma membrane is not necessary for the conversion process in inherited prion disease.

In both mouse fibroblast and mouse neuroblastoma cell lines the aggregation and protease

resistance of mutant PrP increases with the number of octapeptide repeats, correlating with the finding that increasing numbers of repeats is associated with an earlier onset of familial CJD (Capellari *et al*., 1997). However, while in mouse fibroblast cells expressed PrP molecules with greater than five copies of the octapeptide repeat show increase in aggregation and protease resistance (Priola & Chesebro, 1998), in neuroblastoma cells only PrP molecules with nine or eleven copies of the octapeptide motif show an increase in aggregation and PK resistance. The different results suggest that the cell type in which PrP is expressed is an important determinant of whether or not mutant PrP acquires abnormal properties. As the addition of up to six octapeptide segments does not change the efficiency of PrP^{Sc} conversion in ScN_2a cells (Rogers *et al*., 1993), it appears that the *de novo* synthesis of prions is not accelerated in the presence of exogenous PrP^{Sc} molecules. This would be another indication that *de novo* prion synthesis and PrP^{Sc}-induced prion propagation are independent processes (Fig. 1) which take place at different locations in the cell.

The amber mutation at codon 145, which has been found in the *Prnp* of a Japanese patient who died following a prolonged GSS illness (Kitamoto *et al*., 1993), yields a truncated protein PrP^{145} that lacks the C-terminal region containing the two α-helices and concomitantly the single disulfide-bond (Fig. 3A), the two sites for *N*-glycosylation, and the GPI anchor. Yet, the heterozygous stop mutation is associated with a phenotype not basically different from that of the GSS subtypes linked to a single point mutation located C-terminal to the amber mutation (Ghetti *et al.*, 1996). In transfected human neuroblastoma cells, PrP^{145} is expressed in two forms, one of which conserves the signal peptide (Zanusso *et al*., 1999). Both forms are unstable and are rapidly degraded through the proteasomal pathway, presumably at the cytosolic face of the ER membrane. Following inhibition of proteosomal degradation, PrP^{145} accumulates primarily in the ER and Golgi in a detergent-soluble form resistant to mild PK treatment. However, none of the PrP^{145} forms were found to be bound to any of the major ER-specific chaperones.

6.3 *Transmembrane PrP forms*

Although conversion of PrP^{C} to PrP^{Sc} appears to be central to prion disease, the observation of neurodegeneration in the absence of PrP^{Sc} accumulation in some cases (see Hsiao *et al*., 1990; Telling *et al.*, 1996*a*) argues that other aspects of PrP expression, folding, or trafficking may feature in the pathophysiological mechanisms that cause disease. Studies of PrP translocation at the ER membrane revealed unusual features in biogenesis. Whereas most glycoproteins are synthesized in a single orientation with respect to the ER membrane, the PrP synthesized in cell-free translation systems is found in more than one topological form (Hay *et al*., 1987*a*,*b*; Lopez *et al*., 1990; Yost *et al*., 1990): the "normal" form is fully translocated into the ER lumen and enters the endocytic pathway, while two additional PrP forms span the ER membrane with regions of the molecule exposed to the cytosol (Hay *et al*., 1987*a*,*b*; Yost *et al*., 1990). One form, termed ^{Ctm}PrP, has the carboxy-terminus in the ER lumen and the amino-terminus located in the cytosol. The other form, termed ^{Ntm}PrP, has the amino-terminus in the ER lumen and the carboxy-terminus in the cytosol. Both transmembrane forms appear to span the membrane at the same stretch of hydrophobic amino acids comprised of residues 110 to 135 (see Figs. 2A and 3A). The distribution of newly synthesized PrP between transmembrane and secretory forms is

affected by the GSS mutation A117V in the hydrophobic segment spanning the membrane (Hsiao *et al*., 1991; Hegde *et al*., 1998). In brain tissue as well as in cell-free systems the mutation favors the synthesis of ^{Ctm}PrP over the other two topological forms, where ^{Ctm}PrP is associated with scrapie-like neuropathological changes but not with an accumulation of protease-resistant protein. These data support the hypothesis that expression of ^{Ctm}PrP may be involved in the pathological process occurring in at least a subset of heritable prion diseases. Recently, the relationship between the neurodegeneration seen in transmissible prion diseases involving PrP^{Sc} and that associated with ^{Ctm}PrP has been studied using transgenic mouse lines. It was found that the time course of PrP^{Sc} accumulation is followed closely by increased generation of ^{Ctm}PrP, suggesting that the accumulation of PrP^{Sc} modulates in *trans* the events involved in generating or metabolizing the ^{Ctm}PrP form (Hegde *et al.*, 1999). It remains to be established whether inappropriately expressed ^{Ctm}PrP is able to initiate specific signaling events to cause neuronal cell death or accomplishes this end by another mechanism.

7. Physical properties of synthetic PrP

7.1 *Amyloidogenic peptides*

Despite the lack of evidence for the spontaneous transformation of synthetic prion protein or fragments thereof into infectious PrP^{Sc}, *in vitro* experiments with synthetic components give us some knowledge about the tendency of the PrP polypeptide sequence to form β-sheet secondary structure, amyloidogenic aggregates, and protease-resistant conformations. Interestingly, all the peptide fragments of PrP which tend to form β-sheet structure have been found to concomitantly aggregate into amyloid fibrils in buffered solution at neutral or slightly acidic pH. Increased amyloid propensity has been found for peptides whose amino acid sequences correspond to segments 90–141, 169–191, and 195–218 (Fig. 3F). These correspond to regions in PrP^{C} that contain the transmembrane region including the first β-strand, and the second and third α-helix, respectively (Fig. 3A). As outlined in section 5.3 all of these regions are required for prion propagation in miniprions (Fig. 3B). The β-sheet structure formed by peptides in the region of helix 2 is in agreement with secondary structure predictions suggesting high β-sheet propensity for large parts of this polypeptide region (Fig. 3G), whereas helix 3 is predicted to have a high propensity for α-helical secondary structure. The tendency of peptides corresponding to helices 2 and 3 to form amyloid structure suggests that in PrP^{C}, α-helical structure within these segments is stabilized by the single disulfide bond and the formation of a well packed hydrophobic core. Residues outside the hydrophobic core region corresponding to helix 1 are predicted to contain high α-helix propensity (Fig. 3G), in agreement with CD and NMR studies on a polypeptide containing helix 1 of the mouse prion protein (Liu *et al*., 1999*b*).

Of the amyloid forming peptides those corresponding to the region 90 to 141 of the human PrP sequence (Fig. 3F) have been characterized in great detail. The segment 90–145 was originally chosen for peptide studies because residue 90 is the N-terminus of the infectious PrP 27–30 molecule (Prusiner *et al*., 1984) and residue 145 coincides with the amber mutation leading to familial TSE (see Fig. 3A). The conformation of PrP(90–145) depends strongly on solution conditions (Zhang *et al*., 1995): in aqueous solution and in the presence of some organic solvents, the peptide can be induced to form α-helical structures, whereas sodium

chloride in physiological concentrations or acetonitrile induce the peptide to acquire substantial β-sheet, and PK-resistant rod-shaped polymers. When mixed with PrP^{C} purified from hamster brain, PrP(90–145) produces a complex that displays some properties of PrP^{Sc}, including protease-resistance, formation of fibrous aggregates and high β-sheet content. Moreover, the efficiency of the conversion increases after introducing the A117V mutation causing GSS disease (Kaneko *et al.*, 1995; 1997*b*). Dried preparations of PrP(90–145) yield X-ray diffraction patterns similar to those obtained from PrP 27–30 prion rods, suggesting that the amyloidogenic core of PrP is closely modeled by the peptide (Nguyen *et al*., 1995*b*). A dried, magnetically oriented sample of PrP(90–145) shows a cross-β diffraction pattern in which the fiber axis is parallel to the H-bonding (Inouye & Kirschner, 1997), as has been observed in many amyloid fibrillar states of proteins and peptides (reviewed in Sunde & Blake, 1998). The most compact structure based on the X-ray diffraction analysis shows that the smaller residues of segment 109–122 fold back and are hydrogen bonded with the smaller residues of segment 129–141 (Inouye & Kirschner, 1998), indicating that perturbation of the packing environment of the highly conserved residues 109 to 141 (Fig. 2A) may be a mechanism for triggering the conversion of PrP^{C} into the PrP^{Sc} isoform.

The amino acid sequence corresponding to residues 109–122 of Syrian hamster PrP is predicted to form α-helical structure (Fig. 3G), but the corresponding peptide is highly amyloidogenic (Fig. 3F). The peptide does not have the potential to convert purified PrP^{C} into PrP^{Sc}, although it converts the α-helical secondary structure of two other peptides, 104–122 and 129–141, into β-sheet structure (Nguyen *et al*., 1995*a*). The conversion is sequence-specific since mouse PrP(109–122) is inefficient at converting human PrP(104–122) into the β-sheet form. A slightly longer peptide corresponding to residues 106–126 of human PrP forms straight fibrils similar to those extracted from brains of GSS victims, the mayor component of which is an 11 kDa fragment of PrP that spans approximately residues 58 to 150 (Tagliavini *et al*., 1991; 1993). The partially protease-resistant peptide (Selvaggini *et al.*, 1993) was reported to be toxic to cultured rat hippocampal neurons (Forloni *et al*., 1993). Apparently contradicting results were obtained recently by Kunz *et al*. (1999) who showed that the viability of these and other neuronal cell types were found not to be impaired in the presence of the same peptide under widely varied sets of conditions. In the presence of micelles formed by a 5% solution of sodium dodecyl sulfate, PrP(106–126) shows a high content of α-helix (De Gioia *et al*., 1994). However, when the peptide is dissolved in phosphate buffer and incubated with liposomes, it changes from a dominantly random coil form to a β-sheet conformation. The environment-dependent polymorphism of PrP(106–126) and its marked tendency to form β-sheet structures at acidic pH (Salmona *et al*., 1999) could be associated with an initiation of the PrP^{C} to PrP^{Sc} conversion in an endosomal-lysosomal compartment.

7.2 *Folding intermediates*

Longer portions of the PrP sequence have been expressed in bacteria (see Hornemann & Glockshuber, 1996; Mehlhorn *et al*., 1996; Zahn *et al*., 1997) and used in PrP folding studies. The amino-terminally truncated segment of the mouse prion protein comprising residues 121–231 has been shown to constitute an autonomous folding unit, whose folding and solubility does not require *N*-glycosylation (Hornemann & Glockshuber, 1996). Under non-reducing

conditions, refolding of chemically denatured mPrP(121–231) is cooperative and reversible, and follows a two-state mechanism with a free energy of about 22 kJ/mol at neutral pH. The kinetics of folding of mPrP(121–231) has been investigated by stopped-flow fluorescence using the variant F175W (Wildegger *et al*., 1999). The variant folds into the native conformation extremely rapidly, with a microscopic rate constant of about 4000 s^{-1}. The high fractional solvent accessibility of the folding transition state relative to the native state indicates that the compactness of the transition state is closer to the unfolded polypeptide than to the native protein. At acidic pH, both the mPrP(121–231) and the structured domain in human and hamster PrP(90–231) adopts an alternative conformation with spectral characteristics of a β-sheet protein (Swietnicki *et al*., 1997; Zhang *et al*., 1997; Hornemann & Glockshuber, 1998). The equilibrium unfolding intermediate of mouse PrP(121–231) is maximally populated at 3.5 M urea, and is soluble and in rapid equilibrium with the native and unfolded state (Hornemann & Glockshuber, 1998). Incubation of the human PrP(90–231) in the presence of 1 M guanidine hydrochloride results in a time-dependent transition from an α-helical to a β-sheet conformation and oligomerization into large molecular weight aggregates with increased resistance to PK digestion and a fibrillar morphology (Swietnicki *et al*., 2000).

Reduction of the single disulfide bond in human PrP(90–231) at pH 4.0 has been shown to generate a monomeric and soluble protein characterized by a strong β-sheet signal in the CD spectrum (Jackson *et al*., 1999*a*,*b*). In contrast to the aforementioned oxidized folding intermediates, reduced β-PrP is populated in the absence of denaturant. Compared to the PrP^C isoform β-PrP retains a near-UV CD signal from aromatic residues, but with diminished intensity, indicating weaker tertiary interactions. Accordingly, NMR spectra of β-PrP exhibit a low degree of chemical shift dispersion characteristic of the loss of fixed side chain orientations. The switch from β-PrP to PrP^C is reversible, and either isoform can be generated by fully denaturing or refolding at the appropriate pH. Physiological salt concentrations cause precipitation of monomeric β-PrP into irregular spherical particles that associate over several hours to form fibrils with a diameter of up to 20 nm and length of up to 500 nm. The folded β-PrP shows a marked PK resistance, with only a moderate further increase associated with aggregation. These experiments confirm the peptide studies described in the previous section suggesting that the hydrophobic packing of the disulfide bond-connected helices 2 and 3 is the mayor element in stabilizing the folding of α-helical secondary structure in the PrP^C isoform. Whether the reduced or oxidized β-sheet isoforms of recombinant PrP resemble PrP^{Sc} remains to be established.

8. Hypothetical protein X

8.1 *Two species-specific epitopes*

Experimental evidence that an additional factor, provisionally designated protein X, participates in prion propagation originally came from inoculation studies with transgenic mice expressing various PrP constructs. Tg(HuPrP)$Prnp^{+/+}$ mice expressing high levels of the human prion protein compared to endogenous mouse PrP failed to develop CNS dysfunction upon inoculation with human prions more frequently than nontransgenic controls (Telling *et al*., 1994). When the human *Prnp* was introduced into knockout mice where the mouse *Prnp* was

ablated, the resulting Tg(HuPrP)*Prnp*$^{0/0}$ mice were susceptible to human prions (Telling *et al*., 1995). These observations indicated that mouse PrP^{C} inhibits the conversion of human PrP^{C} into PrP^{Sc}, and that inhibition is abolished once mouse PrP^{C} is removed. The finding that Tg(MHu2M)*Prnp*$^{+/+}$ mice expressing a chimeric human/mouse PrP transgene are highly susceptible to human prion (Telling *et al*., 1994) confined the species barrier for transmission of human prions into mice to nine amino acids in the region corresponding to residues 97 and 168 of the human sequence (Figs. 2A and 3C). Hence, two separate segments of human PrP^{C} participate in the formation of PrP^{Sc}: the central domain delimited by residues 97 to 168 that binds to PrP^{Sc} and an additional epitope in human PrP^{C} which binds to protein X (Telling *et al*., 1995). Since the truncation of the N-terminal residues in PrP^{C} still permits the formation of PrP^{Sc} (Rogers *et al*., 1993; Fischer *et al*., 1996), the binding site for protein X was confined to the C-terminal segment comprising residues 169 to 230 (Fig. 3C). Like the binding of PrP^{C} to PrP^{Sc} (Prusiner *et al*., 1990), the binding of PrP^{C} to protein X has been postulated to be most efficient when these proteins are from the same species. An alternative interpretation of the transgenic mice studies would be that mouse PrP^{C} inhibits the conversion by either binding to human PrP^{Sc} or PrP^{C} with high affinity, but such a scenario would be in contrast to the finding that homotypic interactions govern the conversion (Prusiner *et al*., 1990; Scott *et al*., 1993), rather than heterologous interactions.

Similar experiments (Scott *et al.*, 1997*b*) have been repeated with mice expressing a chimeric bovine/mouse PrP transgene, Tg(MBo2M)*Prnp*$^{0/0}$, resulting in eight bovine substitutions in mouse PrP corresponding to human PrP residues 97, 109, 138, 143, 145, 155, 184 and 186 (Fig. 2A). Interestingly, while Tg(BoPrP)*Prnp*$^{0/0}$ mice expressing bovine PrP were susceptible to BSE prions, Tg(MBo2M)*Prnp*$^{0/0}$ mice were found to be resistant. When considering the differences in amino acid sequence between human, bovine, and mouse PrP within residues 187 to 230 (Fig. 2A), it is tempting to speculate from these results that the replacement I203V considerably changes affinity of the chimeric PrP^{C} for BSE prion. On the basis of these experiments it has been suggested that residue 203 together with residues 184, 186 and 205 are involved in a second PrP^{Sc} subepitope.

More recently, data from *in vitro* conversion experiments have been presented in favor of protein X participating in prion propagation (Saborio *et al*., 1999). In these experiments the efficiency of conversion from PrP^{C} into protease-resistant PrP-res was enhanced when using a cell lysate from transfected CHO cells as a source of PrP^{C} instead of purified protein (Kocisko *et al.*, 1994; see also section 5.1). When the PrP^{C} in the cell lysate was purified by affinity chromatography to yield 60 to 70% purified protein (Cashman *et al*., 1990), no protease-resistant protein could be detected any more, but conversion into PrP-res was recovered when a PrP^{C}-depleted fraction of the cell lysate was added. Furthermore, the use of cell lysate reduced the molar excess of PrP^{Sc} over PrP^{C} required to achieve formation of PrP-res (Kocisko *et al.*, 1994) from 50 to 10, and no denaturation of PrP^{Sc} was necessary to achieve conversion as was with purified PrP^{C}. In fact, the pretreatment of the PrP^{Sc} sample with 2 M guanidine hydrochloride diminished the conversion efficiency. Yet, an unknown factor in the cell lysate is required for conversion which might be identical with protein X as postulated from the transgenic mice experiments.

8.2 *Mapping the protein X epitope*

It has been known since the structure determination of mPrP(121–231) that the molecular surface of the potential protein X epitope is formed by two polypeptide segments with low homology among different species, which are close in the three-dimensional structure (Billeter *et al.*, 1997). The two segments of helix 3 and the loop between β-strand 2 and helix 2 (see Fig. 4) are characterized by significant alterations of the electrostatic surface potential among different mammalian species (Fig. 2A): human PrP differs from bovine and mouse PrP in the replacement of the glutamine residues 168 and 219 by glutamic acid residues, as well as by conservative substitutions at positions 166, 215, and 220. Studies with scrapie-infected neuroblastoma cells transfected with a chimeric human/mouse *Prnp* confirmed that single amino acid replacements in the area of the protein X epitope affect the efficiency with which recombinant PrP is converted into PrP^{Sc} (Kaneko *et al.*, 1997*c*). Substitution of residues 168, 215 or 219 with the corresponding residues in human PrP (see Fig. 2A), but not at position 220, diminishes or prevents conversion to PrP^{Sc} in the recombinant construct. The relative affinities of mutant and wild-type protein for protein X were determined by co-transfection studies of mutant and wild-type PrP, which showed that substitution of a basic residue for glutamines occurring at positions 168, 172, or 219 inhibits conversion of both mutant and wild-type PrP owing to the failure of the mutated PrP^{C} to release protein X. Conversely, exchange of glutamines 168 or 219 against glutamic acid prevented conversion of mutant PrP but allowed conversion of wild-type PrP, presumably by weakening mutant PrP^{C}–protein X binding. Based on these data a model has been proposed suggesting that the conversion of PrP^{C} into PrP^{Sc} occurs in a protein X/PrP^{C}/PrP^{Sc} triple complex (Prusiner *et al.*, 1998). However, the fact that residue 168 co-participates in the PrP^{Sc} epitope of PrP^{C} (Fig. 3C) indicates that PrP^{C} presumably binds subsequently to protein X and PrP^{Sc}.

There is an intriguing coincidence between the location of the binding epitope of the putative protein X and the location of the species variations observed when comparing the three-dimensional structures of human, mouse, and hamster PrP^{C} C-terminal domain (Zahn *et al.*, 2000). Although the NMR structures within the C-terminal domain are very similar, local differences between the backbone conformations of the three proteins are manifested in helix 3 and the nearby loop between the β-strand 2 and helix 2. In mouse PrP the helix 3 ends at residue 219, and after a "kink" in the segment 219–222 (Figs. 4 and 7) the chain forms a helix-like turn (Riek *et al.*, 1998). In contrast, a straight, mostly regular α-helix is observed in hPrP (Fig. 7) and shPrP (Liu *et al.*, 1999*a*). Helix 3 in hPrP contains a nearly continuous pattern of medium-range nuclear Overhauser enhancement (NOE) cross peaks $d_{\alpha N}(i, i+3)$ and $d_{\alpha\beta}(i, i+3)$ for the residues 217 to 221 (Fig. 7). Only Tyr218 is missing a medium-range NOE cross peak. In mPrP(121–231) the corresponding medium-range NOE cross peaks are either absent or correspond to distances larger than 5 Å, so that the polypeptide chain is not restricted to form an α-helical secondary structure for the residues 220 to 224 (Wüthrich, 1986). The loop 167–171 between the β-strand 2 and helix 2 has been reported to be well defined in shPrP(90–231), where complete resonance assignments could be obtained for this segment (James *et al.*, 1997; Liu *et al.*, 1999*a*). For hPrP and mPrP some resonances of the loop have not been observed, either at pH 4.5 or at pH 7.0, and due to the resulting scarcity of conformational constraints the structure of this peptide segment is not precisely defined (Fig. 5). To gain more

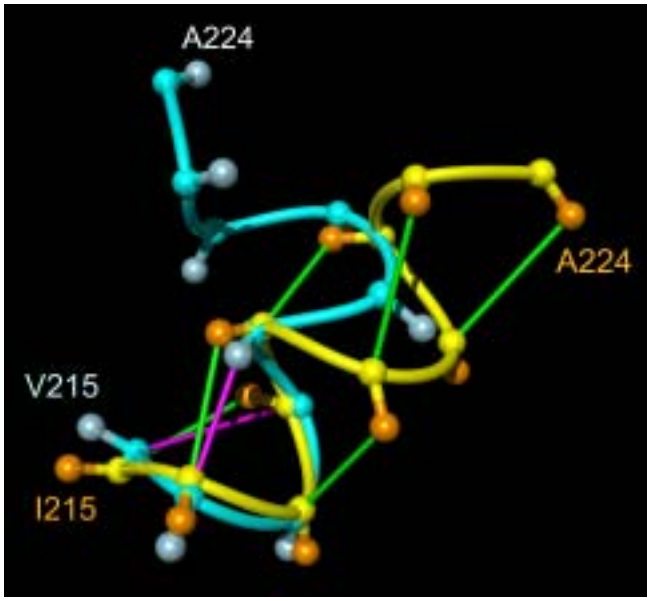

Fig. 7. Comparison of helix 3 in human and mouse PrP, where the backbone of the polypeptide segment 215–224 is represented as a spline function drawn through the C^{α} positions. The figure results from a global superposition of the two proteins for best fit of the backbone atoms of the residues 144–154, 175–193 and 200–219, which correspond to the α-helices in mPrP. The following color code was used: yellow and orange, backbone and C^{β} atoms of hPrP(121–230), respectively; cyan and light blue, backbone and C^{β} atoms of mPrP(121–231), respectively; green, $d_{\alpha\beta}$(i, i+3) and $d_{\alpha N}$(i, i+3) NOE distance constraints observed in hPrP; magenta, same types of NOE constraints observed for mPrP. Reproduced with permission from Zahn *et al*. (2000).

direct insight into the apparent correlations between amino acid sequence and local three-dimensional structure in the region of the protein X epitope, one would have to start structural studies of a selection of variant proteins with single amino acid exchanges relative to wild-type protein (Zahn *et al*., 2000). It is tempting to speculate that species-dependent amino acid replacements might affect the molecular interaction between PrP^{C} and protein X through changes in the local structure and dynamics of the PrP polypeptide chain.

There is also coincidence between the protein X epitope and the epitope of a PrP^{Sc} isoform-specific monoclonal antibody (Korth *et al*., 1997; 1999). The 15B3 antibody recognizes the three peptide sequences 142–148, 162–170, and 214–226 in bovine PrP, where the first epitope segment overlaps with the single epitope of an isoform-unspecific PrP antibody 6H4 and the second and third epitope segments are located within the proposed binding region for protein X (Fig. 3E). From the large spatial separation of the N-terminal segment from either of the two other segments in PrP^{C} it has been suggested that a single continuous 15B3 epitope must be formed either by aggregation of two PrP molecules, or by structural rearrangement of a single PrP molecule (Korth *et al*., 1997). Intramolecular structural rearrangement bringing all three segments of the 15B3 epitope into close spatial proximity might involve an extension of the existing small β-sheet into the polypeptide segment forming the first α-helix in the PrP^{C} isoform (Glockshuber *et al*., 1997). Thus, in both of these models there is no requirement for a structural rearrangement of the protein X epitope during the PrP^{C} to PrP^{Sc} conversion.

The involvement of helix 3 in a protein X-mediated PrP conversion also corresponds with cell-free conversion experiments (Horiuchi & Caughey, 1999*a*). The findings that binding of

polyclonal antibodies (α219–232) inhibits the binding of PrP^{C} to PrP^{Sc} and the subsequent generation of PrP-res, but that on the other hand removal of the α219–232 epitope from PrP^{C} does not affect PrP^{Sc} binding, can be interpreted in different terms. Firstly, binding of α219–232 leads to steric blocking of a binding site that is close to, but does not include, the PrP^{Sc} epitope of PrP^{C} (Horiuchi & Caughey, 1999*a*,*b*). Secondly, the binding of antibodies inhibits conversion by stabilizing the native conformation of helix 3, which affects the overall stability of the PrP^{C} isoform. In this respect it is interesting to note that sequence alignment of PrP with the recently discovered PrP-like protein (Moore *et al*., 1999) suggests the formation of an intramolecular disulfide bond between residues corresponding to Met166 and Arg220 in human PrP. The function of the additional disulfide bond in Dpl could be to stabilize local protein conformation.

9. Chaperone-mediated PrP conversion

9.1 *Hsp60 and Hsp10 chaperonins*

Chaperonins are large, double-ring-shaped protein complexes whose function *in vivo* is to assist the post-translational folding of polypeptides into the native protein conformation and the refolding of stress-denatured proteins (Ellis, 1996; Hartl, 1996; Netzer & Hartl, 1998). They have been identified in all three life kingdoms as well as in endosymbiotically derived cellular organelles. Based on their sequence homology, chaperonins can be classified into two groups. Group I chaperonins consist of members from eubacteria (GroEL), mitochondria (Hsp60), and chloroplasts (Rubisco binding protein), while the group II chaperonins consist of members from archaea (thermosome/TF55) and the eukaryotic cytosol (TCP1/CCT). The structure and function of chaperonins has been analysed in great detail using GroEL and its co-chaperonin GroES as a model protein (reviewed in Fenton & Horwich, 1997; Sigler *et al*., 1998). The three-dimensional structure of GroEL shows a hollow cylinder of fourteen identical 57 kDa subunits arranged in two seven-membered rings (Braig *et al*., 1994; 1995), where each monomer is composed of three domains (Fig. 8): an apical domain that is responsible for polypeptide binding, an equatorial domain that contains the ATP-binding site, and an intermediate hinge domain that connects the apical and equatorial domain. The apical domain of residues 191 to 376 provides a hydrophobic binding site, which prevents aggregation of folding intermediates (e.g. Buchner *et al*., 1991; Mendoza *et al*., 1991; Zahn & Plückthun, 1992) and causes unfolding of misfolded states (Walter *et al*, 1996; Zahn *et al*., 1996*c*,*d*). In the asymmetrical bacterial holo-chaperonin (Fig. 8), GroES caps the apical surface of the GroEL *cis* ring, anchoring the elevated orientations of the apical domains and closing off the end of the GroEL channel (Xu *et al*., 1997). The role of ATP hydrolysis within the equatorial domain and the transient binding of the GroES to the apical domain is to dissociate the substrate with a native-like conformation (see Goloubinoff *et al.*, 1989; Laminet *et al*., 1990; Martin *et al*., 1991). Recent biochemical and structural discoveries on the folding of proteins from their initial unstructured state to their mature form promoted by chaperonins have recently been reviewed (Gottesman & Hendrickson, 2000; Feldman & Frydman, 2000; Agashe & Hartl, 2000).

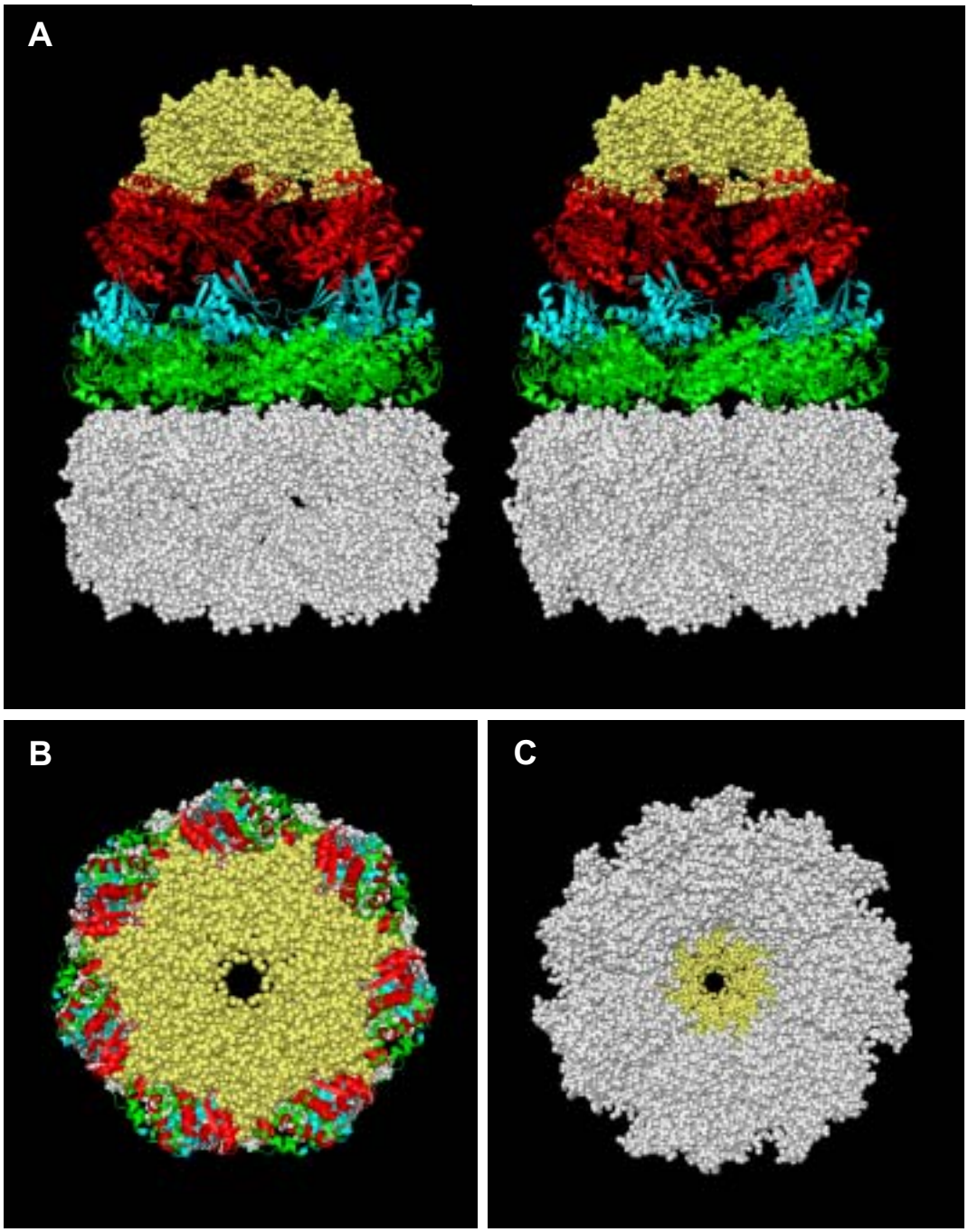

Fig. 8. Overall architecture of the GroEL–GroES holo-chaperonin complex (Xu *et al.*, 1997). (A) Side-view in stereo presentation. The *trans* GroEL ring (white) and GroES ring (yellow) are represented as van der Waals space-filling models (only heavy atoms are shown). The *cis* GroEL ring is drawn as ribbon model. The protein domains of the *cis* ring are color coded as follows: green for equatorial domain, cyan for intermediate domain, and red for apical domain. (B) Top view of (A) looking down from the GroES-binding site. (C) Bottom view of (A) looking down from the *trans* ring. The figures were prepared with the program MOLMOL (Koradi *et al*., 1996).

9.2 *GroEL promoted PrP-res formation*

The chaperonins Hsp60 and GroEL share their substrate specifity for binding to prion protein. Winnacker and co-workers showed that Syrian hamster PrP specifically binds to Hsp60 when recombinantly expressed into *Saccharomyces cerevisiae* (Edenhofer *et al*., 1996). Sequencing

of nine out of fifty-five clones isolated by two-hybrid screening of a HeLa cell line cDNA library identified N-terminally truncated Hsp60 molecules starting at residues 146, 228, and 298 corresponding to residues 122, 204, and 274 of the GroEL sequence (Fig. 2B). Specific PrP binding could be confirmed *in vitro* using immunoblot analysis with an N-terminally glutathione S-transferase (GST)-immobilized shPrP(23–231) construct. Moreover, GroEL was found to interact with intact PrP as well as shPrP(90–231) when immobilized *via* the GST fusion, and affinity chromatography indicated that the equilibrium constant for dissociation is in the micromolar range or smaller. Employing immunoblotting to six synthetic GST-fusion peptides of shPrP the GroEL and Hsp60 epitopes were mapped to residues 180 to 210 of the PrP sequence (Fig. 3D), whereas peptides comprising the segments 23–52, 53–93, 90–109, 129–175, and 218–231 of PrP failed to interact with both chaperonins.

The Lindquist group investigated a possible involvement of the major cellular chaperones Hsp10 (GroES), Hsp26, Hsp40, Hsp60 (GroEL), Hsp70, Hsp90, and Hsp104 in the conversion of prion protein using a modified cell-free conversion assay (Kocisko *et al*., 1994; Caughey *et al*., 1995), wherein metabolically labeled ^{35}S-PrP^{C}, purified from cultured cells in an acid-treated state, is converted into PrP-res (DebBurman *et al*., 1997). Over a broad range of concentrations, alone and in various combinations, none of the chaperones investigated promoted the conversion of PrP^{C} to PrP-res in the absence of PrP^{Sc}, recapitulating the requirement of pre-existing PrP^{Sc} in the conversion process. However, GroEL was found to facilitate the conversion of up to 30% of PrP^{C} into PrP-res in the presence of PrP^{Sc}. Notably, the chaperone not only reduced by ten-fold the quantity of PrP^{Sc} required for detectable conversion, but also achieved efficient conversion without partial chemical denaturation of PrP^{Sc}. Conversion was only observed in the presence of ATP, and was strongly reduced in the presence of point mutants of GroEL which have been shown to block efficient folding of the substrate (Fenton *et al*., 1994). Furthermore, the chaperone-mediated conversion was consistently eliminated by GroES, and was more efficient both for a PrP mutant lacking the GPI anchor and when using unglycosylated PrP^{C}. A kinetic analysis suggested that the conversion reaction resembles a two-step process with GroEL specifically increasing the rate at which PrP^{C} aggregates, whereas the slower rate of conversion into PrP-res remains unchanged in the presence of chaperone. The use of partially denatured PrP^{Sc} in 4 M urea altered the character of conversions promoted by GroEL, with the conversion losing ATP-dependence and becoming resistant to GroES inhibition.

9.3 *Membrane-associated chaperonins*

As has been outlined in section 5.2, the subcellular location of prion propagation is either proximal to the plasma membrane or within coated invaginations of the plasma membrane which form during endocytosis. Assuming that Hsp60 does not leave the mitochondrial matrix, there is no interaction between Hsp60 and PrP during their life cycle, apparently contradicting the hypothesis that chaperonins are potential candidates participating in the PrP conversion. In recent years, however, an increasing number of proteins that are targeted to mitochondria have been found at unexpected, yet very specific, locations (reviewed in Soltys & Gupta, 1999). All these mitochondrial matrix proteins are single protein products of single nuclear genes, but have been found at extramitochondrial locations. Most of these proteins are found in specific

membranous locations and are not present in the cytosol. Immunoelectron-microscopy studies in a wide variety of cells and tissues show that 15 to 20% of Hsp60 activity is present at discrete extramitochondrial sites, including the extracellular cell membrane (Soltys & Gupta, 1997), unidentified cytoplasmic vesicles and granules, peroxisomes, the endoplasmic reticulum (Soltys & Gupta, 1996), and mature insulin-secretory granules in pancreatic β-cells (Brudzynski *et al*., 1992). Moreover, early pregnancy factor has been shown to be identical to Hsp10 suggesting that a physiological mechanism that is responsible for secretion of Hsp10 exists (Cavanagh & Morton, 1994), and immunoelectron microscopy has shown that Hsp10 together with Hsp60 is present in the secretory pathway of pancreatic acinar cells (Velez-Granell *et al*., 1994). Several studies show that extramitochondrial Hsp60 is present as the mature form of the protein, indicating that the chaperonin has been initially imported into mitochondria (Soltys & Gupta, 1996) where the N-terminal mitochondrial targeting sequence is removed. The pathway Hsp60 and other proteins take to arrive at extramitochondrial locations is unresolved. Three scenarios of extramitochondrial transport may be envisaged. The mitochondrial protein could be exported through a yet unknown membrane transport system perhaps including mechanisms used by bacterial pathogens (Finlay & Falkow, 1997), or it may be released in conjunction with membrane vesicles as has been observed for Gram-negative bacteria (Li *et al*., 1998). A third putative transport mechanism would rely on transient fusion of mitochondria with target membranes of other organelles, including the ER and the plasma membrane (Crotty & Ledbetter, 1973).

There are various lines of evidence that Hsp60 specifically binds to plasma membrane-associated proteins and may serve as a chaperone for the folding of these proteins. In cross-linking experiments with oncogenic T cells, the $p21^{ras}$ protein was found to complex transiently with mature Hsp60 in the plasma membrane, where Hsp60 appears to be integral to the function of $p21^{ras}$ as a GTP-binding signaling molecule (Ikawa & Weinberg, 1992). Mutants of CHO cells, which were selected for resistance to increasing concentrations of alanine, show increases in the abundance of Hsp60 that are positively correlated with increases in the A system of amino acid transport (Moffett *et al*., 1988; Jones *et al*., 1994). Because the amino acid composition of mature Hsp60 is not indicative of a protein having extensive membrane spanning domains (Picketts *et al*., 1989), it has been suggested that the chaperonin associates in the manner of a peripheral membrane protein with the extracellular domains of the transmembrane amino acid transport system (Jones *et al*., 1994). In human primary T lymphocytes (Laxminarayana *et al*., 1993; Kammer *et al*., 1994) and in the human leukemic $CD4^+$ T cell line (Khan *et al*., 1998), Hsp60 has been shown to co-immunoprecipitate with membrane-associated histone 2B, where this membrane association is regulated by the phosphorylation status of both the chaperone and the substrate molecule. The phosphorylation of Hsp60 and histone 2B by extracellular type I protein kinase A rapidly severs their physical association, resulting in immediate expulsion of histone 2B, but not chaperonin, from the plasma membrane into the extracellular milieu. After dephosphorylation by a phosphatase, Hsp60 is able to repeat the cycle. Hsp60 contains a total of six serine and threonine residues which could potentially be phosphorylated by the protein kinase including the tripeptide segment Lys226–Ile227–Ser228 located near the peptide binding site within the apical domain (Fig. 2B). Interestingly, the tripeptide segments Lys101–Pro102–Ser103, Arg220–Glu221–Ser222 and Arg228–Gly229–Ser230 in the sequence of human PrP (the latter

two located within the putative protein X epitope; Fig. 2A) also constitute potential phosphorylations sites (Edelman *et al.*, 1987). If kinases recognize these sites, changes in the phosphorylation pattern could have drastic effects on the molecular interaction between Hsp60 and the PrP substrate.

Recently, it has been shown that soluble GroEL chaperonin has high affinity for model lipid membranes (Török *et al.*, 1997). The conserved C-terminus of chaperonin is involved in membrane binding, which is apparently governed by the composition and the physical state of the host bilayer. Fluorescence anisotropy measurements on large unilamellar vesicles revealed that the interaction of GroEL tetradecamers with lipid membrane increases the molecular order in the liquid crystalline state. Asymmetrical GroEL–GroES and symmetrical GroEL–$(GroES)_2$ heterooligomers penetrate into the hydrophobic core of the lipid bilayer, while protein folding and ATPase activities remain remarkably unchanged as compared with soluble chaperonin. From these experiments it has been suggested that, during stress, chaperonins can assume the functions of assisting the folding of both soluble and membrane-associated proteins while concomitantly stabilizing membranes.

9.4 *Preference of GroEL for positive charges*

The nature of chaperonin-polypeptide interactions is promiscuous: in addition to hydrophobic binding (see Mendoza *et al*., 1991; 1992; Luo & Horowitz, 1993; Hayer-Hartl *et al*., 1994) electrostatic interactions are important for the binding of GroEL to several proteins (Zahn *et al*., 1994*a*; Perrett *et al*., 1997). Mutagenesis studies carried out in the Fersht lab have shown that positively charged side chains tend to interact favorably with GroEL, whereas negatively charged side chains tend to disfavor interaction (Itzhaki *et al*., 1995). An effect on binding could be observed when a single amino acid with a charged side chain was exchanged against an uncharged residue, and *vice versa*. Moreover, the more efficient conversion of PrP^C into PrP-res by GroEL in the absence of N-linked sugars or the GPI anchor (DebBurman *et al*., 1997) coincides with the finding that glycosylated forms of invertase are less efficiently arrested by GroEL during refolding than non-glycosylated invertase (Kern *et al.*, 1992), and can also be explained by a preference of the chaperonin for positive charges.

The preference of GroEL for binding positively charged polypeptides coincides with the observation that substitution of a basic residue at positions Gln168, Gln172, or Gln219 increases binding affinity of chimeric human/mouse PrP^C to protein X rendering it unavailable for prion propagation, whereas introduction of a negative charge at positions Gln168 and Gln219 decreases affinity of PrP^C for binding to protein X (see section 8.2).

9.5 *Potential GroEL/Hsp60 epitopes on PrP*

The characteristics of polypeptide sequence motifs that bind to GroEL have been analysed by using affinity panning of immobilized monomeric fragments encompassing the apical domain of GroEL designed “minichaperones” that are active in chaperoning protein folding *in vitro* and *in vivo* (Zahn *et al*., 1996*a*; Chatellier *et al*., 1998; Golbik *et al.*, 1998). Suitable mutants from a library of bacteriophages that display the fungal cellulose-binding domain of the enzyme cellobiohydrolase I confirmed that side chains recognized by GroEL do not have to be totally

hydrophobic, rather that polar and positively charged chains can be accommodated (Chatellier *et al*., 1999). The ten residues of selected peptides exhibit a linear binding motif with similar dimensions and chemical characteristics to the GroEL-bound mobile loop of GroES (Landry *et al*., 1993; Hunt *et al*., 1996), suggesting that the binding mode and/or site of the co-chaperonin to GroEL are likely to mimic substrate polypeptide binding.

Alignment of the "consensus" sequence for binding, RGSLLPGSSL, and the human PrP sequence (Schätzl *et al.*, 1995) reveals 67% identity within a six amino acid overlap corresponding to the peptide segment 35–40, and 33% identity in a nine amino acid overlap corresponding to the segment 126–133. Both of these segments are highly conserved in mammalian PrPs (Fig. 2A). The less conserved region of residues 229–232 comprising the GPI-attachment site shows 75% identity when compared to the consensus sequence. These results suggest that GroEL and presumably Hsp60 can bind to several segments on PrP including residues of the flexible tail, the first β-strand, and the C-terminal end, as well as the segment of residues 180–210 (see section 9.2) comprising helices 2 and 3 (Fig. 3D). Three of the potential Hsp60 epitopes belong to the minimal PrP sequence required for prion propagation (Fig. 3B), and may together with other regions contribute to cooperative binding to chaperonin.

9.6 *Conformations of chaperonin-bound PrP*

Until recently structural details of the binding of proteins to GroEL have been lacking. Application of high resolution X-ray crystallography to chaperonin-substrate complex appears to be difficult, and the large molecular mass of the chaperonins does not allow direct observation by solution NMR methods because of line broadening owing to slow molecular tumbling (Wüthrich, 1986). Amide proton exchange detected by NMR has provided some detailed information on the secondary structure of proteins when complexed with GroEL (Zahn *et al*., 1994*b*), and indicate that substrate protein can be completely unfolded during binding (Zahn *et al*., 1996*c*,*d*). Complex formation with the chaperone thus allows the correction of misfolded conformations in an isolated environment without the danger of intermolecular aggregation reactions.

Recently, the minichaperones have been demonstrated to constitute a paradigm for studying GroEL-substrate interactions at the atomic level. The crystal structure of GroEL(191–376) fused to a 17 residue N-terminal tag at 1.7 Å resolution (Buckle *et al*., 1997) revealed specific binding of the N-terminal tag within the polypeptide binding site of neighboring molecules. Within the binding site, the N-terminal tag sequence GLVPRGS adopted a roughly extended conformation (Fig. 9) suggesting that polypeptide binding in the GroEL tetradecamer occurs around the rim of the central channel (Fig. 10). The minichaperones also turned out to be particularly suitable for NMR studies of bound peptides. Transferred NOEs were used to study minichaperone-bound conformations of a synthetic peptide corresponding to the N-terminal α-helix of the mitochondrial rhodanese (Kobayashi *et al*., 1999), a protein whose *in vitro* refolding is mediated by intact GroEL and minichaperones (Martin *et al*., 1991; Zahn *et al*., 1996*a*). The peptide adopted an α-helical conformation upon binding, indicating that the binding site of GroEL is compatible with binding of both α-helices as well as extended β-strands.

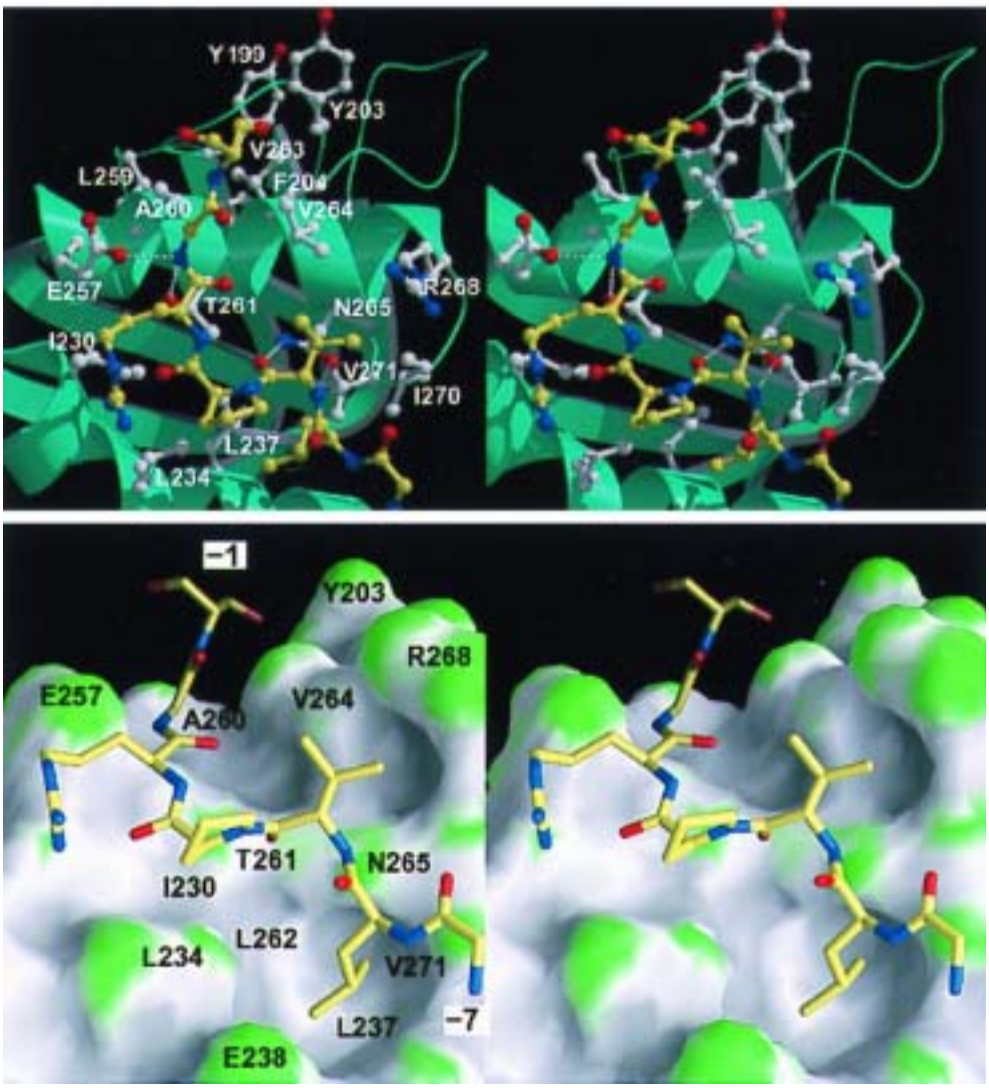

Fig. 9. Polypeptide binding of GroEL minichaperone. (A) Stereoview of the crystal structure of the peptide–GroEL(191–376) complex. Residues −7 to −1 of the N-terminal tag of a neighboring molecule in the crystal are represented by yellow bonds. Neighboring residues of the minichaperone binding site are represented by white bonds. Hydrogen bonds are represented by broken white lines. (B) Same orientation as in (A) but showing the molecular surface of the minichaperone. The surface is colored according to surface curvature to highlight concave surface pockets. Convex, concave, and flat surfaces are colored green, grey, and white, respectively. Residues underlying the surface are labelled. Reproduced with permission from Buckle *et al*. (1997).

The conformation of the bound polypeptides appears to depend on the difference between the intrinsic folding stability of the substrate protein and the net binding energy of the complex between chaperonin and substrate (Zahn *et al*, 1996*b*). Thus, there is a thermodynamic partitioning between two equilibria: the folding equilibrium of the substrate protein converting between native and unfolded conformations, and the binding equilibrium between free and bound substrate (Zahn & Plückthun, 1994; Zahn *et al.*, 1994*a*). This model suggests that PrP^C would be either partially or fully unfolded when complexed to Hsp60, dependent on parameters of the cellular environment.

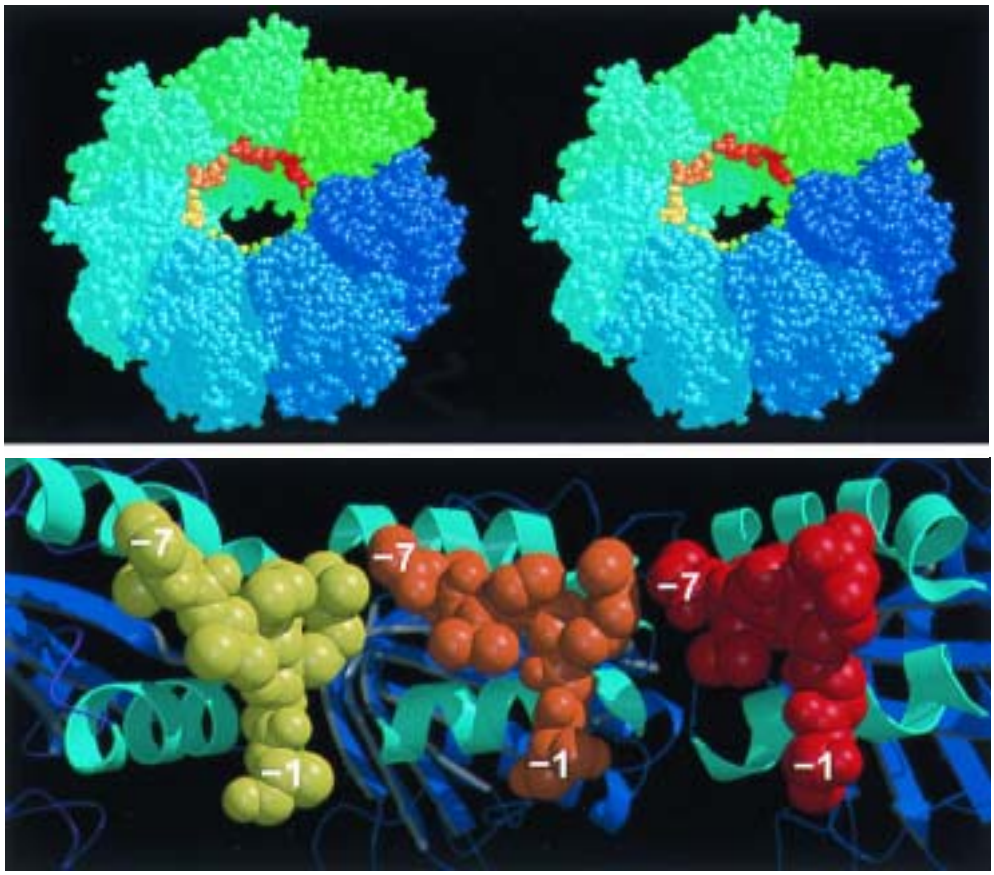

Fig. 10. Structural model for polypeptide binding in intact GroEL. (A) Stereoview of one heptameric ring of the GroEL tetradecamer showing the position of the N-terminal tag bound to each apical domain, near the opening to the central channel. This model was generated by the superposition of the minichaperone GroEL(191–376) with each of the corresponding apical domains in intact GroEL (the second ring of the GroEL cylinder is not shown). Subunits are color coded going clockwise around the ring from blue to green. Superimposed bound peptides are colored from green to red going clockwise around the ring. (B) Cross section of the model shown in (A) looking directly at the inner wall of the chamber, and showing the apical domains from three subunits with modeled peptide. The helices H8 and H9 are colored cyan, and the modeled peptides are colored yellow, orange, and red, respectively. Each of the separate peptides (residues −7 to −1) could be linked together by small peptide segments so that a longer polypeptide chain could bind from one contiguous site to the next. Reproduced with permission from Buckle *et al*. (1997).

9.7 *Conserved Hsp60 substrate binding sites*

The polypeptide binding site for GroEL has been defined by mutagenesis studies (Fenton *et al*., 1994) to be within the apical domain and comprises of the loop between β-strands S7 and S8, helices H8 and H9, and the adjacent loop between helix H9 and β-strand S11 (Fig. 2B). These sites coincide well with the substrate binding sites of monomeric GroEL minichaperones as defined by crystallography studies (Buckle *et al*., 1997), NMR spectroscopy (Kobayashi *et al*., 1999), and fluorescence anisotropy measurements using synthetic peptides and denatured proteins (Tanaka & Fersht, 1999). Little change was observed for NMR chemical shifts and fluorescence outside these regions. The aforementioned preference of GroEL for positively charged side chains can be rationalized by the two Glu residues at positions 238 and 257 within

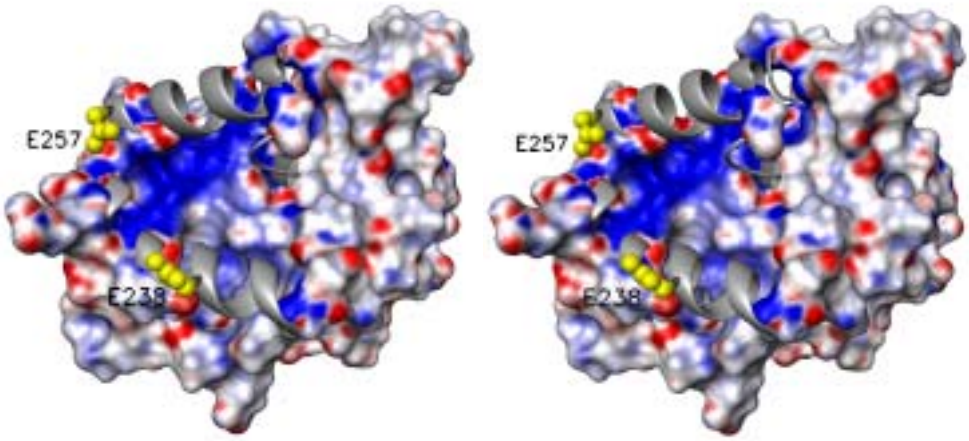

Fig. 11. Stereoview of the GroEL substrate binding site. Residues involved in polypeptide binding (see Fig. 2B) are shown as a ribbon drawing model, with the Glu side chains represented as yellow ball-and-stick models. Residues outside the binding site are represented by surface plot. The surface is colored according to the electrostatic surface potential, with blue for positive charges and red for negative charges. The molecular orientation is approximately the same as in figure 9. The figure was prepared with the program MOLMOL (Koradi *et al*., 1996).

the binding site (Fig. 11), where Glu257 plays a key role in peptide binding as it is also involved in hydrogen bonding with the substrate (Fig. 9A,B). Affinity for positive charges can only be explained by these two residues, since the remaining residues nearby the binding site are either neutral or positively charged (Fig. 11).

A comparison of the binding sites of GroEL and Hsp60 reveals that the amino acid sequence is only marginally conserved between bacterial and mitochondrial group I chaperonins (Fig. 2B). However, the two negatively charged side chains of the binding site are conserved between bacterial and mitochondrial chaperonins (Fig. 2B), indicating their importance for polypeptide binding. Within the mitochondrial chaperonins the amino acid sequence is highly conserved. In fact, human and mouse Hsp60 differ by only a single amino acid replacement of Ile against Val at position 230 (position given relative to the *E. coli* open reading frame). If Hsp60 is identical to protein X, this would mean that the more efficient conversion of chimeric human/mouse PrP compared to human PrP in transgenic mice or mouse neuroblastoma cells as described in section 8, is caused by amino acid exchanges in PrP rather than by the sequence of host protein X. Thus, the preference of protein X for mouse PrP over human PrP could be explained by the net charges of −2 and −4 within the residues 169 to 230 (Fig. 2A) from the two species, respectively.

9.8 *Requirement of ATP-hydrolysis*

It has emerged from a large variety of studies that the nature of chaperonin-mediated protein folding depends critically on the substrate protein. There is a spectrum of mechanisms for chaperonin-mediated protein folding, with minichaperones at one end and the complete chaperonin system represented by GroEL, GroES and ATP at the other end (Ben-Zvi *et al*., 1998; Hayer-Hartl *et al*., 1999, Rye *et al*., 1999). Under permissive conditions proteins such as

cyclophilin A and rhodanese have a significant background of spontaneous refolding. For these proteins, the minichaperones or GroEL alone in the absence of GroES are able to support protein folding (Zahn *et al*., 1996*a*). Permissible proteins require a minimal mechanism for GroEL-mediated protein folding, namely the ability of the chaperonin to undergo recurrent transitions between high-affinity T and low affinity R states (Ben-Zvi *et al*., 1998). The minimal requirement for a chaperonin to mediate protein folding is to provide a flexible hydrophobic surface (Zahn *et al*., 1993) that can bind the sticky folding intermediates or misfolded states, eventually causing the unfolding of compact states (Zahn *et al*., 1996*c*,*d*), and giving them an additional chance to fold successfully in a shielded environment before release from the R state. Nonpermissive proteins such as mitochondrial malate dehydrogenase show a strict requirement for the complete chaperonin system under conditions where spontaneous refolding is extremely inefficient (Ben-Zvi *et al*., 1998; Hayer-Hartl *et al*., 1999; Yifrach & Horovitz, 2000). In the "encapsulation" model for chaperonin-mediated protein folding (see Mayhew *et al*., 1996; Weissman *et al.*, 1996), the critical role of the GroEL–GroES complex (see Fig. 8) is to provide a protected folding chamber with physical properties that are distinct from that of the bulk solution. It has been suggested that the folding chamber can also detect the folded state of a protein therein and signal for GroES release once the protein is fully folded (Ben-Zvi *et al*., 1998). Hence, the co-chaperonin would carry the complementary roles of controlling the formation and the stabilization of the folding chamber in the R state and thereby efficiently preventing premature dissociation and aggregation of early folding intermediates from the chaperonin complex.

How can the enhancing effect of GroEL on the conversion of PrP^{C} into PrP-res as described in section 9.2 be interpreted on the basis of the various mechanisms for chaperonin-mediated protein folding? In the presence of the complete chaperonin system PrP-res formation presumably is prevented (DebBurman *et al*., 1997) because GroES optimizes the chaperone activity of GroEL and allows a dissociation of PrP from the R chamber only when the substrate adopts a PrP^{C}-like conformation. Under these permissive conditions PrP folding in the GroEL ring follows the optimal mechanism. In the absence of GroES, the folding mechanism of PrP changes from permissive to nonpermissive. The fact that GroEL-mediated PrP conversion is ATP dependent (DebBurman *et al*., 1997) indicates that chaperone activity is required for the conversion process. Thus, in the presence of ATP the bound PrP goes through the complete chaperonin cycle, and may be released from the R state in a non-native conformation PrP^{D} which is prone to aggregation, but, in the presence of preexisting PrP^{Sc} may refold into the PrP-res isoform. In the absence of ATP no conversion into PrP-res takes place presumably because PrP forms a stable complex with the T state where the substrate is protected against aggregation, in agreement with the finding that GroEL and Hsp60 form a stable complex with PrP (Edenhofer *et al*., 1996). Accordingly, the GroEL variant D87K does not promote conversion into PrP-res (DebBurman *et al*., 1997) presumably because the mutation inhibits hydrolysis of ATP (Fenton *et al*., 1994) and consequently an efficient release of the bound substrate. The mutation G337S/I349E in GroEL, which hydrolyzes ATP but does not efficiently bind the GroES chaperonin (Fenton *et al*., 1994), inhibits *in vitro* conversion presumably because PrP dissociates in a conformation that does not interact with the PrP^{Sc} template. In this respect this variant of GroEL would be an interesting subject for future studies on molecular mechanism preventing PrP-res or PrP^{Sc} formation.

A model of chaperonin-mediated PrP conversion at the cell surface implies that ATP would be available at the extracellular matrix. Of course, it is difficult to measure the extracellular ATP concentration, which presumably varies from tissue to tissue. However, extracellular ATP is known to exert potent effects on the activity of cells in the nervous system, where it can act as a neurotransmitter or as a modulator regulating the activity of other neurohormones (Burnstock *et al*., 1972; Phillis & Wu, 1983; Silinsky & Ginsborg, 1983). Furthermore, it has been shown that ecto-protein kinases use extracellular ATP to phosphorylate proteins localized at the external surface of the plasma membrane in neuronal cells (Ehrlich *et al*., 1986), and Alzheimer β-amyloid precursor protein (APP) is phosphorylated at various sites including the extracellular domain in cultured cells (Hung *et al*., 1994; Walter *et al*., 1997). As the dissociation constant for binding of ATP to GroEL is in the micromolar range (Gray & Fersht, 1991; Jackson *et al*., 1993), relatively low concentrations of nucleotide would be enough to allow chaperonin-mediated protein folding on cellular membranes as described in section 9.3.

9.9 *Chaperone-mediated prion propagation*

As described with reference to the previous section it remains an open question why *in vivo* Hsp60 should not be able to interact with Hsp10 and concomitantly prevent PrP conversion. From the three-dimensional structure of the holo-chaperonin (see Fig. 8) it is tempting to speculate that the immobilization of PrP to the plasma membrane by its C-terminal GPI-anchor, which is essential for prion propagation (Caughey *et al*., 1991*b*; Borchelt *et al*., 1992; Rogers *et al*., 1993), prevents the binding of Hsp10 to the Hsp60 and thus encapsulation of the immobilized PrP. Hence, folding of the substrate occurs under nonpermissive conditions, and in the absence of PrP^{Sc} the chaperonin-released PrP presumably forms amorphous protein aggregates which are removed by cellular proteases. This chaperone-mediated degradation of PrP^{C} could be part of a cellular mechanism regulating the total concentration of functional prion protein. In the presence of PrP^{Sc}, however, the aggregation process might be guided towards the protease-resistant PrP^{Sc} isoform which cannot be removed by cellular proteinases and thus accumulates into pathogenic protein aggregates. In conclusion, there are many arguments for prion propagation mediated by chaperonin (Table 1).

Apart from Hsp60, the major classes of general chaperones are the Hsp40, Hsp70, Hsp90, Hsp100, and the small heat shock proteins (for review see Fink, 1999). Recent investigations have shown that not only do the major classes of chaperones often function with protein cofactors, but direct interactions between members of the different heat-shock protein families may be frequent. For example, the order of events in mitochondrial import suggests that mitochondrial Hsp70 and Hsp60 act sequentially. A kinetic study on the interaction of imported preproteins with chaperones showed that an initial interaction with Hsp70 is followed by binding to Hsp60 (Manning-Krieg *et al*., 1991). The same sequence of chaperone action was reported for the bacterial system, GroEL and DnaK (Hsp70), in a reconstitution study (Langer *et al*., 1992.). Bukau and co-workers (Buchberger *et al*., 1996) have recently suggested that during folding of newly synthesized proteins, DnaK and GroEL form a lateral network of cooperating proteins. So it seems possible that chaperones like Hsp70, although they have not been shown to facilitate PrP conversion *in vitr*o (see section 9.2), under physiological conditions may be relevant for propagation of prions at the plasma membrane. Indeed, like

Table 1. *Arguments for prion propagation being mediated by chaperonin*.

1. PrP specifically binds to Hsp60 when recombinantly expressed in an *Saccharomyces cerevisiae* environment.
2. The equilibrium constant for dissociation of Hsp60 or GroEL and PrP is in the micromolar range or smaller.
3. PrP contains several linear epitopes for binding to GroEL and Hsp60.
4. GroEL and protein X share a preference for binding to positively charged side chains.
5. There are extramitochondrial Hsp60 forms that specifically bind to plasma membrane-associated proteins.
6. Of the major cellular chaperones only chaperonin promotes the conversion of PrP^{C} into PrP-res.
7. The more efficient *in vitro* conversion of PrP in the absence of N-linked sugars coincides with the low affinity of GroEL for glycosylated substrates.
8. The effects of GroEL on *in vitro* conversion can be interpreted within a framework involving various mechanisms for chaperonin-mediated protein folding.
9. Immobilization of PrP to the plasma membrane could support PrP^{Sc} formation by preventing the formation of holo-chaperonin complex.

Hsp60 (see section 9.3), mitochondrial Hsp70 has been identified at unexpected cellular locations. The peptide-binding protein PBP72/74, a protein involved in antigen presentation, is identical to Hsp70 (Dahlseid *et al*., 1994), and mortalin, a protein responsible for cell senescence, is also identical to mitochondrial Hsp70 (Wadhwa *et al*., 1993). Furthermore, immunoelectron microscopy suggests that significant amounts of mitochondrial Hsp70 are present at the plasma membrane, in cytoplasmic vesicles and in cytoplasmic granules (VanBuskirk *et al.*, 1991; Singh *et al*., 1997).

10. Template-assisted annealing model

Two general models have been proposed to answer the following questions: why is spontaneous formation of PrP^{Sc} an extremely rare event and how does infection with PrP^{Sc} promote the conversion of the cellular isoform? The “nucleated polymerization” or “seeding” model for PrP^{Sc} formation (Jarrett & Lansbury, 1993; Come *et al*., 1993) proposes that PrP^{C} and PrP^{Sc} are in a rapidly established equilibrium, and that the conformation of PrP^{Sc} is thermodynamically stable only when trapped within a crystal-like seed (Fig. 12A). The proposed process is akin to other well-characterized nucleation-dependent protein polymerization processes, including microtubule assembly, flagellum assembly, and sickle-cell hemoglobin fibril formation, where the kinetic barrier is imposed by nucleus formation around single molecules. To explain exponential conversion rates, it must be assumed that the aggregates are continuously

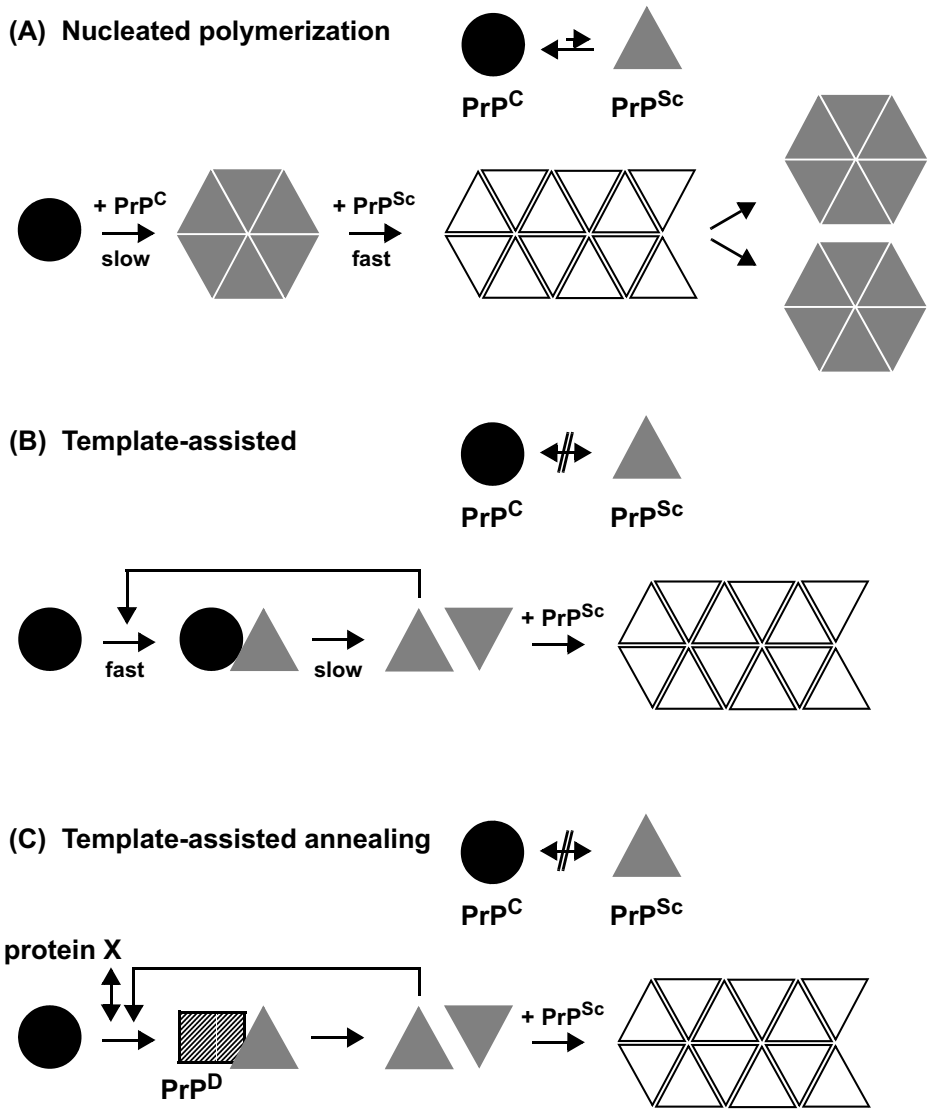

Fig. 12. Mechanistic models for the conformational conversion of PrP^{C} (black circle) to PrP^{Sc} (triangle). (A) In the nucleated polymerization model, the rate-limiting step for PrP conversion is the formation of a nucleus or seed (grey triangles). Once formed, the nucleus grows rapidly and forms larger aggregates or fibrils (white triangles), which dissociate at some stage in order to produce new nuclei. (B) The template-assisted model does not require that the PrP^{C} and PrP^{Sc} isoforms are in a thermodynamic equilibrium. The conversion reaction is catalyzed by the formation of a PrP^{C}–PrP^{Sc} heterodimer complex. After the conversion homodimeric PrP^{Sc} dissociates into monomers, which at some concentration form large protein aggregates. (C) In the template-assisted annealing model, the conversion reaction occurs as in (B), but is promoted by the unfolding activity of a chaperone-like protein X. The resulting folding intermediate PrP^{D} (hatched rectangle) refolds into PrP^{Sc} only in the presence of a preexisting PrP^{Sc} template molecule.

fragmented to present increasing surface for accretion, although the mechanism of fragmentation remains to be explained. The "template-assisted" or "heterodimer" model for PrP^{Sc} formation (Prusiner *et al*., 1990; Prusiner, 1991) proposes that PrP^{C} is unfolded to some extent and refolded under the influence of a PrP^{Sc} molecule functioning as a template (Fig. 12B). A high energy barrier is postulated to make this conversion improbable without catalysis by preexisting PrP^{Sc}. The conformational change is proposed to be kinetically

controlled by the dissociation of a PrP^{C}–PrP^{Sc} heterodimer into two PrP^{Sc} molecules, and can be treated as an induced fit enzymatic reaction following autocatalytic Michaelis-Menten kinetics. Once conversion has been initiated it gives rise to an exponential conversion cascade as long as the PrP^{Sc} dimer dissociates rapidly into monomers. A disadvantage of the template-assisted model is that it does not explain why PrP^{Sc} after propagation should aggregate into protein fibrils. Eigen has presented a comparative kinetic analysis of the two proposed mechanisms of prion disease (Eigen, 1996). He found that logically both models are possible, in principle, but that the conditions under which they work seem to be too narrow and unrealistic. The autocatalytic template-assisted model requires cooperativity in order to work, but it then becomes phenomenologically indistinguishable from the nucleation model which is also a form of (passive) autocatalysis. Though the two kind of mechanisms still may differ on the question which of the two monomeric protein conformations is the favored equilibrium state, they both require an aggregated state as the from that is eventually favored at equilibrium and that presumably resembles the pathogenic form of the prion protein. Eigen concluded that more experimental evidence is needed in order to judge which of the two models is the right one.

In principle, neither of the models for prion propagation do not rule out a possible assistance by molecular chaperones. In the nucleated polymerization model (Fig. 12A) the PrP conformational conversion could be facilitated by chaperones which preferentially bind PrP^{Sc} shifting the folding equilibrium between the two isoforms towards the PrP^{Sc} form. However, assuming that the substrate is bound to the surface it appears unlikely that six PrP molecules (according to Lansbury this is the minimal size of a seed effective in initializing the aggregation of PrP^{Sc} molecules) can approach one another to form a nucleus because of steric hindrance by the generally larger chaperones. Moreover, in many chaperones like Hsp60 large parts of the bound polypeptide chain are sequestered and would thus *per se* not be available for nucleated polymerization. More likely, molecular chaperones would facilitate PrP conversion through a mechanism which is based on the template-assisted model (Fig. 12B) as suggested by Prusiner *et al*. (1998). In this model, which I here term "template-assisted annealing" model for PrP^{Sc} formation (Fig. 12C), partially denatured PrP^{D} forms a complex with a chaperone-like protein X, and subsequently binds to PrP^{Sc}. Here, the function of PrP^{Sc} is that of a template as in the model of figure 12B, but the unfolding activity is provided by the protein X component. Unfolding and refolding into a different protein conformation constitutes an annealing process where the binding energy the of the PrP^{D}–protein X complex is used to overcome the high energy barrier for folding of PrP^{C} into PrP^{Sc}. Indeed, it has been demonstrated for GroEL that chaperonins have the potential to act as annealing machines and are able to catalyse unfolding of compact protein conformations (Zahn *et al*., 1996*d*; Shtilerman *et al*., 1999).

11. ACKNOWLEDGMENTS

I am grateful to Alan Fersht, Andreas Plückthun and Kurt Wüthrich for generous support, and Fred Damberger for critical reading of the manuscript.

12. REFERENCES

AGASHE, V. R. & HARTL, F. U. (2000). Roles of molecular chaperones in cytoplasmic protein

folding. *Semin. Cell. Dev. Biol*. **11**, 15–25.

ALPER, T., CRAMP, W. A., HAIG, D. A. & CLARKE, M. C. (1967). Does the agent of scrapie replicate without nucleic acid? *Nature* **214**, 764–766.

ALPER, T., HAIG, D. A. & CLARKE, M. C. (1966). The exceptionally small size of the scrapie agent. *Biochem. Biophys. Res. Commun.* **22**, 278–284.

ANDERSON, R. G. (1998). The caveolae membrane system. *Annu. Rev. Biochem*. **67**, 199–225.

ANDERSON, R. G., KAMEN, B. A., ROTHBERG, K. G. & LACEY, S. W. (1992). Potocytosis: sequestration and transport of small molecules by caveolae. *Science* **255**, 410–411.

ANFINSEN, C. B. (1973). Principles that govern the folding of protein chains. *Science* **181**, 223–230.

ARNOLD, J. E., TIPLER, C., LASZLO, L., HOPE, J., LANDON, M. & MAYER, R. J. (1995). The abnormal isoform of the prion protein accumulates in late-endosome-like organelles in scrapie-infected mouse brain. *J. Pathol.* **176**, 403–411.

BARRY, R. A., MCKINLEY, M. P., BENDHEIM, P. E., LEWIS, G. K., DEARMOND, S. J. & PRUSINER, S. B. (1985). Antibodies to the scrapie protein decorate prion rods. *J. Immunol.* **135**, 603–613.

BASLER, K., OESCH, B., SCOTT, M., WESTAWAY, D., WÄLCHLI, M., GROTH, D. F., MCKINLEY, M. P., PRUSINER, S. B. & WEISSMANN, C. (1986). Scrapie and cellular PrP isoforms are encoded by the same chromosomal gene. *Cell* **46**, 417–428.

BELLINGER-KAWAHARA, C. G., KEMPNER, E., GROTH, D., GABIZON, R., & PRUSINER, S. B. (1988). Scrapie prion liposomes and rods exhibit target sizes of 55,000 Da. *Virology* **164**, 537–541.

BENDHEIM, P. E., BARRY, R. A., DEARMOND, S. J., STITES, D. P. & PRUSINER, S. B. (1984). Antibodies to a scrapie prion protein. *Nature* **310**, 418–421.

BENDHEIM, P. E., BOCKMAN, J. M., MCKINLEY, M. P., KINGSBURY, D. T. & PRUSINER, S. B. (1985). Scrapie and Creutzfeldt-Jakob disease prion proteins share physical properties and antigenic determinants. *Proc. Natl. Acad. Sci. USA* **82**, 997–1001.

BEN-ZVI, A. P., CHATELLIER, J., FERSHT, A. R. & GOLOUBINOFF, P. (1998). Minimal and optimal mechanisms for GroE-mediated protein folding. *Proc. Natl. Acad. Sci. USA* **95**, 15275–15280.

BESSEN, R. A. & MARSH, R. F. (1994). Distinct PrP properties suggest the molecular basis of strain variation in transmissible mink encephalopathy. *J. Virol.* **68**, 7859–7868.

BESSEN, R. A., KOCISKO, D. A., RAYMOND, G. J., NANDAN, S., LANSBURY, P. T. & CAUGHEY, B. (1995). Non-genetic propagation of strain-specific properties of scrapie prion protein. *Nature* **375**, 698–700.

BILLETER, M., KLINE, A. D., BRAUN, W., HUBER, R. & WÜTHRICH, K. (1989). Comparison of the high-resolution structures of the α-amylase inhibitor Tendamistat determined by nuclear magnetic resonance in solution and by X-ray diffraction in single crystals. *J. Mol. Biol.* **206**, 677–687.

BILLETER, M., RIEK, R., WIDER, G., HORNEMANN, S., GLOCKSHUBER, R. & WÜTHRICH, K. (1997). Prion protein NMR structure and species barrier for prion diseases. *Proc. Natl. Acad. Sci USA* **94**, 7281–7285.

BOCKMAN, J. M., PRUSINER, S. B., TATEISHI, J. & KINGSBURY, D. T. (1987). Immunoblotting of Creutzfeldt-Jakob disease prion proteins: host species-specific epitopes. *Ann. Neurol*. **21**,

589–595.

BOLTON, D. C., BENDHEIM, P. E., MARMORSTEIN, A. D. & POTEMPSKA, A. (1987). Isolation and structural studies of the intact scrapie agent protein. *Arch. Biochem. Biophys*. **258**, 579–590.

BOLTON, D. C., MCKINLEY, M. P. & PRUSINER, S. B. (1982). Identification of a protein that purifies with the scrapie prion. *Science* **218**, 1309–1311.

BOLTON, D. C., MCKINLEY, M. P. & PRUSINER, S. B. (1984). Molecular characteristics of the major scrapie prion protein. *Biochemistry* **23**, 5898–5906.

BORCHELT, D. R., ROGERS, M., STAHL, N., TELLING, G. & PRUSINER, S. B. (1993). Release of the cellular prion protein from cultured cells after loss of its glycoinositol phospholipid anchor. *Glycobiology* **3**, 319–329.

BORCHELT, D. R., SCOTT, M., TARABOULOS, A., STAHL, N. & PRUSINER, S. B. (1990). Scrapie and cellular prion proteins differ in their kinetics of synthesis and topology in cultured cells. *J. Cell. Biol*. **110**, 743–752.

BORCHELT, D. R., TARABOULOS, A. & PRUSINER, S. B. (1992). Evidence for synthesis of scrapie prion proteins in the endocytic pathway. *J. Biol. Chem*. **267**, 16188–16199.

BRAIG, K., ADAMS, P. D. AND BRÜNGER, A. T. (1995). Conformational variability in the refined structure of the chaperonin GroEL at 2.8 Å resolution. *Nat. Struct. Biol.* **2**, 1083–1094.

BRAIG, K., OTWINOWSKI, Z., HEGDE, R., BOISVERT, D. C., JOACHIMIAK, A., HORWICH, A. L. & SIGLER, P. B. (1994). The crystal structure of the bacterial chaperonin GroEL at 2.8 Å. *Nature* **371**, 578–586.

BROWN, D. R. & BESINGER, A. (1998). Prion protein expression and superoxide dismutase activity. *Biochem. J*. **334**, 423–429.

BROWN, D. R., QIN, K., HERMS, J. W., MADLUNG, A., MANSON, J., STROME, R., FRASER, P. E., KRUCK, T., VON BOHLEN, A., SCHULZ-SCHAEFFER, W., GIESE, A., WESTAWAY, D. & KRETZSCHMAR, H. (1997*a*). The cellular prion protein binds copper *in vivo*. *Nature* **390**, 684–687.

BROWN, D. R., SCHMIDT, B. & KRETZSCHMAR, H. A. (1997*b*). Effects of oxidative stress on prion protein expression in PC12 cells. *Int. J. Dev. Neurosci.* **15**, 961–972.

BROWN, D. R., SCHULZ-SCHAEFFER, W. J., SCHMIDT, B. & KRETZSCHMAR, H. A. (1997*c*). Prion protein-deficient cells show altered response to oxidative stress due to decreased SOD–1 activity. *Exp. Neurol.* **146**, 104–112.

BROWN, D. R., WONG, B.-S., HAFIZ, F., CLIVE, C., HASWELL, S. J. & JONES, I. M. (1999). Normal prion protein has an activity like that of superoxide dismutase. *Biochem. J*. **344**, 1–5.

BROWN, P., LIBERSKI, P. P., WOLFF, A. & GAJDUSEK, D. C. (1990). Resistance of scrapie infectivity to steam autoclaving after formaldehyde fixation and limited survival after ashing at 360 °C: practical and theoretical implications. *J. Infect. Dis.* **161**, 467–472.

BRUDZYNSKI, K., MARTINEZ, V. & GUPTA, R. S. (1992). Immunocytochemical localization of heat-shock protein 60-related protein in β-cell secretory granules and its altered distribution in non-obese diabetic mice. *Diabetologia* **35**, 316–324.

BUCHBERGER, A., SCHRÖDER, H., HESTERKAMP, T., SCHÖNFELD, H. J. & BUKAU, B. (1996). Substrate shuttling between the DnaK and GroEL systems indicates a chaperone network promoting protein folding. *J. Mol. Biol*. **261**, 328–333.

BUCHNER, J., SCHMIDT, M., FUCHS, M., JAENICKE, R., RUDOLPH, R., SCHMID, F. X. &

KIEFHABER, T. (1991). GroE facilitates refolding of citrate synthase by suppressing aggregation. *Biochemistry* **30**, 1586–1591.

BUCKLE, A. M., ZAHN, R. & FERSHT, A. R. (1997). A structural model for GroEL–polypeptide recognition. *Proc. Natl. Acad. Sci. USA* **94**, 3571–3575.

BÜELER, H., AGUZZI, A., SAILER, A., GREINER, R.-A., AUTENRIED, P., AGUET, M. & WEISSMANN, C. (1993). Mice devoid of PrP are resistant to scrapie. *Cell* **73**, 1339–1347.

BURNSTOCK, G. (1972). Purinergic nerves. *Pharmacol. Rev.* **24**, 509–581.

BUTLER, D. A., SCOTT, M. R., BOCKMAN, J. M., BORCHELT, D. R., TARABOULOS, A., HSIAO, K. K., KINGSBURY, D. T. & PRUSINER, S. B. (1988). Scrapie-infected murine neuroblastoma cells produce protease-resistant prion proteins. *J. Virol.* **62**, 1558–1564.

CAPELLARI, S., VITAL, C., PARCHI, P., PETERSEN, R. B., FERRER, X., JARNIER, D., PEGORARO, E., GAMBETTI, P. & JULIEN, J. (1997). Familial prion disease with a novel 144-bp insertion in the prion protein gene in a Basque family. *Neurology* **49**, 133–141.

CARLSON, G. A., KINGSBURY, D. T., GOODMAN, P. A., COLEMAN, S., MARSHALL, S. T., DEARMOND, S., WESTAWAY, D. & PRUSINER, S. B. (1986). Linkage of prion protein and scrapie incubation time genes. *Cell* **46**, 503–511.

CASHMAN, N. R., LOERTSCHER, R., NALBANTOGLU, J., SHAW, I., KASCSAK, R. J., BOLTON, D. C. & BENDHEIM, P. E. (1990). Cellular isoform of the scrapie agent protein participates in lymphocyte activation. *Cell* **61**, 185–192.

CAUGHEY, B. & RAYMOND, G. J. (1991). The scrapie-associated form of PrP is made from a cell surface precursor that is both protease- and phospholipase-sensitive. *J. Biol. Chem*. **266**, 18217–18223.

CAUGHEY, B., KOCISKO, D. A., RAYMOND, G. J. & LANSBURY, P. T., JR. (1995). Aggregates of scrapie-associated prion protein induce the cell-free conversion of protease-sensitive prion protein to the protease-resistant state. *Chem. Biol.* **2**, 807–817.

CAUGHEY, B., NEARY, K., BULLER, R., ERNST, D., PERRY, L. L., CHESEBRO, B. & RACE, R. E. (1990). Normal and scrapie-associated forms of prion protein differ in their sensitivities to phospholipase and proteases in intact neuroblastoma cells. *J. Virol.* **64**, 1093–1101.

CAUGHEY, B., RACE, R. E., ERNST, D., BUCHMEIER, M. J. & CHESEBRO, B. (1989). Prion protein biosynthesis in scrapie-infected and uninfected neuroblastoma cells. *J. Virol.* **63**, 175–181.

CAUGHEY, B., RAYMOND, G. J., ERNST, D. & RACE, R. E. (1991*b*). N-terminal truncation of the scrapie-associated form of PrP by lysosomal protease(s): implications regarding the site of conversion of PrP to the protease-resistant state. *J. Virol*. **65**, 6597–6603.

CAUGHEY, B. W., DONG, A., BHAT, K. S., ERNST, D., HAYES, S. F. & CAUGHEY, W. S. (1991*a*). Secondary structure analysis of the scrapie-associated protein PrP 27–30 in water by infrared spectroscopy. *Biochemistry* **30**, 7672–7680.

CAVANAGH, A. C. & MORTON, H. (1994). The purification of early-pregnancy factor to homogeneity from human platelets and identification as chaperonin 10. *Eur. J. Biochem*. **222**, 551–560.

CHABRY, J., CAUGHEY, B. & CHESEBRO, B. (1998). Specific inhibition of *in vitro* formation of protease-resistant prion protein by synthetic peptides. *J. Biol. Chem*. **273**, 13203–13207.

CHANDLER, R. L. (1963). Experimental scrapie in mouse. *Res. Vet. Sci.* **4**, 276–285.

CHATELLIER, J., BUCKLE, A. M. & FERSHT, A. R. (1999). GroEL recognises sequential and

non-sequential linear structural motifs compatible with extended β-strands and α-helices. *J. Mol. Biol.* **292**, 163–172.

CHATELLIER, J., HILL, F., LUND, P. A. & FERSHT, A. R. (1998). *In vivo* activities of GroEL minichaperones. *Proc. Natl. Acad. Sci. USA* **95**, 9861–9866.

COHEN, F. E., PAN, K.-M., HUANG, Z., BALDWIN, M., FLETTERICK, R. J. & PRUSINER, S. B. (1994). Structural clues to prion replication. *Science* **264**, 530–531.

COLLINGE, J., SIDLE, K. C. L., MEADS, J., IRONSIDE, J. & HILL, A. F. (1996). Molecular analysis of prion strain variation and the aetiology of 'new variant' CJD. *Nature* **383**, 685–690.

COLLINGE, J., WHITTINGTON, M. A., SIDLE, K. C., SMITH, C. J., PALMER, M. S., CLARKE, A. R. & JEFFERYS, J. G. (1994). Prion protein is necessary for normal synaptic function. *Nature* **370**, 295–297.

COME, J. H., FRASER, P. E. & LANSBURY, P. T., JR. (1993). A kinetic model for amyloid formation in the prion diseases: importance of seeding. *Proc. Natl. Acad. Sci. USA* **90**, 5959–5963.

CORRALES, F. J. & FERSHT, A. R. (1996*a*). Kinetic significance of $GroEL_{14}$–$(GroES_7)_2$ complexes in molecular chaperone activity. *Fold. Des.* **1**, 265–273.

CORRALES, F. J. & FERSHT, A. R. (1996*b*). Toward a mechanism for GroEL–GroES chaperone activity: an ATPase-gated and -pulsed folding and annealing cage. *Proc. Natl. Acad. Sci. USA* **93**, 4509–4512.

CROTTY, W. J. & LEDBETTER, M. C. (1973). Membrane continuities involving chloroplasts and other organelles in plant cells. *Science* **182**, 839–841.

DAHLSEID, J. N., LILL, R., GREEN, J. M., XU, X., QIU, Y. & PIERCE, S. K. (1994). PBP74, a new member of the mammalian 70-kDa heat shock protein family, is a mitochondrial protein. *Mol. Biol. Cell* **5**, 1265–1275.

DAUDE, N., LEHMANN, S. & HARRIS, D. A. (1997). Identification of intermediate steps in the conversion of a mutant prion protein to a scrapie-like form in cultured cells. *J. Biol. Chem*. **272**, 11604–11612.

DEARMOND, S. J., MCKINLEY, M. P., BARRY, R. A., BRAUNFELD, M. B., MCCOLLOCH, J. R. & PRUSINER, S. B. (1985). Identification of prion amyloid filaments in scrapie-infected brain. *Cell* **41**, 221–235.

DEARMOND, S. J., SÁNCHEZ, H., YEHIELY, F., QIU, Y., NINCHAK-CASEY, A., DAGGETT, V., CAMERINO, A. P., CAYETANO, J., ROGERS, M., GROTH, D., TORCHIA, M., TREMBLAY, P., SCOTT, M. R., COHEN, F. E. & PRUSINER, S. B. (1997). Selective neuronal targeting in prion disease. *Neuron* **19**, 1337–1348.

DEBBURMAN, S. K., RAYMOND, G. J., CAUGHEY, B. & LINDQUIST, S. (1997). Chaperone-supervised conversion of prion protein to its protease-resistant form. *Proc. Natl. Acad. Sci. USA* **94**, 13938–13943.

DE GIOIA, L., SELVAGGINI, C., GHIBAUDI, E., DIOMEDE, L., BUGIANI, O., FORLONI, G., TAGLIAVINI, F. & SALMONA, M. (1994). Conformational polymorphism of the amyloidogenic and neurotoxic peptide homologous to residues 106–126 of the prion protein. *J. Biol. Chem*. **269**, 7859–7862.

DIRINGER, H., GELDERBLOM, H., HILMERT, H., ÖZEL, M., EDELBLUTH, C., KIMBERLIN, R. H. (1983). Scrapie infectivity, fibrils and low molecular weight protein. *Nature* **306**, 476–478.

DOH-URA, K., TATEISHI, J., SASAKI, H., KITAMOTO, T. & SAKAKI, Y. (1989). Pro-leu change at

position 102 of prion protein is the most common but not the sole mutation related to Gerstmann-Sträussler syndrome. *Biochem. Biophys. Res. Commun*. **163**, 974–979.

DONNE, D. G., VILES, J. H., GROTH, D., MEHLHORN, I., JAMES, T. L., COHEN, F. E., PRUSINER, S. B., WRIGHT, P. E. & DYSON, H. J. (1997). Structure of the recombinant full-length hamster prion protein PrP(29–231): the N terminus is highly flexible. *Proc. Natl. Acad. Sci. USA* **94**, 13452–13457.

EDELMAN, A. M., BLUMENTHAL, D. K. & KREBS, E. G. (1987). Protein serine/threonine kinases. *Annu. Rev. Biochem*. **56**, 567–613.

EDENHOFER, F., RIEGER, R., FAMULOK, M., WENDLER, W., WEISS, S. & WINNACKER, E.-L. (1996). Prion protein PrP^C interacts with molecular chaperones of the Hsp60 family. *J. Virol.* **70**, 4724–4728.

EHRLICH, Y. H., DAVIS, T. B., BOCK, E., KORNECKI, E. & LENOX, R. H. (1986). Ecto-protein kinase activity on the external surface of neural cells. *Nature* **320**, 67–70.

EIGEN, M. (1996). Prionics or the kinetic basis of prion diseases. *Biophys. Chem*. **63**, A1–A18.

ELLIS, R. J. (1996). *The chaperonins.* San Diego: Academic Press.

ELLIS, R. J., VAN DER VIES, S. M. & HEMMINGSEN, S. M. (1989). The molecular chaperone concept. *Biochem. Soc. Symp*. **55**, 145–153.

ENDO, T., GROTH, D., PRUSINER, S. B. & KOBATA, A. (1989). Diversity of oligosaccharide structures linked to asparagines of the scrapie prion protein. *Biochemistry* **28**, 8380–8388.

FELDMAN, D. E. & FRYDMAN, J. (2000). Protein folding *in vivo*: the importance of molecular chaperones. *Curr. Opin. Struct. Biol.* **10**, 26–33.

FENTON, W. A. & HORWICH, A. L. (1997). GroEL-mediated protein folding. *Protein Sci.* **6**, 743–760.

FENTON, W. A., KASHI, Y., FURTAK, K. & HORWICH, A. L. (1994). Residues in chaperonin GroEL required for polypeptide binding and release. *Nature* **371**, 614–619.

FINK, A. L. (1999). Chaperone-mediated protein folding. *Physiol. Rev.* **79**, 425–449.

FINLAY, B. B. & FALKOW, S. (1997). Common themes in microbial pathogenicity revisited. *Microbiol. Mol. Biol. Rev*. **61**, 136–169.

FISCHER, M., RÜLICKE, T., RAEBER, A., SAILER, A., MOSER, M., OESCH, B., BRANDNER, S., AGUZZI, A. & WEISSMANN, C. (1996). Prion protein (PrP) with amino-proximal deletions restoring susceptibility of PrP knockout mice to scrapie. *EMBO J.* **15**, 1255–1264.

FORLONI, G., ANGERETTI, N., CHIESA, R., MONZANI, E., SALMONA, M., BUGIANI, O. & TAGLIAVINI, F. (1993). Neurotoxicity of a prion protein fragment. *Nature* **362**, 543–546.

FRASER, H. & DICKINSON, A. G. (1968). The sequential development of the brain lesion of scrapie in three strains of mice. *J. Comp. Pathol*. **78**, 301–311.

GABIZON, R., MCKINLEY, M. P., PRUSINER, S. B. (1987). Purified prion proteins and scrapie infectivity copartition into liposomes. *Proc. Natl. Acad. Sci. USA* **84**, 4017–4021.

GABIZON, R., TELLING, G., MEINER, Z., HALIMI, M., KAHANA, I. & PRUSINER, S. B. (1996). Insoluble wild-type and protease-resistant mutant prion protein in brains of patients with inherited prion disease. *Nat. Med*. **2**, 59–64.

GASSET, M., BALDWIN, M. A., FLETTERICK, R. J. & PRUSINER, S. B. (1993). Perturbation of the secondary structure of the scrapie prion protein under conditions that alter infectivity. *Proc. Natl. Acad. Sci. USA* **90**, 1–5.

GASSET, M., BALDWIN, M. A., LLOYD, D. H., GABRIEL, J.-M., HOLTZMAN, D. M., COHEN, F.,

FLETTERICK, R. & PRUSINER, S. B. (1992). Predicted α-helical regions of the prion protein when synthesized as peptides form amyloid. *Proc. Natl. Acad. Sci. USA* **89**, 10940–10944.

GEIGER, T. & CLARKE, S. (1987). Deamidation, isomerization, and racemization at asparaginyl and aspartyl residues in peptides. Succinimide-linked reactions that contribute to protein degradation. *J. Biol. Chem*. **262**, 785–794.

GHETTI, B., PICCARDO, P., FRANGIONE, B., BUGIANI, O., GIACCONE, G., YOUNG, K., PRELLI, F., FARLOW, M. R., DLOUHY, S. R. & TAGLIAVINI, F. (1996). Prion protein amyloidosis. *Brain Pathol*. **6**, 127–145.

GIBBS, C. J., JR., GAJDUSEK, D. C. & LATARJET, R. (1978). Unusual resistance to ionizing radiation of the viruses of kuru, Creutzfeldt-Jakob disease, and scrapie. *Proc. Natl. Acad. Sci USA* **75**, 6268–6270.

GLOCKSHUBER, R., HORNEMANN, S., RIEK, R., WIDER, G., BILLETER, M. & WÜTHRICH, K. (1997). Three-dimensional NMR structure of a self-folding domain of the prion protein PrP(121–231). *Trends Biochem. Sci.* **22**, 241–242.

GOLBIK, R., ZAHN, R., HARDING, S. E. & FERSHT, A. R. (1998). Thermodynamic stability and folding of GroEL minichaperones. *J. Mol. Biol*. **276**, 505–515.

GOLDFARB, L. G., BROWN, P., HALTIA, M., GHISO, J., FRANGIONE, B. & GAJDUSEK, D. C. (1993). Synthetic peptides corresponding to different mutated regions of the amyloid gene in familial Creutzfeldt-Jakob disease show enhanced *in vitro* formation of morphologically different amyloid fibrils. *Proc. Natl. Acad. Sci. USA* **90**, 4451–4454.

GOLDGABER, D., GOLDFARB, L. G., BROWN, P., ASHER, D. M., BROWN, W. T., LIN, S., TEENER, J. W., FEINSTONE, S. M., RUBENSTEIN, R., KASCSAK, R. J., BOELLAARD, J. W. & GAJDUSEK D. C. (1989). Mutations in familial Creutzfeldt-Jakob disease and Gerstmann-Sträussler-Scheinker's syndrome. *Exp. Neurol.* **106**, 204–206.

GOLOUBINOFF, P., CHRISTELLER, J. T., GATENBY, A. A. & LORIMER, G. H. (1989). Reconstitution of active dimeric ribulose biphosphate carboxylase from an unfolded state depends on two chaperonin proteins and Mg–ATP. *Nature* **342**, 884–889.

GOORMAGHTIGH, E., CABIAUX, V. & RUYSSCHAERT, J. M. (1990). Secondary structure and dosage of soluble and membrane proteins by attenuated total reflection Fourier-transform infrared spectroscopy on hydrated films. *Eur. J. Biochem*. **193**, 409–420.

GORODINSKY, A. & HARRIS, D. A. (1995). Glycolipid-anchored proteins in neuroblastoma cells form detergent-resistant complexes without caveolin. *J. Cell Biol*. **129**, 619–627.

GOTTESMAN, M. E. & HENDRICKSON. W. A. (2000). Protein folding and unfolding by *Escherichia coli* chaperones and chaperonins. *Curr. Opin. Microbiol*. **3**, 197–202.

GRAY, T. E. & FERSHT, A. R. (1991). Cooperativity in ATP hydrolysis by GroEL is increased by GroES. *FEBS Lett*. **292**, 254–258.

GRIFFITH, J. S. (1967). Self-replication and scrapie. *Nature* **215**, 1043–1044.

GUERMEUR, Y. (1997). *Combinaison de classifieurs statistiques, application à la prédiction de la structure secondaire des protéines*. Thèse da Doctorat de l'Université Paris 6, Paris.

HARAGUCHI, T., FISHER, S., OLOFSSON, S., ENDO, T., GROTH, D., TARENTINO, A., BORCHELT, D. R., TEPLOW, D., HOOD, L., BURLINGAME, A., LYCKE, E., KOBATA, A. & PRUSINER, S. B. (1989). Asparagine-linked glycosylation of the scrapie and cellular prion proteins. *Arch. Biochem. Biophys*. **274**, 1–13.

HARMEY, J. H., DOYLE, D., BROWN, V. & ROGERS, M. S. (1995). The cellular isoform of the

prion protein, PrP^C, is associated with caveolae in mouse neuroblastoma (N_2a) cells. *Biochem. Biophys. Res. Commun*. **210**, 753–759.

HARRIS, D. A., GORODINSKY, A., LEHMANN, S., MOULDER, K. & SHYNG, S. L. (1996). Cell biology of the prion protein. *Curr. Top. Microbiol. Immunol.* **207**, 77–93.

HARTL, F. U. (1996). Molecular chaperones in cellular protein folding. *Nature* **381**, 571–580.

HARTTER, D. E. & BARNEA, A. (1988). Brain tissue accumulates ^{67}Copper by two ligand-dependent saturable processes. A high affinity, low capacity and a low affinity, high capacity process. *J. Biol. Chem*. **263**, 799–805.

HAY, B., BARRY, R. A., LIEBERBURG, I., PRUSINER, S. B. & LINGAPPA, V. R. (1987*a*). Biogenesis and transmembrane orientation of the cellular isoform of the scrapie prion protein. *Mol. Cell. Biol.* **7**, 914–920.

HAY, B., PRUSINER, S. B. & LINGAPPA, V. R. (1987*b*). Evidence for a secretory form of the cellular prion protein. *Biochemistry* **26**, 8110–8115.

HAYER-HARTL, M. K., EWBANK, J. J., CREIGHTON, T. E. & HARTL, F. U. (1994). Conformational specificity of the chaperonin GroEL for the compact folding intermediates of α-lactalbumin. *EMBO J.* **13**, 3192–3202.

HAYER-HARTL, M. K., EWALT, K. L. & HARTL, F. U. (1999). On the role of symmetrical and asymmetrical chaperonin complexes in assisted protein folding. *Biol. Chem*. **380**, 531–540.

HECKER, R., TARABOULOS, A., SCOTT, M., PAN, K.-M., YANG, S.-L., TORCHIA, M., JENDROSKA, K., DEARMOND, S. J. & PRUSINER, S. B. (1992). Replication of distinct scrapie prion isolates is region specific in brains of transgenic mice and hamsters. *Genes Dev.* **6**, 1213–1228.

HEGDE, R. S., MASTRIANNI, J. A., SCOTT, M. R., DEFEA, K. A., TREMBLAY, P., TORCHIA, M., DEARMOND, S. J., PRUSINER, S. B. & LINGAPPA, V. R. (1998). A transmembrane form of the prion protein in neurodegenerative disease. *Science* **279**, 827–834.

HEGDE, R. S., TREMBLAY, P., GROTH, D., DEARMOND, S. J., PRUSINER, S. B. & LINGAPPA, V. R. (1999). Transmissible and genetic prion diseases share a common pathway of neurodegeneration. *Nature* **402**, 822–826.

HELLER, J., KOLBERT, A. C., LARSEN, R., ERNST, M., BEKKER, T., BALDWIN, M., PRUSINER, S. B., PINES, A. & WEMMER, D. E. (1996). Solid-state NMR studies of the prion protein H1 fragment. *Protein Sci.* **5**, 1655–1661.

HERRMANN, L. M. & CAUGHEY, B. (1998). The importance of the disulfide bond in prion protein conversion. *Neuroreport* **9**, 2457–2461.

HILL, A. F., ANTONIOU, M. & COLLINGE, J. (1999). Protease-resistant prion protein produced *in vitro* lacks detectable infectivity. *J. Gen. Virol*. **80**, 11–14.

HOPE, J., MORTON, L. J. D., FARQUHAR, C. F., MULTHAUP, G., BEYREUTHER, K. & KIMBERLIN, R. H. (1986). The major polypeptide of scrapie-associated fibrils (SAF) has the same size, charge distribution and N-terminal protein sequence as predicted for the normal brain protein (PrP). *EMBO J.* **5**, 2591–2597.

HOPE, J., MULTHAUP, G., REEKIE, L. J. D., KIMBERLIN, R. H. & BEYREUTHER, K. (1988). Molecular pathology of scrapie-associated fibril protein (PrP) in mouse brain affected by the ME7 strain of scrapie. *Eur. J. Biochem*. **172**, 271–277.

HORIUCHI, M. & CAUGHEY, B. (1999*a*). Specific binding of normal prion protein to the scrapie form via a localized domain initiates its conversion to the protease-resistant state. *EMBO J.*

18, 3193–3203.

HORIUCHI, M. & CAUGHEY, B. (1999*b*). Prion protein interconversions and the transmissible spongiform encephalopathies. *Structure Fold. Des.* **7,** R231–R240.

HORNEMANN, S. & GLOCKSHUBER, R. (1996). Autonomous and reversible folding of a soluble amino-terminally truncated segment of the mouse prion protein. *J. Mol. Biol.* **261**, 614–619.

HORNEMANN, S. & GLOCKSHUBER, R. (1998). A scrapie-like unfolding intermediate of the prion protein domain PrP(121–231) induced by acidic pH. *Proc. Natl. Acad. Sci. USA* **95**, 6010–6014.

HORNSHAW, M. P., MCDERMOTT, J. R. & CANDY, J. M. (1995). Copper binding to the N-terminal tandem repeat regions of mammalian and avian prion protein. *Biochem. Biophys. Res. Commun.* **207**, 621–629.

HSIAO, K., BAKER, H. F., CROW, T. J., POULTER, M., OWEN, F., TERWILLIGER, J. D., WESTAWAY, D., OTT, J. & PRUSINER, S. B. (1989). Linkage of a prion protein missense variant to Gerstmann-Sträussler syndrome. *Nature* **338**, 342–345.

HSIAO, K. K., CASS, C., SCHELLENBERG, G. D., BIRD, T., DEVINE-GAGE, E., WISNIEWSKI, H. & PRUSINER, S. B. (1991). A prion protein variant in a family with the telencephalic form of Gerstmann-Sträussler-Scheinker syndrome. *Neurology* **41**, 681–684.

HSIAO, K. K., GROTH, D., SCOTT, M., YANG, S.-L., SERBAN, H., RAPP, D., FOSTER, D., TORCHIA, M., DEARMOND, S. J. & PRUSINER, S. B. (1994). Serial transmission in rodents of neurodegeneration from transgenic mice expressing mutant prion protein. *Proc. Natl. Acad. Sci. USA* **91**, 9126–9130.

HSIAO, K. K., SCOTT, M., FOSTER, D., GROTH, D. F., DEARMOND, S. J. & PRUSINER, S. B. (1990). Spontaneous neurodegeneration in transgenic mice with mutant prion protein. *Science* **250**, 1587–1590.

HUANG, Z., GABRIEL, J.-M., BALDWIN, M. A., FLETTERICK, R. J., PRUSINER, S. B. & COHEN, F. E. (1994). Proposed three-dimensional structure for the cellular prion protein. *Proc. Natl. Acad. Sci. USA* **91**, 7139–7143.

HUANG, Z., PRUSINER, S. B. & COHEN, F. E. (1995). Scrapie prions: a three-dimensional model of an infectious fragment. *Fold. Des*. **1**, 13–19.

HUNG, A. Y. & SELKOE, D. J. (1994). Selective ectodomain phosphorylation and regulated cleavage of beta-amyloid precursor protein. *EMBO J.* **13**, 534–542.

HUNT, J. F., WEAVER, A. J., LANDRY, S. J., GIERASCH, L. & DEISENHOFER, J. (1996). The crystal structure of the GroES co-chaperonin at 2.8 Å resolution. *Nature* **379**, 37–45.

IKAWA, S. & WEINBERG, R. A. (1992). An interaction between $p21^{ras}$ and heat shock protein hsp60, a chaperonin. *Proc. Natl. Acad. Sci. USA* **89**, 2012–2016.

INOUYE, H. & KIRSCHNER, D. A. (1997). X-ray diffraction analysis of scrapie prion: intermediate and folded structures in a peptide containing two putative α-helices. *J. Mol. Biol*. **268**, 375–389.

INOUYE, H. & KIRSCHNER, D. A. (1998). Polypeptide chain folding in the hydrophobic core of hamster scrapie prion: analysis by X-ray diffraction. *J. Struct. Biol*. **122**, 247–255.

ITZHAKI, L. S., OTZEN, D. E. & FERSHT, A. R. (1995). Nature and consequences of GroEL–protein interactions. *Biochemistry* **34**, 14581–14587.

JACKSON, G. S., HILL, A. F., JOSEPH, C., HOSSZU, L., POWER, A., WALTHO, J. P., CLARKE, A. R. & COLLINGE, J. (1999*a*). Multiple folding pathways for heterologously expressed human

prion protein. *Biochim. Biophys. Acta* **1431**, 1–13.

JACKSON, G. S., HOSSZU, L. L., POWER, A., HILL, A. F., KENNEY, J., SAIBIL, H., CRAVEN, C. J., WALTHO, J. P., CLARKE, A. R. & COLLINGE, J. (1999*b*). Reversible conversion of monomeric human prion protein between native and fibrilogenic conformations. *Science* **283**, 1935–1937.

JACKSON, G. S., STANIFORTH, R. A., HALSALL, D. J., ATKINSON, T., HOLBROOK, J. J., CLARKE, A. R. & BURSTON, S. G. (1993). Binding and hydrolysis of nucleotides in the chaperonin catalytic cycle: implications for the mechanism of assisted protein folding. *Biochemistry* **32**, 2554-2563.

JAENICKE, R. & RUDOLPH, R. (1986). Refolding and association of oligomeric proteins. *Methods Enzymol*. **131**, 218–250.

JAMES, T. L., LIU, H., ULYANOV, N. B., FARR-JONES, S., ZHANG, H., DONNE, D. G., KANEKO, K., GROTH, D., MEHLHORN, I., PRUSINER, S. B. & COHEN, F. E. (1997). Solution structure of a 142-residue recombinant prion protein corresponding to the infectious fragment of the scrapie isoform. *Proc. Natl. Acad. Sci. USA* **94**, 10086–10091.

JARRETT, J. T. & LANSBURY, P. T., JR. (1993). Seeding "one-dimensional crystallization" of amyloid: a pathogenic mechanism in Alzheimer's disease and scrapie? *Cell* **73**, 1055–1058.

JONES, M., GUPTA, R. S. & ENGLESBERG, E. (1994). Enhancement in amount of P1 (hsp60) in mutants of Chinese hamster ovary (CHO–K1) cells exhibiting increases in the A system of amino acid transport. *Proc. Natl. Acad. Sci. USA* **91**, 858–862.

KAMMER, G. M., KHAN, I. U. & MALEMUD, C. J. (1994). Deficient type I protein kinase A isozyme activity in systemic lupus erythematosus T lymphocytes. *J. Clin. Invest*. **94**, 422–430.

KANEKO, K., PERETZ, D., PAN, K.-M., BLOCHBERGER, T. C., WILLE, H., GABIZON, R., GRIFFITH, O. H., COHEN, F. E., BALDWIN, M. A. & PRUSINER, S. B. (1995). Prion protein (PrP) synthetic peptides induce cellular PrP to acquire properties of the scrapie isoform. *Proc. Natl. Acad. Sci. USA* **92**, 11160–11164.

KANEKO, K., VEY, M., SCOTT, M., PILKUHN, S., COHEN, F. E. & PRUSINER, S. B. (1997*a*). COOH-terminal sequence of the cellular prion protein directs subcellular trafficking and controls conversion into the scrapie isoform. *Proc. Natl. Acad. Sci. USA* **94**, 2333–2338.

KANEKO, K., WILLE, H., MEHLHORN, I., ZHANG, H., BALL, H., COHEN, F. E., BALDWIN, M. A. & PRUSINER, S. B. (1997*b*). Molecular properties of complexes formed between the prion protein and synthetic peptides. *J. Mol. Biol.* **270**, 574–586.

KANEKO, K., ZULIANELLO, L., SCOTT, M., COOPER, C. M., WALLACE, A. C., JAMES, T. L., COHEN, F. E. & PRUSINER, S. B. (1997*c*). Evidence for protein X binding to a discontinuous epitope on the cellular prion protein during scrapie prion propagation. *Proc. Natl. Acad. Sci. USA* **94**, 10069–10074.

KASCSAK, R. J., RUBENSTEIN, R., MERZ, P. A., CARP, R. I., ROBAKIS, N. K., WISNIEWSKI, H. M. & DIRINGER, H. (1986). Immunological comparison of scrapie-associated fibrils isolated from animals infected with four different scrapie strains. *J. Virol.* **59**, 676–683.

KASCSAK, R. J., RUBENSTEIN, R., MERZ, P. A., TONNA-DEMASI, M., FERSKO, R., CARP, R. I., WISNIEWSKI, H. M. & DIRINGER, H. J. (1987). Mouse polyclonal and monoclonal antibody to scrapie-associated fibril proteins. *Virol*. **61**, 3688–3693.

KELLINGS, K., MEYER, N., MIRENDA, C., PRUSINER, S. B. & RIESNER, D. (1992). Further

analysis of nucleic acids in purified scrapie prion preparations by improved return refocusing gel electrophoresis. *J. Gen. Virol.* **73**, 1025–1029.

KELLINGS, K., PRUSINER, S. B. & RIESNER, D. (1994). Nucleic acids in prion preparations: unspecific background or essential component? *Philos. Trans. R. Soc. Lond. B* **343**, 425–430.

KERN, G., SCHMIDT, M., BUCHNER, J. & JAENICKE, R. (1992). Glycosylation inhibits the interaction of invertase with the chaperone GroEL. *FEBS Lett*. **305**, 203–205.

KHAN, I. U., WALLIN, R., GUPTA, R. S. & KAMMER, G. M. (1998). Protein kinase A-catalyzed phosphorylation of heat shock protein 60 chaperone regulates its attachment to histone 2B in the T lymphocyte plasma membrane. *Proc. Natl. Acad. Sci. USA* **95**, 10425–10430.

KIMBERLIN, R. H. & WALKER, C. A. (1978). Evidence that the transmission of one source of scrapie agent to hamsters involves separation of agent strains from a mixture. *J. Gen. Virol*. **39**, 487–496.

KIMBERLIN, R. H., COLE, S. & WALKER, C. A. (1987). Temporary and permanent modifications to a single strain of mouse scrapie on transmission to rats and hamsters. *J. Gen. Virol*. **68**, 1875–1881.

KIMBERLIN, R. H., WALKER, C. A. & FRASER, H. (1989). The genomic identity of different strains of mouse scrapie is expressed in hamsters and preserved on reisolation in mice. *J. Gen. Virol.* **70**, 2017–2025.

KITAMOTO, T., IIZUKA, R. & TATEISHI, J. (1993). An amber mutation of prion protein in Gerstmann-Sträussler syndrome with mutant PrP plaques. *Biochem. Biophys. Res. Commun*. **192**, 525–531.

KOBAYASHI, N., FREUND, S. M. V., CHATELLIER, J., ZAHN, R. & FERSHT, A. R. (1999). NMR analysis of the binding of a rhodanese peptide to a minichaperone in solution. *J. Mol. Biol.* **292**, 181–190.

KOCISKO, D. A., COME, J. H., PRIOLA, S. A., CHESEBRO, B., RAYMOND, G. J., LANSBURY, P. T. & CAUGHEY, B. (1994). Cell-free formation of protease-resistant prion protein. *Nature* **370**, 471–474.

KOCISKO, D. A., PRIOLA, S. A., RAYMOND, G. J., CHESEBRO, B., LANSBURY, P. T., JR. & CAUGHEY, B. (1995). Species specificity in the cell-free conversion of prion protein to protease-resistant forms: a model for the scrapie species barrier. *Proc. Natl. Acad. Sci. USA* **92**, 3923–3927.

KORADI, R., BILLETER, M. & WÜTHRICH, K. (1996). MOLMOL: a program for display and analysis of macromolecular structures. *J. Mol. Graph*. **14**, 51–55.

KORTH, C., STIERLI, B., STREIT, P., MOSER, M., SCHALLER, O., FISCHER, R., SCHULZ-SCHAEFFER, W., KRETZSCHMAR, H., RAEBER, A., BRAUN, U., EHRENSPERGER, F., HORNEMANN, S., GLOCKSHUBER, R., RIEK, R., BILLETER, M., WÜTHRICH, K. & OESCH, B. (1997). Prion (PrP^{Sc})-specific epitope defined by a monoclonal antibody. *Nature* **390**, 74–77.

KORTH, C., STREIT, P. & OESCH, B. (1999). Monoclonal antibodies specific for the native, disease-associated isoform of the prion protein. *Methods Enzymol.* **309**, 106–122.

KRETZSCHMAR, H. A., HONOLD, G., SEITELBERGER, F., FEUCHT, M., WESSELY, P., MEHRAEIN, P. & BUDKA, H. (1991). Prion protein mutation in family first reported by Gerstmann, Sträussler, and Scheinker. *Lancet* **337**, 1160.

KRETZSCHMAR, H. A., PRUSINER, S. B., STOWRING, L. E. & DEARMOND, S. J. (1986). Scrapie prion proteins are synthesized in neurons. *Am. J. Pathol.* **122**, 1–5.

KUNZ, B., SANDMEIER, E. & CHRISTEN, P. (1999). Neurotoxicity of prion peptide 106–126 not confirmed. *FEBS Lett.* **458**, 65–68.

KUWAJIMA, K. (1989). The molten globule state as a clue for understanding the folding and cooperativity of globular-protein structure. *Proteins* **6**, 87–103.

LAMINET, A. A., ZIEGELHOFFER, T., GEORGOPOULOS, C. & PLÜCKTHUN, A. (1990). The *Escherichia coli* heat shock proteins GroEL and GroES modulate the folding of the β-lactamase precursor. *EMBO J.* **9**, 2315–2319.

LANDRY, S. J., ZEILSTRA-RYALLS, J., FAYET, O., GEORGOPOULOS, C. & GIERASCH, L. M. (1993). Characterization of a functionally important mobile domain of GroES. *Nature* **364**, 255–258.

LANGER, T., LU, C., ECHOLS, H., FLANAGAN, J., HAYER, M. K. & HARTL, F. U. (1992). Successive action of DnaK, DnaJ and GroEL along the pathway of chaperone-mediated protein folding. *Nature* **356**, 683–689.

LATARJET, R., MUEL, B., HAIG, D. A., CLARKE, M. C. & ALPER, T. (1970). Inactivation of the scrapie agent by near monochromatic ultraviolet light. *Nature* **227**, 1341–1343.

LAXMINARAYANA, D., BERRADA, A. & KAMMER, G. M. (1993). Early events of human T lymphocyte activation are associated with type I protein kinase A activity. *J. Clin. Invest*. **92**, 2207–2214.

LEE, R. J., WANG, S. & LOW, P. S. (1996). Measurement of endosome pH following folate receptor-mediated endocytosis. *Biochim. Biophys. Acta* **1312**, 237–242.

LEHMANN, S. & HARRIS, D. A. (1995). A mutant prion protein displays an aberrant membrane association when expressed in cultured cells. *J. Biol. Chem*. **270**, 24589–24597.

LEHMANN, S. & HARRIS, D. A. (1996*a*). Mutant and infectious prion proteins display common biochemical properties in cultured cells. *J. Biol. Chem*. **271**, 1633–1637.

LEHMANN, S. & HARRIS, D. A. (1996*b*). Two mutant prion proteins expressed in cultured cells acquire biochemical properties reminiscent of the scrapie isoform. *Proc. Natl. Acad. Sci. USA* **93**, 5610–5614.

LEHMANN, S. & HARRIS, D. A. (1997). Blockade of glycosylation promotes acquisition of scrapie-like properties by the prion protein in cultured cells. *J. Biol. Chem*. **272**, 21479–21487.

LIEMANN, S. & GLOCKSHUBER, R. (1999). Influence of amino acid substitutions related to inherited human prion diseases on the thermodynamic stability of the cellular prion protein. *Biochemistry* **38**, 3258–3267.

LINDER, M. C. (1991). *Biochemistry of Copper*. New York: Plenum.

LI, Z., CLARKE, A. J. & BEVERIDGE, T. J. (1998). Gram-negative bacteria produce membrane vesicles which are capable of killing other bacteria. *J. Bacteriol*. **180**, 5478–5483.

LIU, H., FARR-JONES, S., ULYANOV, N. B., LLINAS, M., MARQUSEE, S., GROTH, D., COHEN, F. E., PRUSINER, S. B. & JAMES, T. L. (1999*a*). Solution structure of Syrian hamster prion protein rPrP(90–231). *Biochemistry* **38**, 5362–5377.

LIU, A., RIEK, R., ZAHN, R., HORNEMANN, S., GLOCKSHUBER, R & WÜTHRICH, K. (1999*b*). Peptides and proteins in neurodegenerative disease: helix propensity of a polypeptide containing helix 1 of the mouse prion protein studied by NMR and CD spectroscopy. *Biopolymers* **51**, 145–152.

LLEDO, P. M., TREMBLAY, P., DEARMOND, S. J., PRUSINER, S. B. & NICOLL, R. A. (1996). Mice

deficient for prion protein exhibit normal neuronal excitability and synaptic transmission in the hippocampus. *Proc. Natl. Acad. Sci. USA* **93**, 2403–2407.

LOPEZ, C. D., YOST, C. S., PRUSINER, S. B., MYERS, R. M. & LINGAPPA, V. R. (1990). Unusual topogenic sequence directs prion protein biogenesis. *Science* **248**, 226–229.

LUO, G. X. & HOROWITZ, P. M. (1993). The folding and stability of rhodanese are influenced by the replacement of glutamic acid 17 in the NH_2-terminal helix by proline but not by glutamine. *J. Biol. Chem*. **268**, 10246–10251.

MANSON, J., WEST, J. D., THOMSON, V., MCBRIDE, P., KAUFMAN, M. H. & HOPE, J. (1992). The prion protein gene: a role in mouse embryogenesis? *Development* **115**, 117–122.

MARTIN, J., LANGER, T., BOTEVA, R., SCHRAMEL, A., HORWICH, A. L. & HARTL, F.-U. (1991). Chaperonin-mediated protein folding at the surface of groEL through a 'molten globule'-like intermediate. *Nature* **352**, 36–42.

MARTINS, V. R., GRANER, E., GARCIA-ABREU, J., DE SOUZA, S. J., MERCADANTE, A. F., VEIGA, S. S., ZANATA, S. M., NETO, V. M. & BRENTANI, R. R. (1997). Complementary hydropathy identifies a cellular prion protein receptor. *Nat. Med*. **3**, 1376–1382.

MAYHEW, M., DA SILVA, A. C. R., MARTIN, J., ERDJUMENT-BROMAGE, H., TEMPST, P. & HARTL, F. U. (1996). Protein folding in the central cavity of the GroEL–GroES chaperonin complex. *Nature* **379**, 420–426.

MCKINLEY, M. P., BOLTON, D. C. & PRUSINER, S. B. (1983). A protease-resistant protein is a structural component of the scrapie prion. *Cell* **35**, 57–62.

MCKINLEY, M. P., MASIARZ, F. R. & PRUSINER, S. B. (1981). Reversible chemical modification of the scrapie agent. *Science* **214**, 1259–1261.

MCKINLEY, M. P., MEYER, R. K., KENAGA, L., RAHBAR, F., COTTER, R., SERBAN, A. & PRUSINER, S. B. (1991*a*). Scrapie prion rod formation in vitro requires both detergent extraction and limited proteolysis. *J. Virol*. **65**, 1340–1351.

MCKINLEY, M. P., TARABOULOS, A., KENAGA, L., SERBAN, D., STIEBER, A., DEARMOND, S. J., PRUSINER, S. B. & GONATAS, N. (1991*b*). Ultrastructural localization of scrapie prion proteins in cytoplasmic vesicles of infected cultured cells. *Lab. Invest*. **65**, 622–630.

MEHLHORN, I., GROTH, D., STÖCKEL, J., MOFFAT, B., REILLY, D., YANSURA, D., WILLETT, W. S., BALDWIN, M., FLETTERICK, R., COHEN, F. E., VANDLEN, R., HENNER, D. & PRUSINER, S. B. (1996). High-level expression and characterization of a purified 142-residue polypeptide of the prion protein. *Biochemistry* **35**, 5528–5537.

MENDOZA, J.A., BUTLER, M. C. & HOROWITZ, P. M. (1992). Characterization of a stable, reactivatable complex between chaperonin 60 and mitochondrial rhodanese. *J. Biol. Chem*. **267**, 24648–24654.

MENDOZA, J. A., LORIMER, G. H. & HOROWITZ, P. M. (1991). Intermediates in the chaperonin-assisted refolding of rhodanese are trapped at low temperature and show a small stoichiometry. *J. Biol. Chem*. **266**, 16973–16976.

MERZ, P. A., KASCSAK, R. J., RUBENSTEIN, R., CARP, R. I. & WISNIEWSKI, H. M. (1987). Antisera to scrapie-associated fibril protein and prion protein decorate scrapie-associated fibrils. *J. Virol*. **61**, 42–49.

MERZ, P. A., ROHWER, R. G., KASCSAK, R., WISNIEWSKI, H. M., SOMERVILLE, R. A., GIBBS, C. J., JR. & GAJDUSEK, D. C. (1984). Infection-specific particle from the unconventional slow virus diseases. *Science* **225**, 437–440.

MERZ, P. A., SOMERVILLE, R. A., WISNIEWSKI, H. M. & IQBAL, K. (1981). Abnormal fibrils from scrapie-infected brain. *Acta Neuropathol.* **54**, 63–74.

MERZ, P. A., SOMERVILLE, R. A., WISNIEWSKI, H. M., MANUELIDIS, L. & MANUELIDIS, E. E. (1983). Scrapie-associated fibrils in Creutzfeldt-Jakob disease. *Nature* **306**, 474–476.

MEYER, R. K., MCKINLEY, M. P., BOWMAN, K. A., BRAUNFELD, M. B., BARRY, R. A. & PRUSINER, S. B. (1986). Separation and properties of cellular and scrapie prion proteins. *Proc. Natl. Acad. Sci. USA* **83**, 2310–2314.

MIURA, T., HORI-I, A. & TAKEUCHI, H. (1996). Metal-dependent α-helix formation promoted by the glycine-rich octapeptide region of prion protein. *FEBS Lett.* **396**, 248–252.

MOBLEY, W. C., NEVE, R. L., PRUSINER, S. B. & MCKINLEY, M. P. (1988). Nerve growth factor increases mRNA levels for the prion protein and the β-amyloid protein precursor in developing hamster brain. *Proc. Natl. Acad. Sci. USA* **85**, 9811–9815.

MOFFETT, J., MENDIAZ, E., JONES, M. & ENGLESBERG, E. (1988). Two membrane-bound proteins associated with alanine resistance and increased A-system amino acid transport in mutants of CHO–K1. *Somat. Cell Mol. Genet.* **14**, 1–12.

MONARI, L., CHEN, S. G., BROWN, P., PARCHI, P., PETERSEN, R. B., MIKOL, J., GRAY, F., CORTELLI, P., MONTAGNA, P., GHETTI, B., GOLDFARB, L. G., GAJDUSEK, D. C., LUGARESI, E., GAMBETTI, P. & AUTILIO-GAMBETTI, L. (1994). Fatal familial insomnia and familial Creutzfeldt-Jakob disease: different prion proteins determined by a DNA polymorphism. *Proc. Natl. Acad. Sci. USA* **91**, 2839–2842.

MOORE, R. (1997). *Gene targeting studies at the mouse prion protein locus*, PhD thesis, University of Edinburgh, Edinburgh, Scotland.

MOORE, R. C., LEE, I. Y., SILVERMAN, G. L., HARRISON, P. M., STROME, R., HEINRICH, C., KARUNARATNE, A., PASTERNAK, S. H., CHISHTI, M. A., LIANG, Y., MASTRANGELO, P., WANG, K., SMIT, A. F. A., KATAMINE, S., CARLSON, G. A., COHEN, F. E., PRUSINER, S. B., MELTON, D. W., TREMBLAY, P., HOOD, L. E. & WESTAWAY, D. (1999). Ataxia in prion protein (PrP)-deficient mice is associated with upregulation of the novel PrP-like protein doppel. *J. Mol. Biol.* **292**, 797–817.

MURAMOTO, T., DEARMOND, S. J., SCOTT, M., TELLING, G. C., COHEN, F. E. & PRUSINER, S. B. (1997). Heritable disorder resembling neuronal storage disease in mice expressing prion protein with deletion of an α-helix. *Nat. Med.* **3**, 750–755.

MURAMOTO, T., SCOTT, M., COHEN, F. E. & PRUSINER, S. B. (1996). Recombinant scrapie-like prion protein of 106 amino acids is soluble. *Proc. Natl. Acad. Sci. USA* **93**, 15457–15462.

MUSGROVE,. J. E. & ELLIS, R. J. (1986). The rubisco large subunit binding protein. *Phil. Trans. R. Soc. Lond. B* **313**, 419–428.

NARWA, R. & HARRIS, D. A. (1999). Prion proteins carrying pathogenic mutations are resistant to phospholipase cleavage of their glycolipid anchors. *Biochemistry* **38**, 8770–8777.

NASLAVSKY, N., SHMEEDA, H., FRIEDLANDER, G., YANAI, A., FUTERMAN, A. H., BARENHOLZ, Y. & TARABOULOS, A. (1999). Sphingolipid depletion increases formation of the scrapie prion protein in neuroblastoma cells infected with prions. *J. Biol. Chem*. **274**, 20763–20771.

NASLAVSKY, N., STEIN, R., YANAI, A., FRIEDLANDER, G. & TARABOULOS, A. (1997). Characterization of detergent-insoluble complexes containing the cellular prion protein and its scrapie isoform. *J. Biol. Chem*. **272**, 6324–6331.

NETZER, W. J. & HARTL, F. U. (1998). Protein folding in the cytosol: chaperonin-dependent and

-independent mechanisms. *Trends Biochem. Sci.* **23**, 68–73.

NGUYEN, J., BALDWIN, M. A., COHEN, F. E. & PRUSINER, S. B. (1995*a*). Prion protein peptides induce α-helix to β-sheet conformational transitions. *Biochemistry* **34**, 4186–4192.

NGUYEN, J. T., INOUYE, H., BALDWIN, M. A., FLETTERICK, R. J., COHEN, F. E., PRUSINER, S. B. & KIRSCHNER, D. A. (1995*b*). X-ray diffraction of scrapie prion rods and PrP peptides. *J. Mol. Biol*. **252**, 412–422.

NITRINI, R., ROSEMBERG, S., PASSOS-BUENO, M. R., DA SILVA, L. S., IUGHETTI, P., PAPADOPOULOS, M., CARRILHO, P. M., CARAMELLI, P., ALBRECHT, S., ZATZ, M. & LEBLANC, A. (1997). Familial spongiform encephalopathy associated with a novel prion protein gene mutation. *Ann. Neurol.* **42**, 138–146.

OESCH, B., WESTAWAY, D., WÄLCHLI, M., MCKINLEY, M. P., KENT, S. B. H., AEBERSOLD, R., BARRY, R. A., TEMPST, P., TEPLOW, D. B., HOOD, L. E., PRUSINER, S. B. & WEISSMANN, C. (1985). A cellular gene encodes scrapie PrP 27–30 protein. *Cell* **40**, 735–746.

PAN, K.-M., BALDWIN, M., NGUYEN, J., GASSET, M., SERBAN, A., GROTH, D., MEHLHORN, I., HUANG, Z., FLETTERICK, R. J., COHEN, F. E. & PRUSINER, S. B. (1993). Conversion of α-helices into β-sheets features in the formation of the scrapie prion proteins. *Proc. Natl. Acad. Sci. USA* **90**, 10962–10966.

PAN, K.-M., STAHL, N. & PRUSINER, S. B. (1992). Purification and properties of the cellular prion protein from Syrian hamster brain. *Protein Sci.* **1**, 1343–1352.

PARCHI, P. & GAMBETTI, P. (1995). Human prion diseases. *Curr. Opin. Neurol.* **8**, 286–293.

PARCHI, P., CASTELLANI, R., CAPELLARI, S., GHETTI, B., YOUNG, K., CHEN, S. G., FARLOW, M., DICKSON, D. W., SIMA, A. A., TROJANOWSKI, J. Q., PETERSEN, R. B. & GAMBETTI, P. (1996). Molecular basis of phenotypic variability in sporadic Creutzfeldt-Jakob disease. *Ann. Neurol*. **39**, 767–778.

PARGE, H. E., HALLEWELL, R. A. & TAINER, J. A. (1992). Atomic structures of wild-type and thermostable mutant recombinant human Cu,Zn superoxide dismutase. *Proc. Natl. Acad. Sci. USA* **89**, 6109–6113.

PATTISON, I. H. (1965). Scrapie in the welsh mountain breed of sheep and its experimental transmission to goats. *Vet. Rec*. **77**, 1388–1390.

PATTISON, I. H. & JONES, K. M. (1968). Modification of a strain of mouse-adapted scrapie by passage through rats. *Res. Vet. Sci.* **9**, 408–410.

PATTISON, I. H. & MILLSON, G. C. (1961). Scrapie produced experimentally in goats with special reference to the clinical syndrome. *J. Comp. Pathol*. **71**, 101–108.

PAULY, P. C. & HARRIS, D. A. (1998). Copper stimulates endocytosis of the prion protein. *J. Biol. Chem*. **273**, 33107–33110.

PERETZ, D., WILLIAMSON, R. A., MATSUNAGA, Y., SERBAN, H., PINILLA, C., BASTIDAS, R. B., ROZENSHTEYN R., JAMES, T. L., HOUGHTEN, R. A., COHEN, F. E., PRUSINER, S. B. & BURTON, D. R. (1997). A conformational transition at the N terminus of the prion protein features in formation of the scrapie isoform. *J. Mol. Biol*. **273**, 614–622.

PERRETT, S., ZAHN, R., STENBERG, G. & FERSHT, A. R. (1997). Importance of electrostatic interactions in the rapid binding of polypeptides to GroEL. *J. Mol. Biol.* **269**, 892–901.

PETERSEN, R. B., PARCHI, P., RICHARDSON, S. L., URIG, C. B. & GAMBETTI, P. (1996). Effect of the D178N mutation and the codon 129 polymorphism on the metabolism of the prion protein. *J. Biol. Chem*. **271**, 12661–12668.

PHILLIS, J. W. & WU, P. H. in *Physiology and Pharmacology of Adenosine Derivates* (eds Daly, J. W., Kuroda, Y., Phillis, J. W. Shimizu, H. & Ui, M.) 219–236 (Raven, New York, 1983).

PICKETTS, D. J., MAYANIL, C. S. & GUPTA, R. S. (1989). Molecular cloning of a Chinese hamster mitochondrial protein related to the "chaperonin" family of bacterial and plant proteins. *J. Biol. Chem*. **264**, 12001–12008.

PILLOT, T., LINS, L., GOETHALS, M., VANLOO, B., BAERT, J., VANDEKERCKHOVE, J., ROSSENEU, M. & BRASSEUR, R. (1997). The 118–135 peptide of the human prion protein forms amyloid fibrils and induces liposome fusion. *J. Mol. Biol.* **274**, 381–393.

PRIOLA, S. A. & CHESEBRO, B. (1995). A single hamster PrP amino acid blocks conversion to protease-resistant PrP in scrapie-infected mouse neuroblastoma cells. *J. Virol*. **69**, 7754–7758.

PRIOLA, S. A. & CHESEBRO, B. (1998). Abnormal properties of prion protein with insertional mutations in different cell types. *J. Biol. Chem*. **273**, 11980–11985.

PRUSINER, S. B. (1982). Novel proteinaceous infectious particles cause scrapie. *Science* **216**, 136–144.

PRUSINER, S. B. (1987). Prions and neurodegenerative diseases. *N. Engl. J. Med*. **317**, 1571–1581.

PRUSINER, S. B. (1991). Molecular biology of prion diseases. *Science* **252**, 1515–1522.

PRUSINER, S. B. (1997). Prion diseases and the BSE crisis. *Science* **278**, 245–251.

PRUSINER, S. B. (1998). Prions. *Proc. Natl. Acad. Sci. USA* **95**, 13363–13383.

PRUSINER, S. B. & HSIAO, K. K. (1994). Human prion diseases. *Ann. Neurol.* **35**, 385–395.

PRUSINER, S. B., BOLTON, D. C., GROTH, D. F., BOWMAN, K. A., COCHRAN, S. P. & MCKINLEY, M. P. (1982). Further purification and characterization of scrapie prions. *Biochemistry* **21**, 6942–6950.

PRUSINER, S. B., COCHRAN, S. P., DOWNEY, D. E. & GROTH, D. F. (1981*a*). Determination of scrapie agent titer from incubation period measurements in hamsters. *Adv. Exp. Med. Biol.* **134**, 385–399.

PRUSINER, S. B., GROTH, D. F., BOLTON, D. C., KENT, S. B. & HOOD, L. E. (1984). Purification and structural studies of a major scrapie prion protein. *Cell* **38**, 127–134.

PRUSINER, S. B., GROTH, D. F., COCHRAN, S. P., MASIARZ, F. R., MCKINLEY, M. P. & MARTINEZ, H. M. (1980). Molecular properties, partial purification, and assay by incubation period measurements of the hamster scrapie agent. *Biochemistry* **19**, 4883–4891.

PRUSINER, S. B., HADLOW, W. J., EKLUND, C. M. & RACE, R. E. (1977). Sedimentation properties of the scrapie agent. *Proc. Natl. Acad. Sci. USA* **74**, 4656–4660.

PRUSINER, S. B., MCKINLEY, M. P., BOWMAN, K. A., BOLTON, D. C., BENDHEIM, P. E., GROTH, D. F. & GLENNER, G. G. (1983). Scrapie prions aggregate to form amyloid-like birefringent rods. *Cell* **35**, 349–358.

PRUSINER, S. B., MCKINLEY, M. P., GROTH, D. F., BOWMAN, K. A., MOCK, N. I., COCHRAN, S. P. & MASIARZ, F. R. (1981*b*). Scrapie agent contains a hydrophobic protein. *Proc. Natl. Acad. Sci. USA* **78**, 6675–6679.

PRUSINER, S. B., SCOTT, M., FOSTER, D., PAN, K.-M., GROTH, D., MIRENDA, C., TORCHIA, M., YANG, S.-L., SERBAN, D., CARLSON, G. A., HOPPE, P. C., WESTAWAY, D. & DEARMOND, S. J. (1990). Transgenetic studies implicate interactions between homologous PrP isoforms in scrapie prion replication. *Cell* **63**, 673–686.

PRUSINER, S. B., SCOTT, M. R., DEARMOND, S. J. & COHEN & F. E. (1998). Prion protein biology. *Cell* **93**, 337–348.

RAYMOND, G. J., HOPE, J., KOCISKO, D. A., PRIOLA, S. A., RAYMOND, L. D., BOSSERS, A., IRONSIDE, J., WILL, R. G., CHEN, S. G., PETERSEN, R. B., GAMBETTI, P., RUBENSTEIN, R., SMITS, M. A., LANSBURY, P. T., JR. & CAUGHEY, B. (1997). Molecular assessment of the potential transmissibilities of BSE and scrapie to humans. *Nature* **388**, 285–288.

RIEGER, R., EDENHOFER, F., LASMÉZAS, C. I. & WEISS, S. (1997). The human 37-kDa laminin receptor precursor interacts with the prion protein in eukaryotic cells. *Nat. Med.* **3**, 1383–1388.

RIEK, R., HORNEMANN, S., WIDER, G., BILLETER, M., GLOCKSHUBER, R. & WÜTHRICH, K. (1996). NMR structure of the mouse prion protein domain PrP(121–231). *Nature* **382**, 180–182.

RIEK, R., HORNEMANN, S., WIDER, G., GLOCKSHUBER, R. & WÜTHRICH, K. (1997). NMR characterization of the full-length recombinant murine prion protein, *m*PrP(23–231). *FEBS Lett.* **413**, 282–288.

RIEK, R., WIDER, G., BILLETER, M., HORNEMANN, S., GLOCKSHUBER, R. & WÜTHRICH, K. (1998). Prion protein NMR structure and familial human spongiform encephalopathies. *Proc. Natl. Acad. Sci. USA* **95**, 11667–11672.

RIESNER, D., KELLINGS, K., POST, K., WILLE, H., SERBAN, H., GROTH, D., BALDWIN, M. A. & PRUSINER, S. B. (1996). Disruption of prion rods generates 10-nm spherical particles having high α-helical content and lacking scrapie infectivity. *J. Virol.* **70**, 1714–1722.

ROGERS, M., TARABOULOS, A., SCOTT, M., GROTH, D. & PRUSINER, S. B. (1990). Intracellular accumulation of the cellular prion protein after mutagenesis of its Asn-linked glycosylation sites. *Glycobiology* **1**, 101–109.

ROGERS, M., YEHIELY, F., SCOTT, M. & PRUSINER, S. B. (1993). Conversion of truncated and elongated prion proteins into the scrapie isoform in cultured cells. *Proc. Natl. Acad. Sci. USA* **90**, 3182–3186.

ROHER, A. E., LOWENSON, J. D., CLARKE, S., WOLKOW, C., WANG, R., COTTER, R. J., REARDON, I. M., ZURCHER-NEELY, H. A., HEINRIKSON, R. L., BALL, M. J. & GREENBERG, B. D. (1993*a*). Structural alterations in the peptide backbone of β-amyloid core protein may account for its deposition and stability in Alzheimer's disease. *J. Biol. Chem*. **268**, 3072–3083.

ROHER, A. E., LOWENSON, J. D., CLARKE, S., WOODS, A. S., COTTER, R. J., GOWING, E. & BALL, M. J. (1993*b*). β-Amyloid-(1–42) is a major component of cerebrovascular amyloid deposits: implications for the pathology of Alzheimer disease. *Proc. Natl. Acad. Sci. USA* **90**, 10836–10840.

RYE, H. S., ROSEMAN, A. M., CHEN, S., FURTAK, K., FENTON, W. A., SAIBIL, H. R. & HORWICH, A. L. (1999). GroEL-GroES cycling: ATP and nonnative polypeptide direct alternation of folding-active rings. *Cell* **97**, 325–338.

SABORÍO, G. P., SOTO, C., KASCSAK, R. J., LEVY, E., KASCSAK, R., HARRIS, D. A. & FRANGIONE, B. (1999). Cell-lysate conversion of prion protein into its protease-resistant isoform suggests the participation of a cellular chaperone. *Biochem. Biophys. Res. Commun*. **258**, 470–475.

SAFAR, J., ROLLER, P. P., GAJDUSEK, D. C., GIBBS, C. J., JR. (1993*a*). Conformational

transitions, dissociation, and unfolding of scrapie amyloid (prion) protein. *J. Biol. Chem*. **268**, 20276–20284.

SAFAR, J., ROLLER, P. P., GAJDUSEK, D. C. & GIBBS, C. J., JR. (1993*b*). Thermal stability and conformational transitions of scrapie amyloid (prion) protein correlate with infectivity. *Protein Sci.* **2**, 2206–2216.

SAFAR, J., ROLLER, P. P., GAJDUSEK, D. C. & GIBBS, C. J., JR. (1994). Scrapie amyloid (prion) protein has the conformational characteristics of an aggregated molten globule folding intermediate. *Biochemistry* **33**, 8375–8383.

SAFAR, J., WILLE, H., ITRI, V., GROTH, D., SERBAN, H., TORCHIA, M., COHEN, F. E. & PRUSINER, S. B. (1998). Eight prion strains have PrP^{Sc} molecules with different conformations. *Nat. Med*. **4**, 1157–1165.

SAILER, A., BÜELER, H., FISCHER, M., AGUZZI, A. & WEISSMANN, C. (1994). No propagation of prions in mice devoid of PrP. *Cell* **77**, 967–968.

SAKAGUCHI, S., KATAMINE, S., NISHIDA, N., MORIUCHI, R., SHIGEMATSU, K., SUGIMOTO, T., NAKATANI, A., KATAOKA, Y., HOUTANI, T., SHIRABE, S., OKADA, H., HASEGAWA, S., MIYAMOTO, T. & NODA, T. (1996). Loss of cerebellar Purkinje cells in aged mice homozygous for a disrupted PrP gene. *Nature* **380**, 528–531.

SALMONA, M., MALESANI, P., DE GIOIA, L., GORLA, S., BRUSCHI, M., MOLINARI, A., DELLA VEDOVA, F., PEDROTTI, B., MARRARI, M. A., AWAN, T., BUGIANI, O., FORLONI, G. & TAGLIAVINI, F. (1999). Molecular determinants of the physicochemical properties of a critical prion protein region comprising residues 106–126. *Biochem J.* **342**, 207–214.

SCHÄTZL, H. M., DA COSTA, M., TAYLOR, L., COHEN, F. E. & PRUSINER, S. B. (1995). Prion protein gene variation among primates. *J. Mol. Biol.* **245**, 362–374.

SCOTT, M., FOSTER, D., MIRENDA, C., SERBAN, D., COUFAL, F., WÄLCHLI, M., TORCHIA, M., GROTH, D., CARLSON, G., DEARMOND, S. J., WESTAWAY, D. & PRUSINER, S. B. (1989). Transgenic mice expressing hamster prion protein produce species-specific scrapie infectivity and amyloid plaques. *Cell* **59**, 847–857.

SCOTT, M., GROTH, D., FOSTER, D., TORCHIA, M., YANG, S.-L., DEARMOND, S. J. & PRUSINER, S. B. (1993). Propagation of prions with artificial properties in transgenic mice expressing chimeric PrP genes. *Cell* **73**, 979–988.

SCOTT, M. R., GROTH, D., TATZELT, J., TORCHIA, M., TREMBLAY, P., DEARMOND, S. J. & PRUSINER, S. B. (1997*a*). Propagation of prion strains through specific conformers of the prion protein. *J. Virol*. **71**, 9032–9044.

SCOTT, M. R., KOHLER, R., FOSTER, D. & PRUSINER, S. B. (1992). Chimeric prion protein expression in cultured cells and transgenic mice. *Protein Sci.* **1**, 986–997.

SCOTT, M. R., SAFAR, J., TELLING, G., NGUYEN, O., GROTH, D., TORCHIA, M., KOEHLER, R., TREMBLAY, P., WALTHER, D., COHEN, F. E., DEARMOND, S. J. & PRUSINER, S. B. (1997*b*). Identification of a prion protein epitope modulating transmission of bovine spongiform encephalopathy prions to transgenic mice. *Proc. Natl. Acad. Sci. USA* **94**, 14279–14284.

SCOTT, M. R., WILL, R., IRONSIDE, J., NGUYEN, H.-O. B., TREMBLAY, P., DEARMOND, S. J. & PRUSINER, S. B. (1999). Compelling transgenetic evidence for transmission of bovine spongiform encephalopathy prions to humans. *Proc. Natl. Acad. Sci. USA* **96**, 15137–15142.

SELVAGGINI, C., DE GIOIA, L., CANTÙ, L., GHIBAUDI, E., DIOMEDE, L., PASSERINI, F., FORLONI, G., BUGIANI, O., TAGLIAVINI, F. & SALMONA, M. (1993). Molecular

characteristics of a protease-resistant, amyloidogenic and neurotoxic peptide homologous to residues 106–126 of the prion protein. *Biochem. Biophys. Res. Commun*. **194**, 1380–1386.

SHAKED, G. M., FRIDLANDER, G., MEINER, Z., TARABOULOS, A. & GABIZON, R. (1999). Protease-resistant and detergent-insoluble prion protein is not necessarily associated with prion infectivity. *J. Biol. Chem*. **274**, 17981–17986.

SHARMAN, G. J., KENWARD, N., WILLIAMS, H. E., LANDON, M., MAYER, R. J. & SEARLE, M. S. (1998). Prion protein fragments spanning helix 1 and both strands of β sheet (residues 125–170) show evidence for predominantly helical propensity by CD and NMR. *Fold. Des*. **3**, 313–320.

SHMERLING, D., HEGYI, I., FISCHER, M., BLÄTTLER, T., BRANDNER, S., GÖTZ, J., RÜLICKE, T., FLECHSIG, E., COZZIO, A., VON MERING, C., HANGARTNER, C., AGUZZI, A. & WEISSMANN, C. (1998). Expression of amino-terminally truncated PrP in the mouse leading to ataxia and specific cerebellar lesions. *Cell* **93**, 203–214.

SHTILERMAN, M., LORIMER, G. H. & ENGLANDER, S. W. (1999). Chaperonin function: folding by forced unfolding. *Science* **284**, 822–825.

SHYNG, S.-L., HEUSER, J. E. & HARRIS, D. A. (1994). A glycolipid-anchored prion protein is endocytosed via clathrin-coated pits. *J. Cell. Biol.* **125**, 1239–1250.

SHYNG, S.-L., HUBER, M. T. & HARRIS, D. A. (1993). A prion protein cycles between the cell surface and an endocytic compartment in cultured neuroblastoma cells. *J. Biol. Chem*. **268**, 15922–15928.

SHYNG, S.-L., MOULDER, K. L., LESKO, A. & HARRIS, D. A. (1995). The N-terminal domain of a glycolipid-anchored prion protein is essential for its endocytosis via clathrin-coated pits. *J. Biol. Chem*. **270**, 14793–14800.

SIGLER, P. B., XU, Z., RYE, H. S., BURSTON, S. G., FENTON, W. A. & HORWICH, A. L. (1998). Structure and function in GroEL-mediated protein folding. *Annu. Rev. Biochem*. **67**, 581–608.

SILINSKY, E. M. & GINSBORG, B. L. (1983). Inhibition of acetylcholine release from preganglionic frog nerves by ATP but not adenosine. *Nature* **305**, 327–328.

SINGH, B., SOLTYS, B. J., WU, Z. C., PATEL, H. V., FREEMAN, K. B. & GUPTA, R. S. (1997). Cloning and some novel characteristics of mitochondrial Hsp70 from Chinese hamster cells. *Exp. Cell Res*. **234**, 205–216.

SOLTYS, B. J. & GUPTA, R. S. (1996). Immunoelectron microscopic localization of the 60-kDa heat shock chaperonin protein (Hsp60) in mammalian cells. *Exp. Cell. Res*. **222**, 16–27.

SOLTYS, B. J. & GUPTA, R. S. (1997). Cell surface localization of the 60 kDa heat shock chaperonin protein (Hsp60) in mammalian cells. *Cell. Biol. Int.* **21**, 315–320.

SOLTYS, B. J. & GUPTA, R. S. (1999). Mitochondrial-matrix proteins at unexpected locations: are they exported? *Trends Biochem. Sci.* **24**, 174–177.

STAHL, N., BALDWIN, M. A., BURLINGAME, A. L. & PRUSINER, S. B. (1990*a*). Identification of glycoinositol phospholipid linked and truncated forms of the scrapie prion protein. *Biochemistry* **29**, 8879–8884.

STAHL, N., BALDWIN, M. A., TEPLOW, D. B., HOOD, L., GIBSON, B. W., BURLINGAME, A. L. & PRUSINER, S. B. (1993). Structural studies of the scrapie prion protein using mass spectrometry and amino acid sequencing. *Biochemistry* **32**, 1991–2002.

STAHL, N., BORCHELT, D. R., HSIAO, K. & PRUSINER, S. B. (1987). Scrapie prion protein

contains a phosphatidylinositol glycolipid. *Cell* **51**, 229–240.

STAHL, N., BORCHELT, D. R. & PRUSINER, S. B. (1990*b*). Differential release of cellular and scrapie prion proteins from cellular membranes by phosphatidylinositol-specific phospholipase C. *Biochemistry* **29**, 5405–5412.

STÖCKEL, J., SAFAR, J., WALLACE, A. C., COHEN, F. E. & PRUSINER, S. B. (1998). Prion protein selectively binds copper(II) ions. *Biochemistry* **37**, 7185–7193.

SULKOWSKI, E. (1992). Spontaneous conversion of PrP^{C} to PrP^{Sc}. *FEBS Lett.* **307**, 129–130.

SUNDE, M. & BLAKE, C. C. (1998). From the globular to the fibrous state: protein structure and structural conversion in amyloid formation. *Q. Rev. Biophys*. **31**, 1–39.

SUPATTAPONE, S., BOSQUE, P., MURAMOTO, T., WILLE, H., AAGAARD, C., PERETZ, D., NGUYEN, H.-O. B., HEINRICH, C., TORCHIA, M., SAFAR, J., COHEN, F. E., DEARMOND, S. J., PRUSINER, S. B. & SCOTT, M. (1999). Prion protein of 106 residues creates an artificial transmission barrier for prion replication in transgenic mice. *Cell* **96**, 869–878.

SWIETNICKI, W., MORILLAS, M., CHEN, S. G., GAMBETTI, P. & SUREWICZ, W. K. (2000). Aggregation and fibrillization of the recombinant human prion protein huPrP90–231. *Biochemistry* **39**, 424–431.

SWIETNICKI, W., PETERSEN, R., GAMBETTI, P. & SUREWICZ, W. K. (1997). pH-dependent stability and conformation of the recombinant human prion protein PrP(90–231). *J. Biol. Chem*. **272**, 27517–27520.

SWIETNICKI, W., PETERSEN, R. B., GAMBETTI, P. & SUREWICZ, W. K. (1998). Familial mutations and the thermodynamic stability of the recombinant human prion protein. *J. Biol. Chem*. **273**, 31048–31052.

TAGLIAVINI, F., PRELLI, F., GHISO, J., BUGIANI, O., SERBAN, D., PRUSINER, S. B., FARLOW, M. R., GHETTI, B. & FRANGIONE, B. (1991). Amyloid protein of Gerstmann-Sträussler-Scheinker disease (Indiana kindred) is an 11 kd fragment of prion protein with an N-terminal glycine at codon 58. *EMBO J.* **10**, 513–519.

TAGLIAVINI, F., PRELLI, F., VERGA, L., GIACCONE, G., SARMA, R., GOREVIC, P., GHETTI, B., PASSERINI, F., GHIBAUDI, E., FORLONI, G., SALMONA, M., BUGIANI, O. & FRANGIONE, B. (1993). Synthetic peptides homologous to prion protein residues 106–147 form amyloid-like fibrils *in vitro*. *Proc. Natl. Acad. Sci. USA* **90**, 9678–9682.

TANAKA, N. & FERSHT, A. R. (1999). Identification of substrate binding site of GroEL minichaperone in solution. *J. Mol. Biol*. **292**, 173–180.

TARABOULOS, A., ROGERS, M., BORCHELT, D. R., MCKINLEY, M. P., SCOTT, M., SERBAN, D. & PRUSINER, S. B. (1990*a*). Acquisition of protease resistance by prion proteins in scrapie-infected cells does not require asparagine-linked glycosylation. *Proc. Natl. Acad. Sci. USA* **87**, 8262–8266.

TARABOULOS, A., SCOTT, M., SEMENOV, A., AVRAHAMI, D., LASZLO, L. & PRUSINER, S. B. (1995). Cholesterol depletion and modification of COOH-terminal targeting sequence of the prion protein inhibit formation of the scrapie isoform. *J. Cell. Biol.* **129**, 121–132.

TARABOULOS, A., SERBAN, D. & PRUSINER, S. B. (1990*b*). Scrapie prion proteins accumulate in the cytoplasm of persistently infected cultured cells. *J. Cell Biol*. **110**, 2117–2132.

TATZELT, J., PRUSINER, S. B. & WELCH, W. J. (1996). Chemical chaperones interfere with the formation of scrapie prion protein. *EMBO. J.* **15**, 6363–6373.

TELLING, G. C., HAGA, T., TORCHIA, M., TREMBLAY, P., DEARMOND, S. J. & PRUSINER, S. B.

(1996*a*). Interactions between wild-type and mutant prion proteins modulate neurodegeneration in transgenic mice. *Genes Dev*. **10**, 1736–1750.

TELLING, G. C., PARCHI, P., DEARMOND, S. J., CORTELLI, P., MONTAGNA, P., GABIZON, R., MASTRIANNI, J., LUGARESI, E., GAMBETTI, P. & PRUSINER, S. B. (1996*b*). Evidence for the conformation of the pathologic isoform of the prion protein enciphering and propagating prion diversity. *Science* **274**, 2079–2082.

TELLING, G. C., SCOTT, M., HSIAO, K. K., FOSTER, D., YANG, S-L., TORCHIA, M., SIDLE, K. C. L., COLLINGE, J., DEARMOND, S. J. & PRUSINER, S. B. (1994). Transmission of Creutzfeldt-Jakob disease from humans to transgenic mice expressing chimeric human–mouse prion protein. *Proc. Natl. Acad. Sci.* **91**, 9936–9940.

TELLING, G. C., SCOTT, M., MASTRIANNI, J., GABIZON, R., TORCHIA, M., COHEN F. E., DEARMOND, S. J. & PRUSINER, S. B. (1995). Prion propagation in mice expressing human and chimeric PrP transgenes implicates the interaction of cellular PrP with another protein. *Cell* **83**, 79–90.

TOBLER, I., GAUS, S. E., DEBOER, T., ACHERMANN, P., FISCHER, M., RÜLICKE, T., MOSER, M., OESCH, B., MCBRIDE, P. A. & MANSON, J. C. (1996). Altered circadian activity rhythms and sleep in mice devoid of prion protein. *Nature* **380**, 639–642.

TÖRÖK, Z., HORVATH, I., GOLOUBINOFF, P., KOVACS, E., GLATZ, A., BALOGH, G. & VIGH, L. (1997). Evidence for a lipochaperonin: association of active protein-folding GroESL oligomers with lipids can stabilize membranes under heat shock conditions. *Proc. Natl. Acad. Sci. USA* **94**, 2192-2197.

TURK, E., TEPLOW, D. B., HOOD, L. E. & PRUSINER, S. B. (1988). Purification and properties of the cellular and scrapie hamster prion proteins. *Eur. J. Biochem*. **176**, 21–30.

VANBUSKIRK, A. M., DENAGEL, D. C., GUAGLIARDI, L. E., BRODSKY, F. M. & PIERCE, S. K. (1991). Cellular and subcellular distribution of PBP72/74, a peptide-binding protein that plays a role in antigen processing. *J. Immunol*. **146**, 500-506.

VÉLEZ-GRANELL, C. S., ARIAS, A. E., TORRES-RUÍZ, J. A. & BENDAYAN, M. (1994). Molecular chaperones in pancreatic tissue: the presence of cpn10, cpn60 and hsp70 in distinct compartments along the secretory pathway of the acinar cells. *J. Cell. Sci.* **107**, 539–549.

VEY, M., PILKUHN, S., WILLE, H., NIXON, R., DEARMOND, S. J., SMART, E. J., ANDERSON, R. G., TARABOULOS, A. & PRUSINER, S. B. (1996). Subcellular colocalization of the cellular and scrapie prion proteins in caveolae-like membranous domains. *Proc. Natl. Acad. Sci. USA* **93**, 14945–14949.

VILES, J. H., COHEN, F. E., PRUSINER, S. B., GOODIN, D. B., WRIGHT, P. E. & DYSON, H. J. (1999). Copper binding to the prion protein: structural implications of four identical cooperative binding sites. *Proc. Natl. Acad. Sci. USA* **96**, 2042–2047.

WALTER, J., CAPELL, A., HUNG, A. Y., LANGEN, H., SCHNÖLZER, M., THINAKARAN, G., SISODIA, S. S., SELKOE, D. J. & HAASS, C. (1997). Ectodomain phosphorylation of beta-amyloid precursor protein at two distinct cellular locations. *J. Biol. Chem*. **272**, 1896–1903.

WALTER, S., LORIMER, G. H. & SCHMID, F. X. (1996). A thermodynamic coupling mechanism for GroEL-mediated unfolding. *Proc. Natl. Acad. Sci. USA* **93**, 9425–9430.

WEBER, D. J., MCFADDEN, P. N. & CAUGHEY, B. (1998). Measurement of altered aspartyl residues in the scrapie associated form of prion protein. *Biochem. Biophys. Res. Commun*.

246, 606–608.

WEISSMAN, J. S., RYE, H. S., FENTON, W. A., BEECHEM, J. M. & HORWICH, A. L. (1996). Characterization of the active intermediate of a GroEL–GroES-mediated protein folding reaction. *Cell* **84**, 481–490.

WEISSMANN, C. (1999). Molecular genetics of transmissible spongiform encephalopathies. *J. Biol. Chem.* **274**, 3–6.

WILDEGGER, G., LIEMANN, S. & GLOCKSHUBER, R. (1999). Extremely rapid folding of the C-terminal domain of the prion protein without kinetic intermediates. *Nat. Struct. Biol.* **6**, 550–553.

WILLE, H. & PRUSINER, S. B. (1999). Ultrastructural studies on scrapie prion protein crystals obtained from reverse micellar solutions. *Biophys. J.* **76**, 1048–1062.

WU, C., BUTZ, S., YING, Y. & ANDERSON, R. G. (1997). Tyrosine kinase receptors concentrated in caveolae-like domains from neuronal plasma membrane. *J. Biol. Chem*. **272**, 3554–3559.

WÜTHRICH, K. (1986). *NMR of Proteins and Nucleic Acids.* New York: Wiley.

XU, Z., HORWICH, A. L. & SIGLER, P. B. (1997). The crystal structure of the asymmetric GroEL–GroES–$(ADP)_7$ chaperonin complex. *Nature* **388**, 741–750.

YIFRACH, O. & HOROVITZ, A. (2000). Coupling between protein folding and allostery in the GroE chaperonin system. *Proc. Natl. Acad. Sci. USA* **97**, 1521–1524.

YING, Y.-S., ANDERSON, R. G. W. & ROTHBERG, K. G. (1992). *Cold Spring Harbor Symp. Quant. Biol.* **57**, 593–604.

YOST, C. S., LOPEZ, C. D., PRUSINER, S. B., MYERS, R. M. & LINGAPPA, V. R. (1990). Non-hydrophobic extracytoplasmic determinant of stop transfer in the prion protein. *Nature* **343**, 669–672.

YOUNG, K., PICCARDO, P., DLOUHY, S., BUGIANI, O., TAGLIAVINI, F, & GHETTI, B. (1999). The human genetic prion diseases. In *Prions: Molecular and Cellular Biology* (ed. D. A. Harris), pp. 139–175. Wymondham: Horizon Scientific Press.

ZAHN, R. & PLÜCKTHUN, A. (1992). GroE prevents the accumulation of early folding intermediates of pre-β-lactamase without changing the folding pathway. *Biochemistry* **31**, 3249–3255.

ZAHN, R. & PLÜCKTHUN, A. (1994). Thermodynamic partitioning model for hydrophobic binding of polypeptides by GroEL. II. GroEL recognizes thermally unfolded mature β-lactamase. *J. Mol. Biol.* **242**, 165–174.

ZAHN, R., AXMANN, S. E., RÜCKNAGEL, K.-P., JAEGER, E., LAMINET, A. A. & PLÜCKTHUN, A. (1994*a*). Thermodynamic partitioning model for hydrophobic binding of polypeptides by GroEL. I. GroEL recognizes the signal sequences of β-lactamase precursor. *J. Mol. Biol*. **242**, 150–164.

ZAHN, R., BUCKLE, A. M., PERRETT, S., JOHNSON, C. M., CORRALES, F. J., GOLBIK, R., FERSHT, A. R. (1996*a*). Chaperone activity and structure of monomeric polypeptide binding domains of GroEL. *Proc. Natl. Acad. Sci. USA* **93**, 15024–15029.

ZAHN, R., HARRIS, J. R., PFEIFER, G., PLÜCKTHUN, A. & BAUMEISTER, W. (1993). Two-dimensional crystals of the molecular chaperone GroEL reveal structural plasticity. *J. Mol. Biol.* **229**, 579–584.

ZAHN, R., LINDNER, P., AXMANN, S. E. & PLÜCKTHUN, A. (1996*b*). Effect of single point mutations in citrate synthase on binding to GroEL. *FEBS Lett*. **380**, 152–156.

ZAHN, R., LIU, A., LÜHRS, T., RIEK, R., VON SCHROETTER, C., LÓPEZ-GARCÍA, F., BILLETER, M., CALZOLAI, L., WIDER, G. & WÜTHRICH, K. (2000). NMR solution structure of the human prion protein. *Proc. Natl. Acad. Sci. USA* **97**, 145–150.

ZAHN, R., PERRETT, S. & FERSHT, A. R. (1996*c*). Conformational states bound by the molecular chaperones GroEL and SecB: a hidden unfolding (annealing) activity. *J. Mol. Biol*. **261**, 43–61.

ZAHN, R., PERRETT, S., STENBERG, G. & FERSHT, A. R. (1996*d*). Catalysis of amide proton exchange by the molecular chaperones GroEL and SecB. *Science* **271**, 642–645.

ZAHN, R., SPITZFADEN, C., OTTIGER, M., WÜTHRICH, K. & PLÜCKTHUN, A. (1994*b*). Destabilization of the complete protein secondary structure on binding to the chaperone GroEL. *Nature* **368**, 261–265.

ZAHN, R., VON SCHROETTER, C. & WÜTHRICH, K. (1997). Human prion proteins expressed in *Escherichia coli* and purified by high-affinity column refolding. *FEBS Lett.* **417**, 400–404.

ZANUSSO, G., PETERSEN, R. B., JIN, T., JING, Y., KANOUSH, R., FERRARI, S., GAMBETTI, P. & SINGH, N. (1999). Proteasomal degradation and N-terminal protease resistance of the codon 145 mutant prion protein. *J. Biol. Chem*. **274**, 23396–23404.

ZHANG, H., KANEKO, K., NGUYEN, J. T., LIVSHITS, T. L., BALDWIN, M. A., COHEN, F. E., JAMES, T. L. & PRUSINER, S. B. (1995). Conformational transitions in peptides containing two putative α-helices of the prion protein. *J. Mol. Biol.* **250**, 514–526.

ZHANG, H., STÖCKEL, J., MEHLHORN, I., GROTH, D., BALDWIN, M. A., PRUSINER, S. B., JAMES, T. L. & COHEN, F. E. (1997). Physical studies of conformational plasticity in a recombinant prion protein. *Biochemistry* **36**, 3543–3553.